EPRI

Evaluation of Thermal Aging Embrittlement for Cast Austenitic Stainless Steel Components

Technical Report

Evaluation of Thermal Aging Embrittlement for Cast Austenitic Stainless Steel Components

1000976

Final Report, January 2001

EPRI Project Manager
J. Carey

EPRI • 3412 Hillview Avenue, Palo Alto, California 94304 • PO Box 10412, Palo Alto, California 94303 • USA
800.313.3774 • 650.855.2121 • askepri@epri.com • www.epri.com

DISCLAIMER OF WARRANTIES AND LIMITATION OF LIABILITIES

ORGANIZATION(S) THAT PREPARED THIS DOCUMENT

Anatech Corp.
Framatome Technologies, Inc.

ORDERING INFORMATION

Requests for copies of this report should be directed to the EPRI Distribution Center, 207 Coggins Drive, P.O. Box 23205, Pleasant Hill, CA 94523, (800) 313-3774.

CITATIONS

This report was prepared by

Anatech Corp.
5435 Oberlin Drive
San Diego, California 92121

Principal Investigator
R.E. Nickell

Framatome Technologies, Inc.
PO Box 10935
Lynchburg, VA 24506-0935

Principal Investigator
M.A. Rinckel

This report describes research sponsored by EPRI.

The report is a corporate document that should be cited in the literature in the following manner:

Evaluation of Thermal Aging Embrittlement for Cast Austenitic Stainless Steel Components: EPRI, Palo Alto, CA: 2001. 1000976.

REPORT SUMMARY

This report presents screening criteria for evaluating the potential significance of thermal aging embrittlement effects for light water reactor (LWR) Class 1 (reactor coolant system and primary pressure boundary) and Class CS (reactor internals) cast austenitic stainless steel (CASS) components for the license renewal term. For those situations where the effects are found to be potentially significant, evaluation criteria for both detected and postulated flaws are recommended for demonstrating that aging effects are adequately managed.

Background
Prolonged exposure of CASS components to reactor coolant operating temperatures has been shown to lead to some degree of thermal aging embrittlement. The relevant aging effect is a reduction in the material's fracture toughness as a function of time. The magnitude of the reduction depends on the casting method (statically or centrifugally cast), material chemistry (for example, delta ferrite and molybdenum content), and exposure duration at coolant operating temperature. The extensive amount of fracture toughness data available for thermally-aged CASS materials enables delta ferrite content, molybdenum content, casting method, and service temperature history to be used as the basis for screening. Comparing fracture toughness data to those for austenitic stainless steel welds provides the basis for flaw evaluation.

Objective
To develop screening criteria for potential significance of CASS component thermal aging embrittlement; to justify applying austenitic stainless steel weld flaw acceptance criteria to thermally-aged LWR CASS components; and, to obtain Nuclear Regulatory Commission (NRC) acceptance of the complete technical approach.

Approach
The project team examined the extensive set of fracture toughness data in the literature for thermally-aged CASS materials and categorized these data as a function of delta ferrite and molybdenum content, casting method, and duration of aging. The team developed screening criteria for determining the potential significance of thermal aging embrittlement effects by comparing these fracture toughness data with results of flaw tolerance and elastic-plastic fracture toughness evaluations for typical CASS components and loadings. To justify using existing submerged arc weld (SAW) flaw acceptance criteria for CASS component inservice inspections, team members then compared fracture toughness data for the most severely aged CASS materials to crack growth resistance curves for some austenitic stainless steel weld metal, in particular weld metal for submerged arc welds.

Results

The screening criteria illustrate the importance of delta ferrite and molybdenum content. They also show that centrifugally-cast components are more resistant to thermal aging effects than statically-cast components. The similarity of crack growth resistance for severely-aged CASS material and SAW offers the possibility of applying ASME Code Section XI inservice inspection flaw acceptance criteria for SAW and shielded-metal-arc weldments (SMAW) to CASS component inspection results. This report provides screening criteria and justification for applying SAW and SMAW flaw acceptance criteria to CASS component inservice inspection evaluations.

EPRI Perspective

This study is an update of a previous EPRI report (TR-106092, Sept. 1997) and incorporates the experience from reviews of recent license renewal applications. The study examined the extensive set of fracture toughness data in the literature for thermally-aged CASS materials and the categorization of these data as a function of delta ferrite and molybdenum content, casting method, and duration of aging. Screening criteria were developed for determining the potential significance of thermal aging embrittlement effects by comparing these fracture toughness data with results of flaw tolerance and elastic-plastic fracture toughness evaluations for typical CASS components and loadings. Fracture toughness data for the most severely aged CASS materials were then compared to crack growth resistance curves for some austenitic stainless steel weld metal—in particular weld metal for submerged arc welds—to justify using existing SAW flaw acceptance criteria for CASS component inservice inspections.

Keywords

LWR
License renewal
Life assessment
Life-cycle management

ABSTRACT

Prolonged exposure of cast austenitic stainless steels (CASS) to reactor coolant operating temperatures has been shown to lead to some degree of thermal aging embrittlement. The relevant aging effect is a reduction in the fracture toughness of the material as a function of time. The magnitude of the reduction depends upon the type of casting method, the material chemistry, and the duration of exposure at operating temperatures conducive to the embrittlement process. Static castings are more susceptible than centrifugal castings, high-molybdenum-content castings are more susceptible than low-molybdenum-content castings, high-delta-ferrite castings are more susceptible than low-delta-ferrite castings, and operating temperatures of the order of 320°C (610°F) increase the embrittlement rate relative to the rate at operating temperatures of the order of 285°C (550°F). The extensive amount of fracture toughness data available for thermally-aged CASS materials enables delta ferrite, molybdenum content, casting type, and service temperature history to be used as the bases for screening and evaluating components for continued operation during the license renewal term.

In addition, the fracture toughness data for the most severely aged CASS materials were found to be similar to those reported for some austenitic stainless steel weld metal, in particular weld metal from submerged arc welds (SAW). Such similarity offers the possibility for applying periodic inservice inspection flaw acceptance criteria, currently referenced in the ASME Code Section XI, Subsection IWB, for SAW and shielded metal arc weld (SMAW), to CASS component inservice inspection results.

This report presents data to support both the proposed screening criteria for evaluation of the potential significance of the effects of thermal aging embrittlement for Class 1 reactor coolant system and primary pressure boundary CASS components and for Class CS (Core Support) reactor internals components. For those situations where the effects of thermal aging embrittlement are found to be potentially significant, evaluation criteria to determine fitness for continued service are described and justified.

The screening criteria are based on extensive fracture toughness (e.g., J-R crack growth resistance) testing of various CASS materials comprising a wide range of component types, manufacturing methods, and material chemistries, and the comparison of these test data with flaw tolerance calculations. A crack growth resistance of 255 kJ/m^2 (1450 $in\text{-}lb/in^2$) at a crack extension of 2.5 mm (0.1 in) was determined to be a reasonable threshold for defining the screening criteria.

The fitness for continued service evaluation is based on the comparison of the limiting fracture toughness data for Type 316 SAW welds and the lower-bound fracture toughness data reported for high-molybdenum, high-delta-ferrite, statically-cast and centrifugally-cast CASS materials.

The most limiting lower-bound fracture toughness, using the J-R crack growth resistance curve for statically-cast SA 351, Grade CF-8M with a delta ferrite number greater than 15, is slightly below but essentially equivalent to the J-R data for Type 316 SAW used to generate the flaw acceptance criteria for SAW and SMAW in the ASME Code Section XI. While the upper end of the range of delta ferrite from which these data were drawn is limited to about 28%, saturation effects data can be used to extend the comparison to delta ferrite contents that extend up to 40%. (Regulatory interpretation of these data limits the comparison to delta ferrite content of 25% (NUREG-1723, RAI 3.4.8-6) This favorable comparison permits the flaw evaluation procedures specified in IWB-3640 to be applied to Class 1 CASS components and CASS reactor internals for which resistance to crack propagation and growth is a design-basis consideration. Furthermore, these comparisons and the associated flaw acceptance criteria can be used to justify exemptions from current ASME Code Section XI inservice inspection requirements through flaw tolerance evaluation (e.g., see ASME Nuclear Code Case N-481).

For Class CS reactor internals components fabricated from CASS, the NRC staff recognizes that reduction of fracture toughness may be caused by the synergistic effects of thermal embrittlement and irradiation embrittlement. Therefore, the license renewal applicant may demonstrate that the CASS internals components satisfy the thermal embrittlement screening criteria, and that the exposure of CASS components to neutron fluence is limited to 1×10^{17} n/cm^2 ($E > 1$ MeV) during the period of extended operation. If the material can be shown to satisfy the thermal embrittlement and irradiation embrittlement screening criteria for Class CS reactor internals fabricated from CASS, then no further action is required. If the material fails to satisfy the screening criteria, three alternatives are available. First, the mechanical loads can be shown to result in compressive stresses, or tensile stresses below 8 to 10 ksi. Second, the internals components can be shown to be tolerant to mature flaws that may be detected using the existing visual acuity standards in the ASME Code for VT-3 visual examination. Finally, a supplemental visual examination following the BWRVIP visual acuity recommendations can be undertaken.

CONTENTS

LIST OF FIGURES

LIST OF TABLES

1
INTRODUCTION

Test data obtained by Fracture Control Corporation [1, 2], under contract to the Electric Power Research Institute (EPRI), and by Argonne National Laboratory (ANL) [3], under contract to the U. S. Nuclear Regulatory Commission (NRC), indicate that prolonged exposure of cast austenitic stainless steels (CASS) to reactor coolant operating temperatures can lead to thermal aging embrittlement. The relevant aging effect is a reduction in the fracture toughness of the material as a function of time. The magnitude of the reduction depends upon the type of casting method, the material chemistry, and the duration of exposure at operating temperatures conducive to the embrittlement process. Static castings are more susceptible than centrifugal castings, high-molybdenum-content castings are more susceptible than low-molybdenum-content castings, high-delta-ferrite castings are more susceptible than low-delta-ferrite castings, and operating temperatures of the order of 320°C (610°F) increase the embrittlement rate relative to the rate at operating temperatures of the order of 285°C (550°F). From the data presented in References 1 and 2, and elsewhere, thermal aging embrittlement effects may be of concern for any period of operation beyond 40 years, and could possibly be of concern during the current license term.

The potential significance and management of the effects of thermal aging embrittlement for CASS components was one of the open technical issues for a number of the License Renewal Industry Reports (IRs) that were submitted by the Nuclear Management and Resources Council (NUMARC), now the Nuclear Energy Institute (NEI), to the NRC for review and comment during the period 1989-1992. In particular, the issue was addressed in the PWR Reactor Coolant System IR [4] and the BWR Primary Coolant Pressure Boundary IR [5] for Class 1 components that are required to behave in a non-brittle manner, with a correspondingly low probability of abnormal leakage, rapidly propagating fracture, and gross rupture. The industry has continued to evaluate the available technical information, in order to develop a comprehensive and cost-effective strategy for managing the significant effects of thermal aging embrittlement for CASS components through the license renewal term. This strategy is based upon two elements: (1) criteria for screening CASS components to determine whether the reduction of fracture toughness is potentially significant, and (2) for those CASS components for which a significant reduction of fracture toughness is predicted for a license renewal term, methods for evaluating flaws that are either detected during periodic inservice examination or postulated for determining fitness for continued service.

The screening criteria for the determination of potentially significant thermal aging embrittlement effects are based upon measured or calculated delta ferrite content, measured molybdenum content, and casting method–either static or centrifugal casting methods. If the delta ferrite information is not available, or if available information is not used for justification, then further evaluation of the effects of potentially significant thermal aging embrittlement may be required. These screening criteria listed below were determined to be applicable to all CASS

nuclear power plant components manufactured from Grade CF3, CF3A, CF8, CF8A, CF3M, CF3MA, and CF8M material. The flaw evaluation methods are based upon current ASME Code Section XI, Subsection IWB methods for evaluating flaws detected in submerged-arc welds (SAW) and shielded-metal-arc welds (SMAW) [6]. The sequence of steps involved in applying the screening criteria and the flaw evaluation methods is outlined below.

- For screening purposes, the first parameter to be evaluated is molybdenum (Mo) content, as obtained from the component certified material test reports. CF-3 and CF-8 grades with Mo limited to 0.50 wt% should be evaluated separately from the CF-3M and CF-8M grades that may contain Mo up to 3.0 wt%.
- For screening purposes, the second parameter to be evaluated is the casting procedure for the component product form. Centrifugally-cast material should be evaluated separately from statically-cast material.
- For screening purposes, another parameter that may be used, provided that the required material property information is available or can be measured, is the calculated or measured delta ferrite.
- Low-molybdenum (e.g., SA 351 Grade CF-3 and CF-8) material that has been cast centrifugally is not subject to significant thermal aging embrittlement during exposure to service temperatures less than 320°C (610°F) for 525,000 hours (60 years). Low-molybdenum material that has been cast statically is not subject to potentially significant loss of fracture toughness after exposure to service temperatures less than 320°C (610°F) for 525,000 hours (60 years), provided that the delta ferrite content of the material can be shown by either calculation or measurement to be 20%, or less. Management of potential loss of fracture toughness for low-molybdenum, statically-cast components is required, in terms of inservice examination and flaw evaluation program elements, if the delta ferrite content of the material cannot be shown to be 20%, or less.
- High-molybdenum (e.g., SA 351 Grade CF-3M and CF-8M) material that has been cast centrifugally is not subject to potentially significant loss of fracture toughness after exposures to temperatures less than 320°C (610°F) for 525,000 hours (60 years), provided that the delta ferrite content of the material can be shown by either calculation or measurement to be 20%, or less. Management of potential reduction of fracture toughness for high-molybdenum, centrifugally-cast components is required, in terms of inservice examination and flaw evaluation program elements, if the delta ferrite content of the material cannot be shown to be 20%, or less.
- High-molybdenum (e.g., SA 351 Grade CF-3M and CF-8M) that has been cast statically is not subject to potentially significant loss of fracture toughness after exposures to temperatures less than 320°C (610°F) for 525,000 hours (60 years), provided that the delta ferrite content of the material can be shown by either calculation or measurement to be 14%, or less. Management of potential reduction of fracture toughness for high-molybdenum, statically-cast components is required, in terms of inservice examination and flaw evaluation program elements, if the delta ferrite content cannot be shown to be 14%, or less.
- In accordance with the NRC position regarding irradiation embrittlement of reactor internals parts fabricated from CASS in NUREG-1723, reduction of fracture toughness due to irradiation embrittlement is not applicable if the fluence is less than 1.0E17 (n/cm^2).

Management of potential reduction of fracture toughness for Class 1 reactor coolant system and primary pressure boundary CASS components should be based upon a combination of periodic inservice examination and flaw evaluation, in accordance with the provisions of the ASME Code Section XI, IWB-3640 [6], or through the use of justified alternatives, such as the ASME Nuclear Code Case N-481 [7]. Similarly, management of potential reduction of fracture toughness for Class CS reactor internals components should be based on a combination of periodic inservice examination and flaw evaluation, in accordance with the provisions of the ASME Code Section XI, IWB-3520 [6], as supplemented by any examinations necessary to characterize relevant conditions and subsequent indications.

Flaw acceptance criteria can be justified by the license renewal applicant, based upon the arguments contained in this report. Flaw tolerance procedures that use reference flaw sizes, crack growth rates, and elastic-plastic fracture toughness (J-R values) justified by the license renewal applicant may be used to validate the frequency of such periodic examinations, and to define appropriate locations for the examinations. The evaluations should be based on a general, but flexible, procedure that does not impose the use of saturated elastic-plastic fracture toughness data.

The B&W Owners Group Generic License Renewal Program (GLRP) Reactor Coolant System Piping Report [8] identified reduction of fracture toughness as an applicable aging effect for SA 351 Grade CF-8M materials used for the manufacture of valve bodies and bonnets in B&W plants. The components evaluated in Reference 8 were all manufactured from high-molybdenum grade material and were cast statically. Therefore, the screening criteria listed here did not apply. Instead, Reference 8 provided an adapted ASME Code Section XI inservice examination program as the means for managing the effects of thermal aging embrittlement for the CASS components that were evaluated. This program contains inservice examination and flaw evaluation elements that are essentially equivalent with the second portion of the approach outlined above for managing thermal aging embrittlement effects for CASS components.

Both the approach cited in the B&W Owners Group GLRP and the approach presented in this report are based upon the observation that the fracture toughness of some austenitic stainless steel welds, especially those for Type 316 submerged-arc weld (SAW) metal, is comparable to the lower-bound fracture toughness for aged SA 351 CF-8M castings. This comparison is helpful, since Type 316 SAW metal fracture toughness properties were used to help develop the evaluation procedures and acceptance criteria for austenitic stainless steel piping contained in the ASME Code Section XI, IWB-3640 [9].

This report has three purposes. One is to provide the technical justification for the CASS thermal aging embrittlement screening criteria proposed above for simplifying the aging management review for Class 1 and Class CS CASS components for which the effects of embrittlement may be potentially significant. These screening criteria are based on molybdenum content, casting type, and delta ferrite content. In addition, a more conservative approach is provided for those license renewal applicants for whom measurement or calculation of delta ferrite content is not feasible, either because of the lack of measurements or the lack of appropriate material chemistry data. The screening criteria will permit scarce industry resources to be concentrated on those components that truly require further evaluation of potentially significant thermal aging embrittlement effects.

The second purpose is to document the comparison of the limiting fracture toughness data for Type 316 SAW welds and the lower-bound fracture toughness data reported for high-molybdenum, high-delta-ferrite, statically-cast CASS materials in References 3 and 11. The successful comparison of fracture toughness data for SAW/SMAW welds with data for high-molybdenum, statically-cast, high-delta-ferrite CASS material would provide the justification for applying the evaluation procedures and end-of-life flaw acceptance standards for austenitic stainless steel piping and fitting weldments contained in IWB-3640 to CASS components.

The third purpose is to compare the proposed screening criteria and thermal aging embritlement effects management program elements with the evaluation carried out by NRC staff and reported in Reference 17. Reference 17 provides the basis for acceptance by the NRC staff of the approach outlined above and virtually all of the detailed elements of the approach. The slight differences between this approach discussed here and the approach accepted by the NRC staff are pointed out in the text of this report.

2
MATERIAL CONSIDERATIONS

2.1 Importance of Delta Ferrite and Casting Method

Thermal aging embrittlement in duplex stainless steels manifests itself microstructurally as a combination of precipitation/growth of carbides and nitrides in the boundaries between the ferrite and austenite phases, and by deleterious changes in the cleavage fracture resistance of the ferrite phase itself [3]. Therefore, the time-temperature dependency of the loss of fracture toughness is associated with the kinetics of phase boundary precipitation and ferrite phase transformation, and with those material constituents (e.g., ferrite formers) that promote these processes. In particular, if the amount of delta ferrite and brittle phase boundary portion of the material matrix is sufficient, a continuous microstructural fracture path can develop that leads to reduced fracture toughness. These effects eventually saturate when the driving potential falls below the threshold for diffusion-controlled precipitation and growth of brittle phase. Macrostructural studies of thermally-embrittled CASS materials have enhanced understanding of the processes involved.

Reference 3 provides an excellent review of the available data on the issue. Although the discussion is inconclusive about the engineering significance of these data, Figure 2-1 (Figure 2 from Reference 3) is instructive. This figure shows the effect of delta ferrite content, and aging temperature and time, on a crude measure of fracture toughness, the impact energy at room temperature. The 6 percent delta ferrite impact energy after aging for 560,000 hours (60 years) is between 60 and 220 J (45 and 160 ft-lb), depending upon aging temperature, while the 14 percent delta ferrite impact energy after aging for 560,000 hours is between 20 and 200 J (15 and 150 ft-lb). The 40 percent delta ferrite values are well below the 6 and 14 percent values. Data at intermediate delta ferrite levels are not shown. The inference to be drawn is that, for an assumed significance threshold of 50 ft-lb at around 500,000 hours of service at temperature, an impact energy for 6% delta ferrite material is acceptable; however, a relatively small number of 14% delta ferrite components may be affected and components with 40% delta ferrite require some form of evaluation.

The data summarized in Reference 3 were based on 10 heats of SA 351 material: (1) Heat P1, a centrifugally-cast pipe of Grade CF-8; (2) Heat 68, a statically-cast slab of Grade CF-8; (3) Heat P2, a centrifugally-cast pipe of Grade CF-3; (4) Heat I, a statically-cast pump impeller of Grade CF-3; (5) Heat 69, a statically-cast slab of Grade CF-3; (6) EPRI Heat, a statically-cast plate of Grade CF-3; (7) Heat 75, a statically-cast slab of Grade CF-8M; (8) Heat 205, a centrifugally-cast pipe of Grade CF-8M; (9) Heat 758, a statically-cast elbow of Grade CF-8M; and (10) Heat L, a statically-cast plate of Grade CF-8M. The calculated delta ferrite levels for these heats were 18%, 15%, 12%, 20%, 21%, 36%, 25%, 21%, 24%, and 19%, respectively. Therefore, the detailed evaluation included three centrifugally-cast and seven statically-cast heats with a wide range of delta ferrite levels. The data are characterized here and in Table 2-1.

This characterization is based on a comparison between the predicted and measured unaged and fully-aged (saturated) crack growth resistance (J-R) curves as shown in Figures 2-2 through 2-11 (Figures 8 through 17 of Reference 11). For comparison purposes, the threshold level of marginal crack growth resistance is chosen to be about 255 kJ/m^2 (1450 in-lb/in^2) at a crack extension of 2.5 mm (0.1 in). This threshold is based on flaw tolerance calculations described in Appendices A and B, as supplemented by Appendices 9 and 10, plus Attachments E, F and G of the EPRI Cast Austenitic Stainless Steel Sourcebook [12].

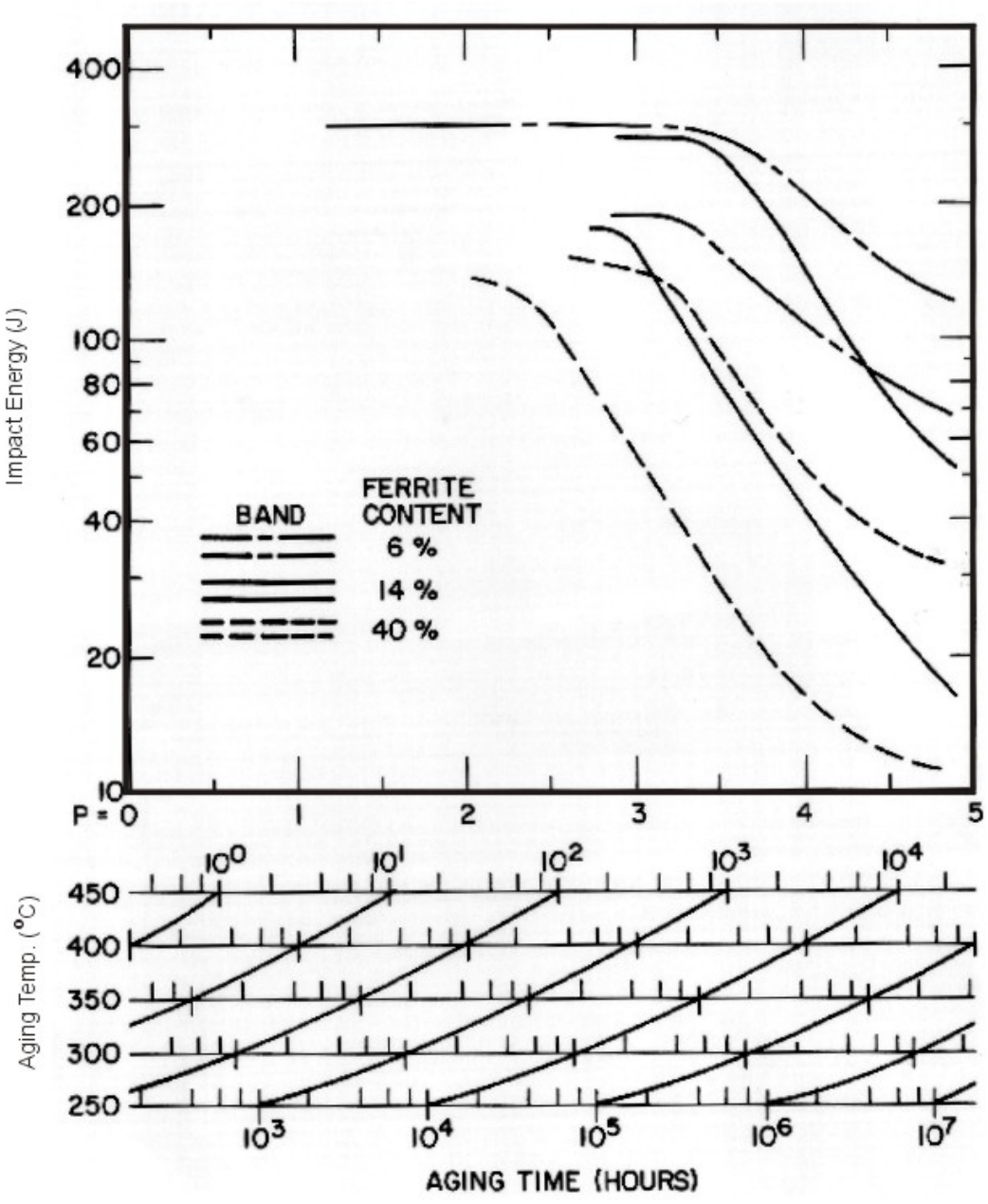

Figure 2-1
Influence of Ferrite Content on the Embrittlement of Cast Austenitic Stainless Steel as a Function of the Aging Parameter P (Figure 2 from Reference 3)

Table 2-1
Characterization of Predicted and Measured Unaged and Fully-Aged Fracture Toughness Data

Heat ID	Grade	Delta Ferrite	Casting Type	Discussion
P1	CF-8	18%	Centrifugally-Cast	Fully-aged data in good agreement with saturation curve at RT, very conservative at 290°C. Saturation curve represents good toughness.
68	CF-8	15%	Statically-Cast	No fully-aged data at 290°C. Saturation curve very conservative with respect to fully-aged data at RT. Good saturation toughness.
P2	CF-3	12%	Centrifugally-Cast	Saturation curves extremely conservative with respect to all fully-aged data. Even saturation curves have good toughness.
I	CF-3	20%	Statically-Cast	No fully-aged data. Saturation curves represent good toughness.
69	CF-3	21%	Statically-Cast	No fully-aged data at 290°C. Fully-aged data at RT in good agreement with saturation curve. Good toughness.
EPRI	CF-3	36%	Statically-Cast	Fully-aged data at RT in good agreement with saturation curve. Saturation curve too conservative at 300°C. Toughness marginal.
75	CF-8M	25%	Statically-Cast	No fully-aged data at 290°C. Fully-aged data at RT is a factor of 2 higher than saturation curve. Actual toughness marginal.
205	CF-8M	21%	Centrifugally-Cast	Saturation curves extremely conservative relative to fully-aged data at RT and 290°C–a factor of almost 3 and 2, respectively. Actual toughness is good.
758	CF-8M	24%	Statically-Cast	Excellent agreement between fully-aged data at RT and 290°C, and saturation curves. Toughness is marginal.
L	CF-8M	19%	Statically-Cast	Excellent agreement between fully-aged data at RT and 320°C, and saturation curves. Toughness is marginal.

Based upon this crack growth resistance threshold and the subsequent characterizations presented in Table 2-1, the predicted saturation toughness (or the actual toughness, as denoted by the data points in Figures 2-2 through 2-11, if the prediction is inaccurate) is marginal only for two situations – statically-cast CF-8M with delta ferrite of at least 19% and statically-cast CF-3 with delta ferrite of 36%. Therefore, it would appear to be conservative to use 20% delta ferrite as the screening value for significance for all cases except for high-molybdenum, statically-cast CF-8M, where a lower value is appropriate. This conclusion is confirmed by Hedgecock [10] who, after reviewing the data and analyses, found that a reasonable threshold value for potentially significant thermal aging embrittlement effects for CASS components was a measured delta ferrite value of 20 percent, by weight. Figure 2-12 (Figure 3-4 from Reference 10) illustrates some of the data upon which this judgment was based.

From these observations, a delta ferrite screening threshold for all materials would appear to be about 30% or greater, with the exception of statically-cast CF-8M. For statically-cast CF-8M, the screening threshold would appear to be 25% or somewhat less. Therefore, a conservative approach would be to use a 20% delta ferrite screening threshold for all materials except statically-cast CF-8M, for which a 14-15% delta ferrite threshold would apply. This conservatism would account for any high-side material chemistry of nitrogen and carbon (potential precipitation agents).

2.2 Importance of Material Chemistry

Further confirmation of the importance of delta ferrite and the additional role of material chemistry is provided by Figure 2-12 (Figure 46 from Reference 3), which shows the minimum impact energy at room temperature as a function of an aging parameter, Φ. Φ is defined by the product of the ferrite spacing, material chemistry, and the square of the measured or calculated ferrite content. The authors of Reference 3 recognized that ferrite spacing would not be a readily-measured parameter, thereby limiting the role of Φ as a useful evaluation measure. However, the remainder of the definition of Φ, including the squared dependency on delta ferrite, seemed to confirm the choice of delta ferrite as a measure for screening, and introduces some elements of material chemistry to the screening criteria, as well.

In later work [11b], ANL provided two new definitions of the aging parameter Φ, one for the higher molybdenum (Mo) bearing grades of CASS material (e.g., SA 351 Grade CF-8M) and another for SA 351 Grades CF-3 and CF-8. The former is given by

$$\Phi = \delta_c (C + 0.4N) (Ni + Si + Mn)^2/5,$$

and the latter is given by

$$\Phi = \delta_c (Cr + Si) (C + 0.4N),$$

where δ_c is the calculated delta ferrite, and Cr, C, N, Ni, Mn, and Si are the weight percentages of chromium, carbon, nitrogen, nickel, manganese, and silicon, respectively, from the material chemistry records.

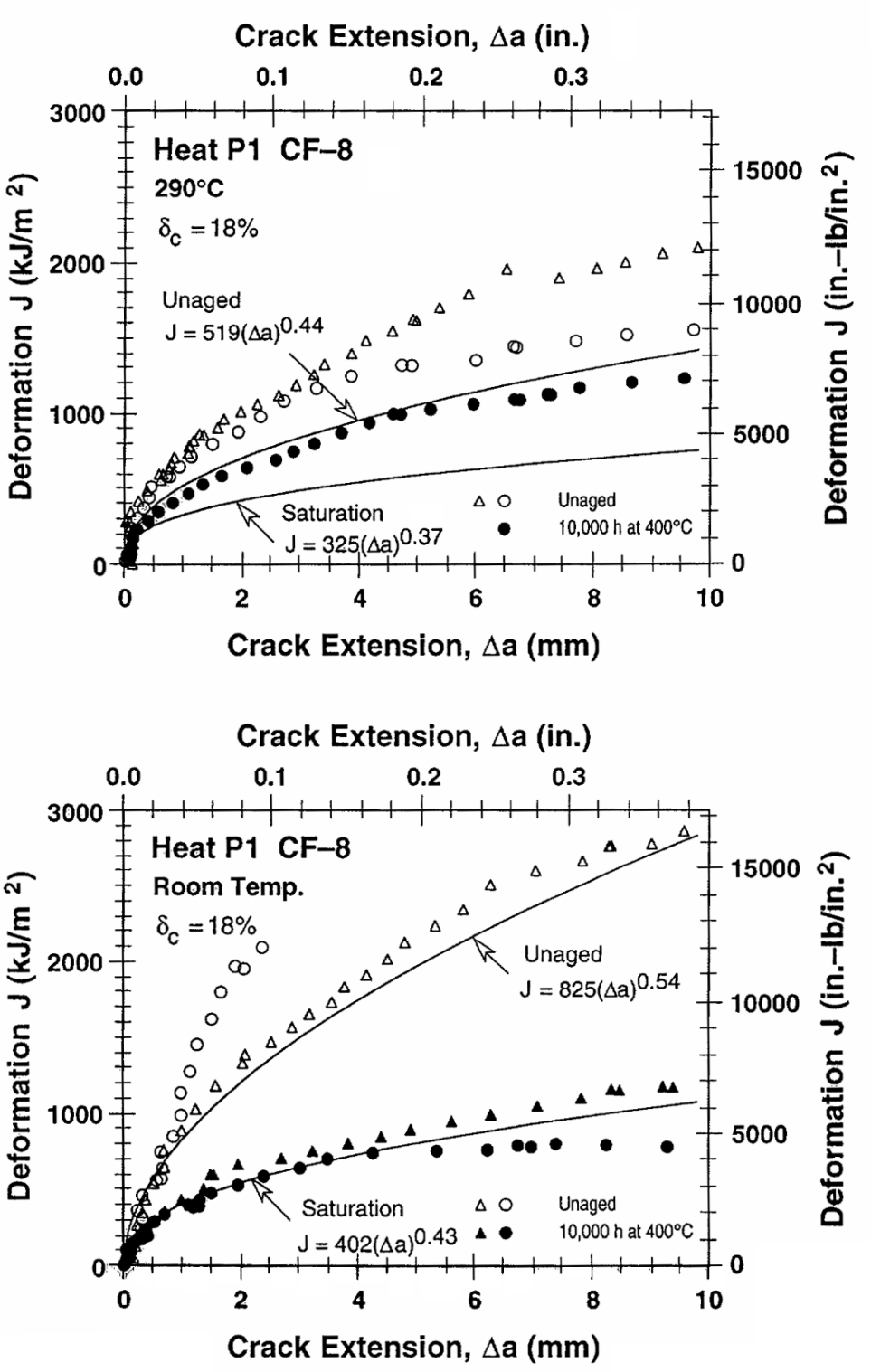

Figure 2-2
Experimental and Estimated J-R Curves for Unaged and Fully-Aged Centrifugally-Cast Pipe of CF-8 Steel (Figure 8 from Reference 11)

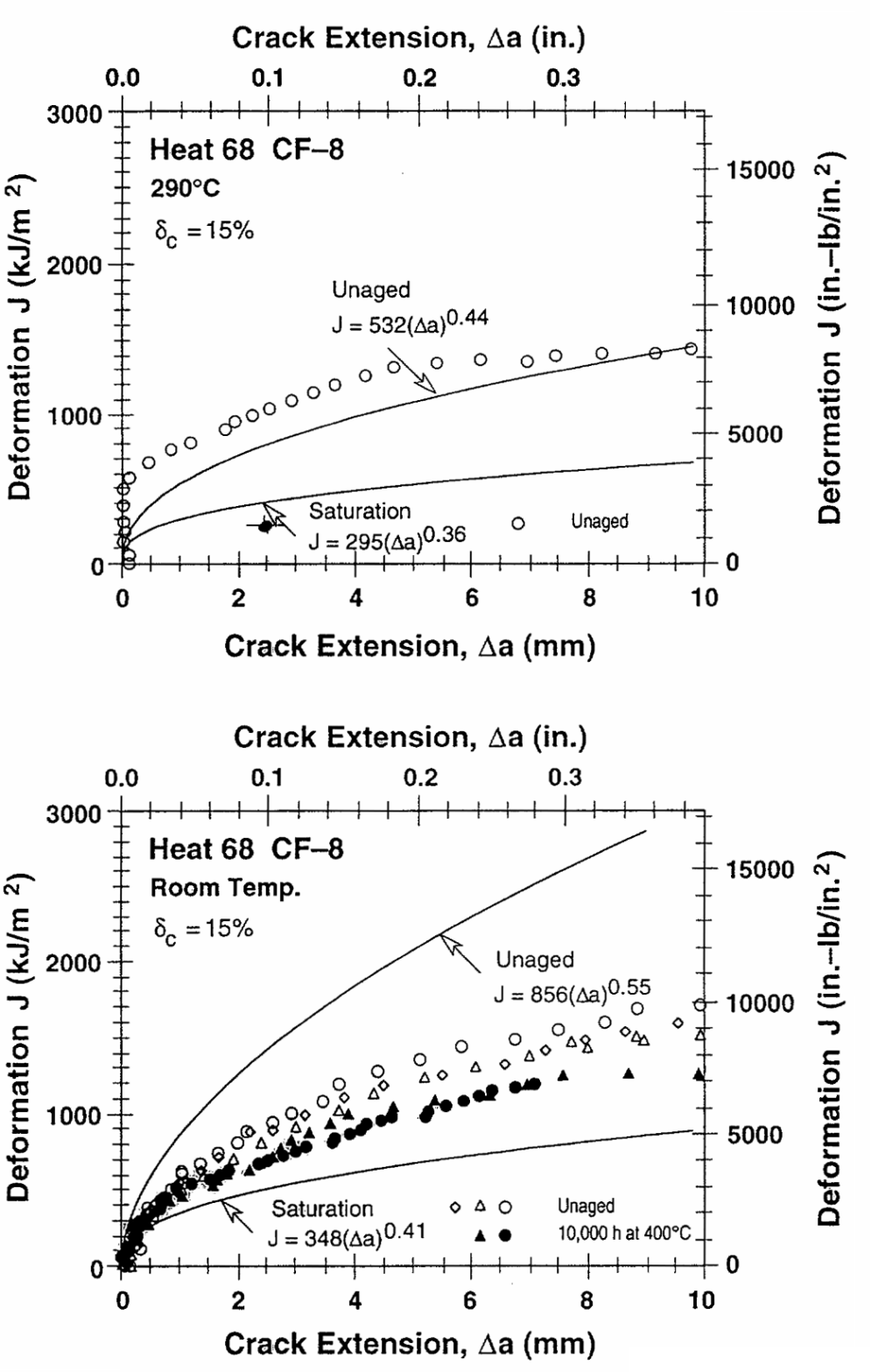

Figure 2-3
Experimental and Estimated J-R Curves for Unaged and Fully-Aged Statically-Cast Slab of CF-8 Steel (Figure 9 from Reference 11)

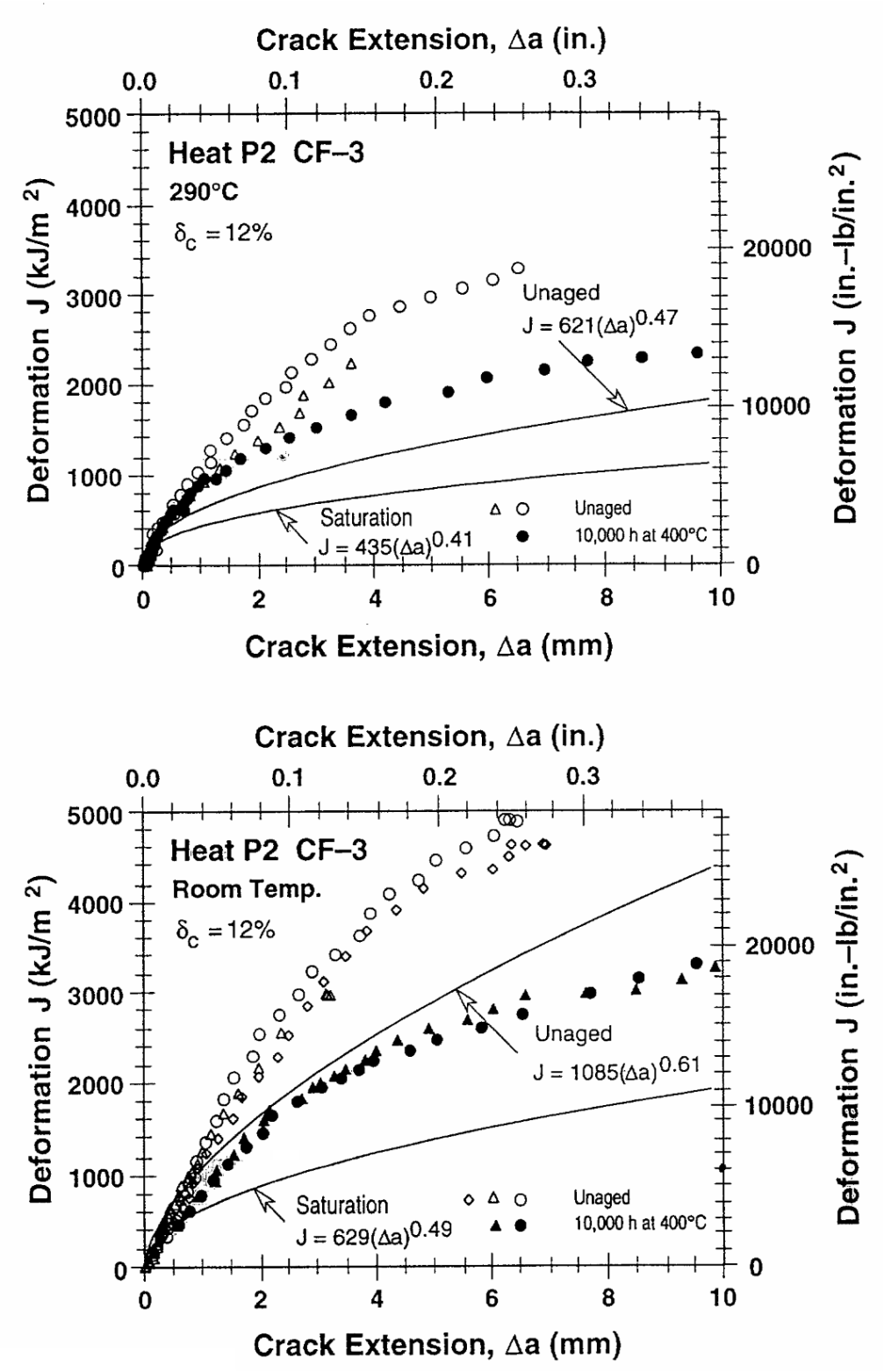

Figure 2-4
Experimental and Estimated J-R Curves for Unaged and Fully-Aged Centrifugally-Cast Pipe of CF-3 Steel (Figure 10 from Reference 11)

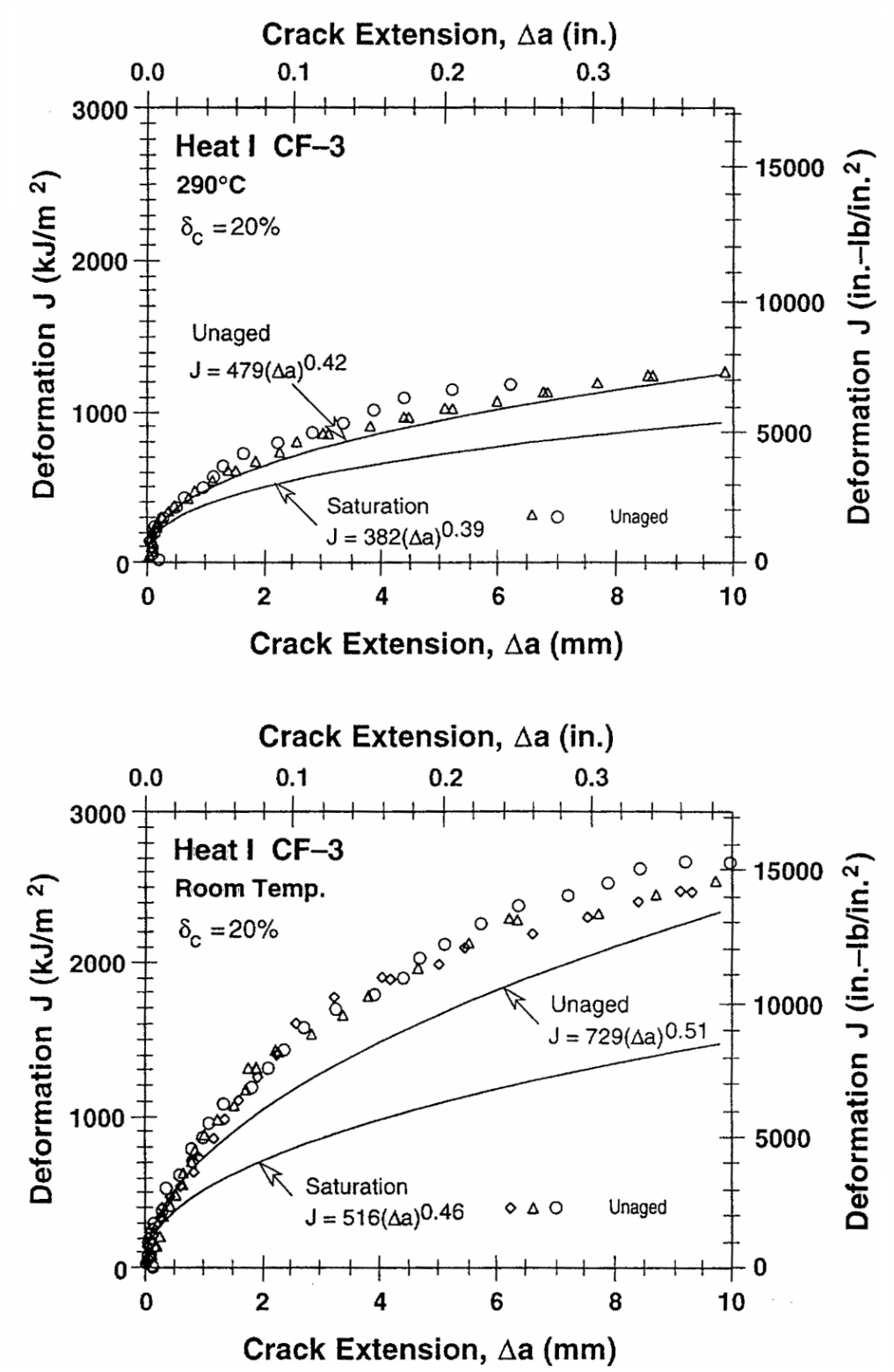

Figure 2-5
Experimental and Estimated J-R Curves for Unaged and Fully-Aged Statically-Cast Pump Impeller of CF-3 Steel (Figure 11 from Reference 11)

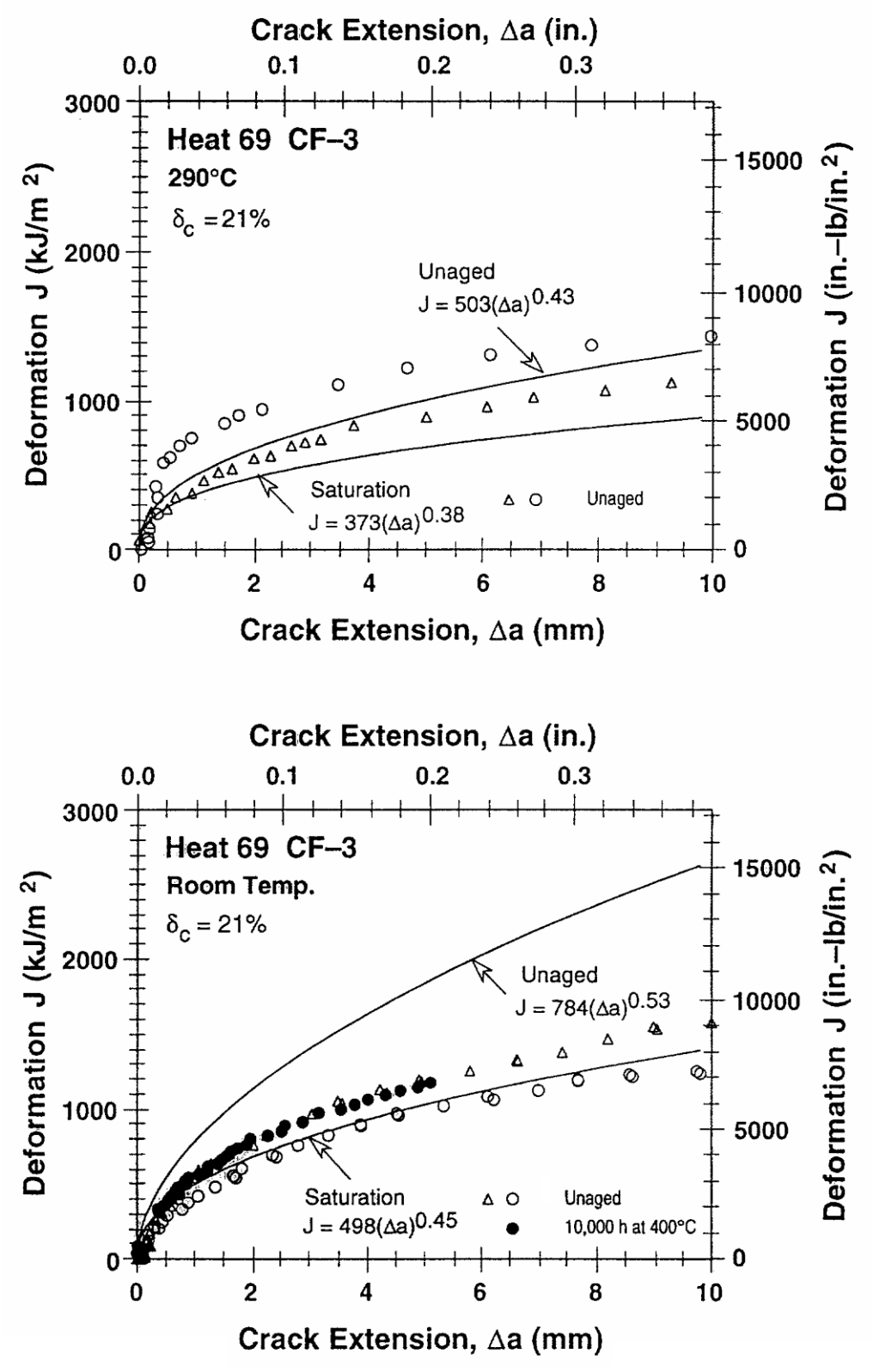

Figure 2-6
Experimental and Estimated J-R Curves for Unaged and Fully-Aged Statically-Cast Slab of CF-3 Steel (Figure 12 from Reference 11)

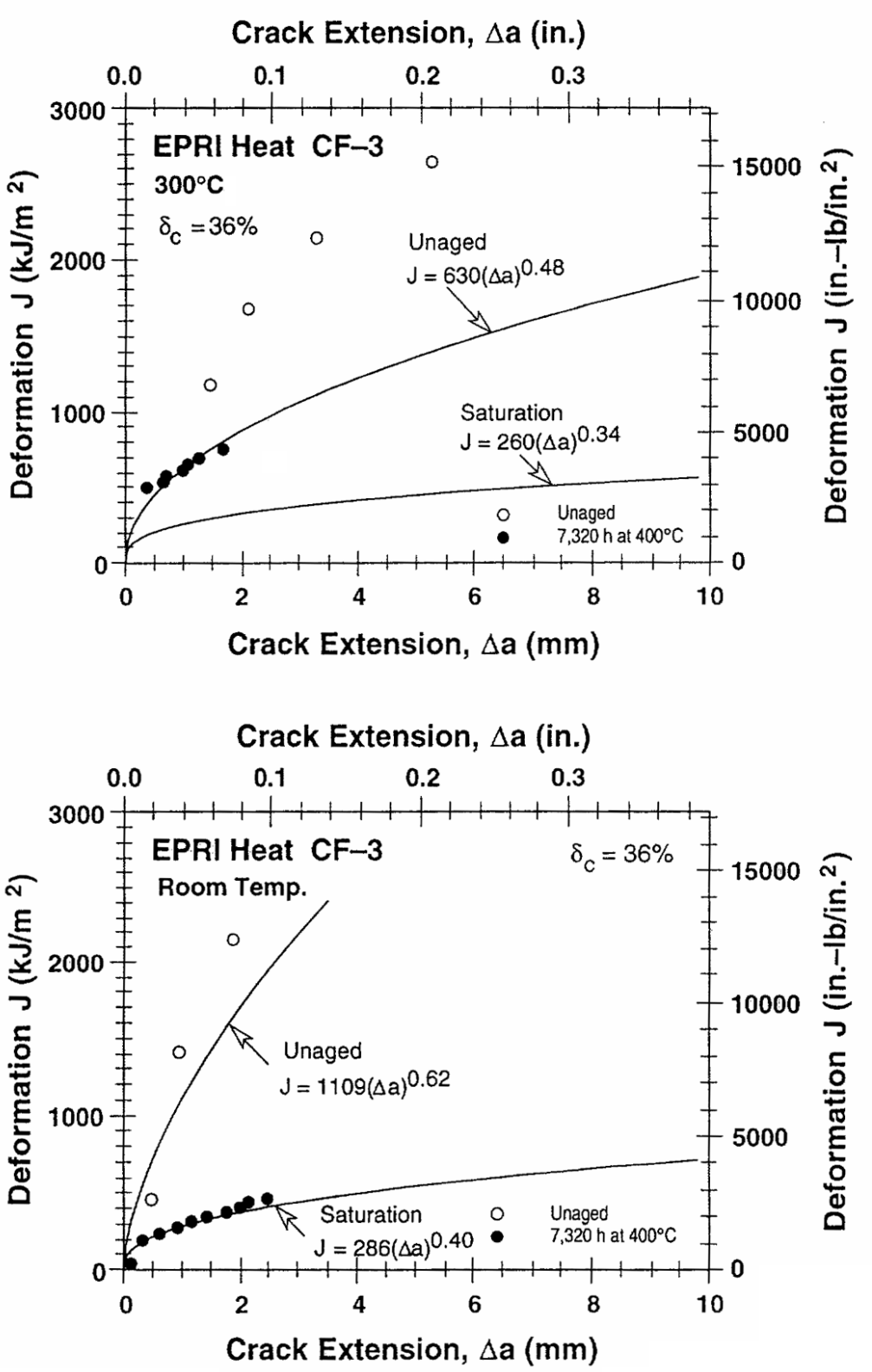

Figure 2-7
Experimental and Estimated J-R Curves for Unaged and Fully-Aged Statically-Cast Plate of CF-3 Steel (Figure 13 from Reference 11)

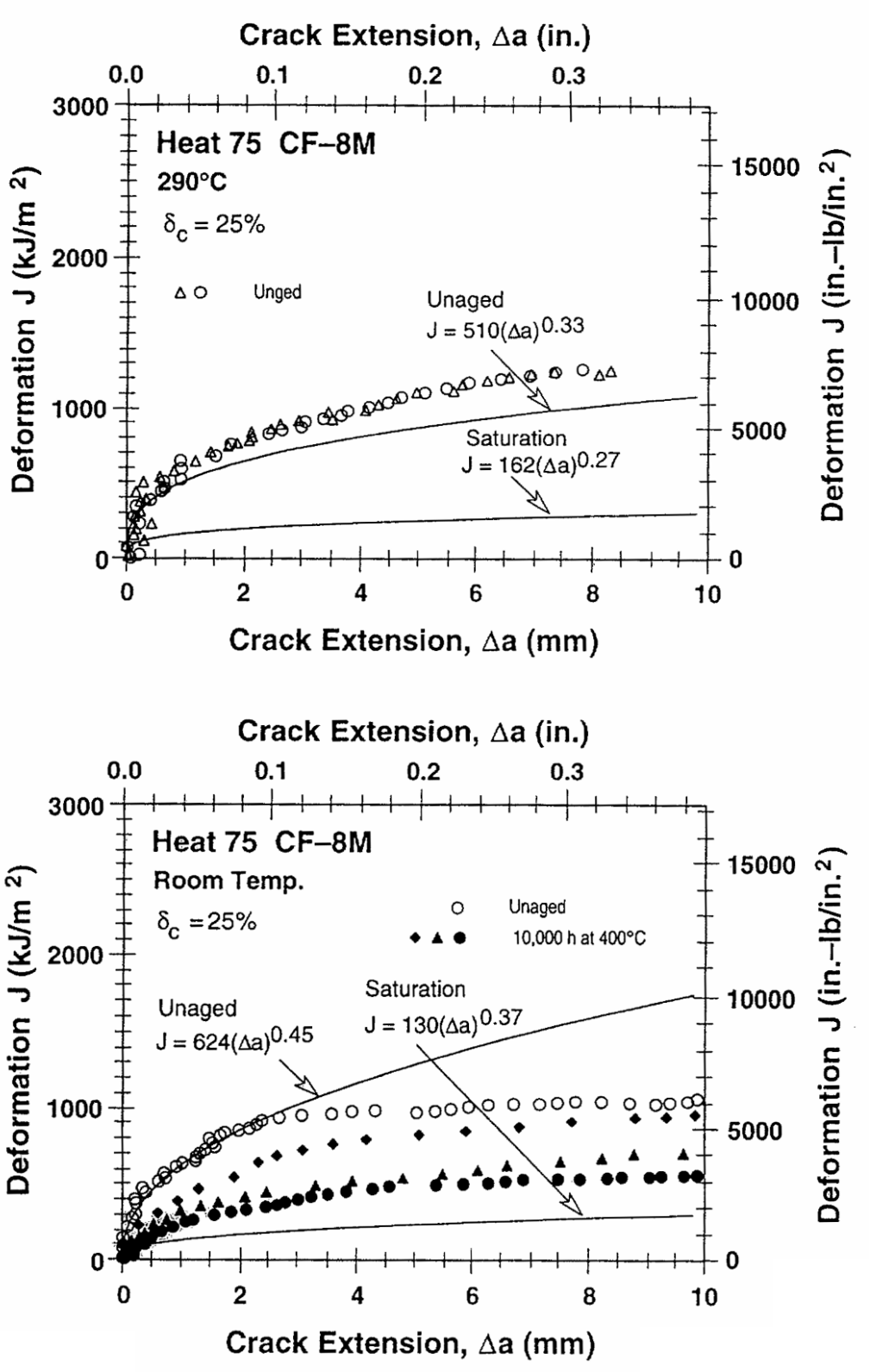

Figure 2-8
Experimental and Estimated J-R Curves for Unaged and Fully-Aged Statically-Cast Slab of CF-8M Steel (Figure 14 from Reference 11)

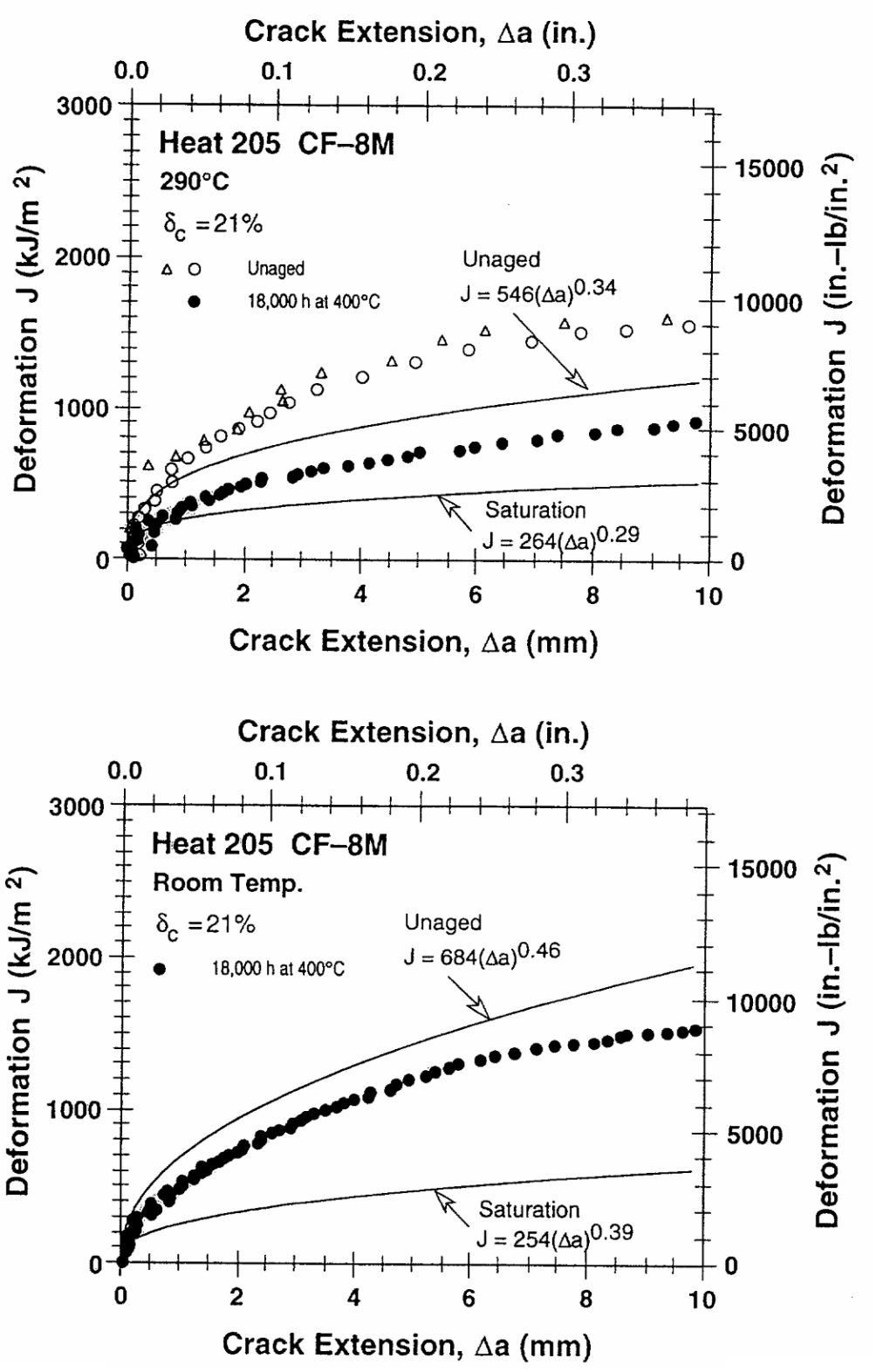

Figure 2-9
Experimental and Estimated J-R Curves for Unaged and Fully-Aged Centrifugally-Cast Pipe of CF-8M Steel (Figure 15 from Reference 11)

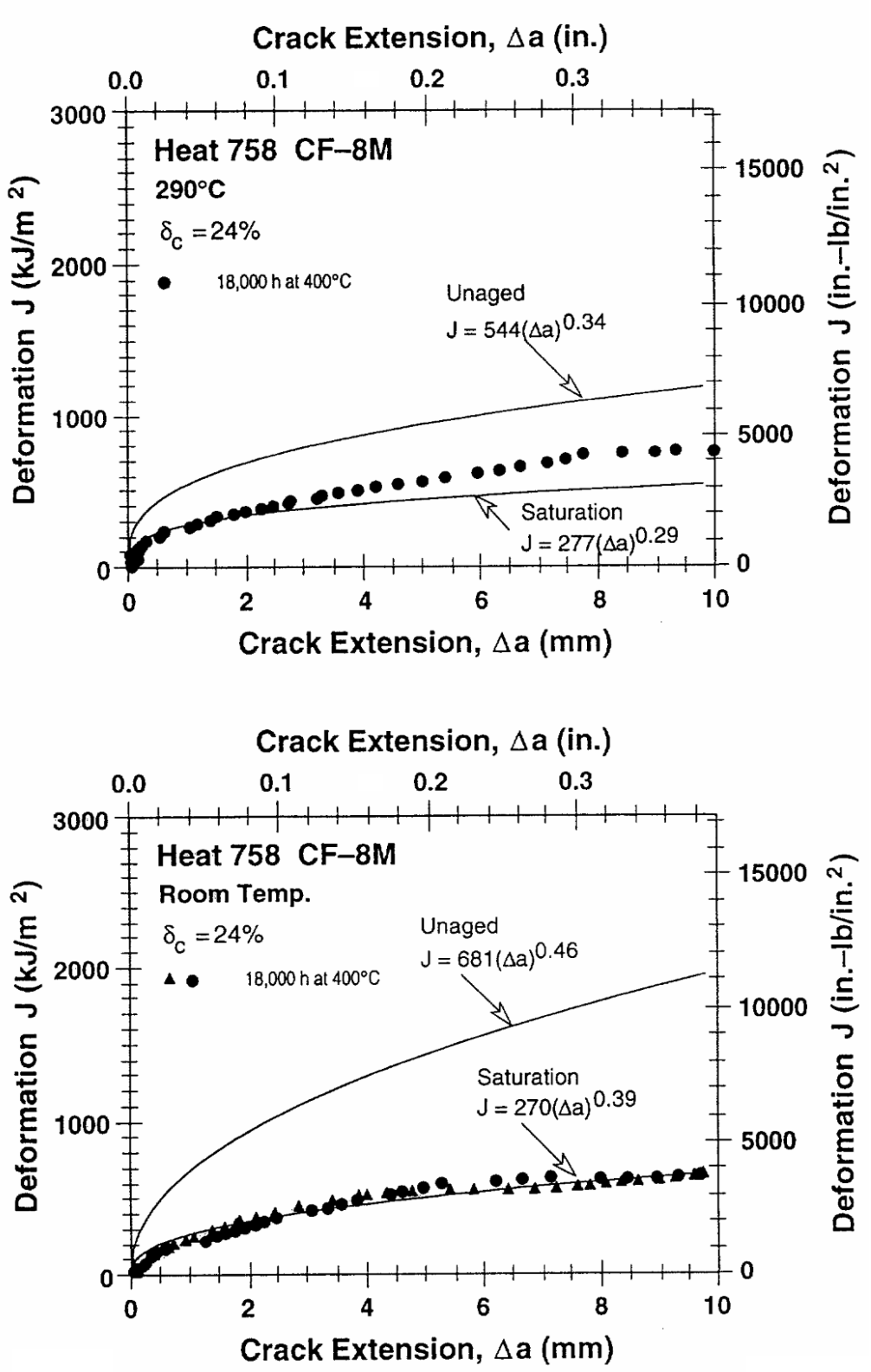

Figure 2-10
Experimental and Estimated J-R Curves for Unaged and Fully-Aged Statically-Cast Elbow of CF-8M Steel (Figure 16 from Reference 11)

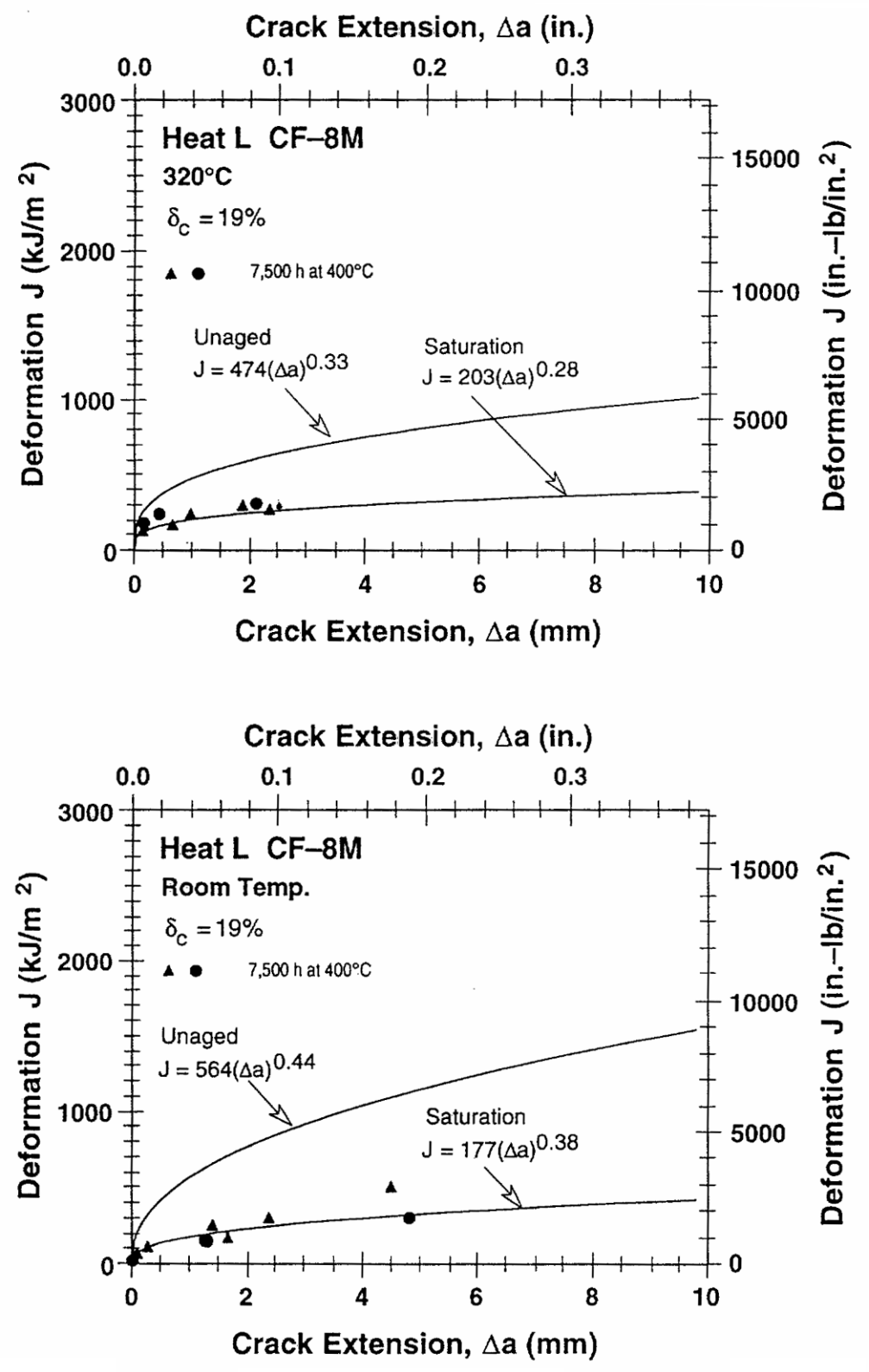

Figure 2-11
Experimental and Estimated J-R Curves for Unaged and Fully-Aged Statically-Cast Plate of CF-8M Steel (Figure 17 from Reference 11)

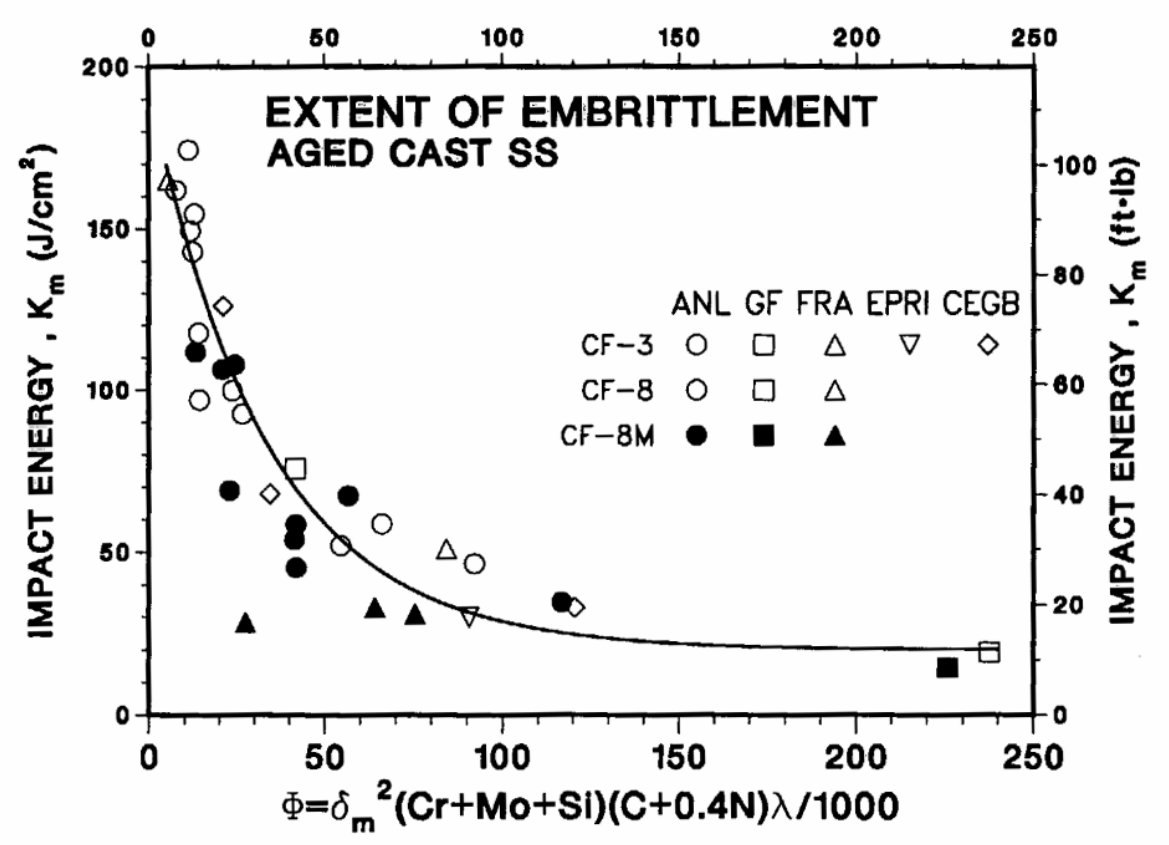

Figure 2-12
Correlation Between Minimum Room Temperature Impact Energy and Material Parameter Φ for Aged Cast Stainless Steel (Figure 46 from Reference 3)

The intent of the factors modifying the delta ferrite content is to further emphasize the ferrite "formers", such as Cr and Si, in the expressions (even though they are already implicitly included in the calculated delta ferrite value), and to explicitly account for nitride/carbide precipitation agents in the correlations. From these expressions, the major items to consider are delta ferrite content and Mo content, with secondary consideration of ferrite formers and precipitation agents.

The conservatism in these expressions for an aging parameter is exposed when they are used for estimating the saturation values of elastic-plastic fracture toughness at room temperature and at service temperatures (290°C - 320°C), in terms of measured saturated impact energies, as shown in Figures 2-2 through 2-11. These figures illustrate that the correlations and their predictive capability are extremely conservative and are accurate only for the worst-case situations (e.g., statically-cast CF-8M material with delta ferrite greater than 20%–see Figure 2-10). For centrifugally-cast product forms, the saturation toughness is very conservative, even for CF-8M with delta ferrite of 21% (see Figure 2-9).

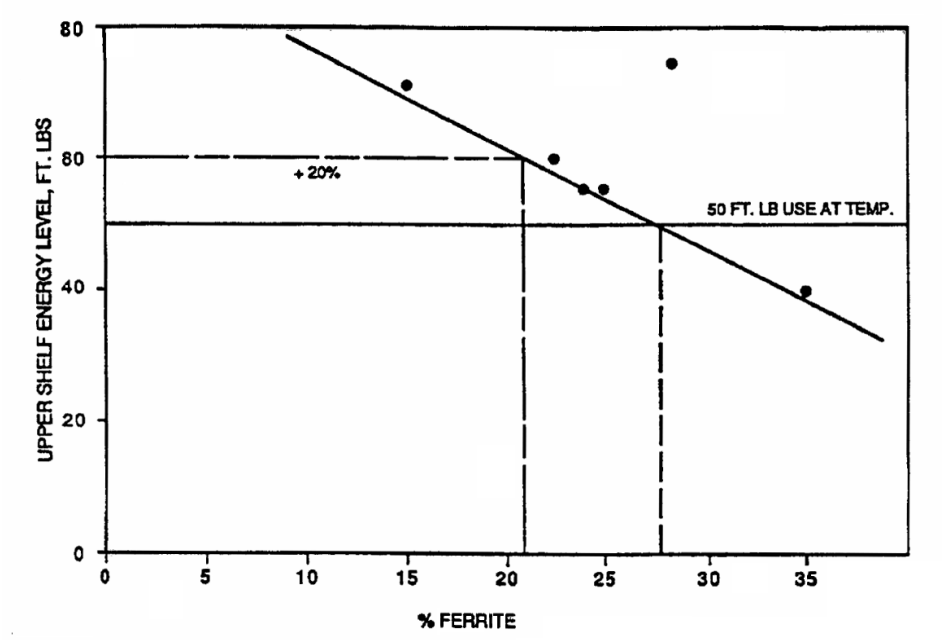

Figure 2-13
Observed Upper Shelf Energy Level as a Function of Delta Ferrite Level (Figure 3-4 from Reference 10)

2.3 Estimation of Fracture Toughness

The estimations contained in Reference 11a reinforce observations derived in Reference 3. The earlier report attempted to calculate intermediate, or partially-aged, fracture toughness data through the use of a chemistry-dependent activation energy, with interpolation between the initial (unaged) and saturation values. Some of the measured data obtained on the heats discussed previously (P1, 68, P2, I, 69, EPRI, and 75) were compared to these interpolated values, along with measured data for two other heats – a CF-8 pump cover plate with a calculated delta ferrite of 28% and Heat C1488, a centrifugally-cast CF-8M pipe with 21% calculated delta ferrite.

In order to provide a basis for the evaluation of a reduction of fracture toughness, a screening crack growth resistance (J-R) value of 255 kJ/m^2 (1,450 in-lb/in^2) at a crack extension of 2.5 mm (0.1 in) was determined, in accordance with the flaw tolerance calculations in Appendix A, Appendix B, and Reference 12. Using this criterion, the results and comparisons from Figures 2-14 through 2-22 (Figures 22 through 30 of Reference 11) are characterized below.

- Heat P1 of centrifugally-cast CF-8 (18% delta ferrite) has more than adequate toughness, even for the conservative predictions. The conservatively predicted saturation toughness at a crack extension of 2.5 mm (0.1 in) is well above 255 kJ/m^2 (1,450 in-lb/in^2) at both room temperature and 290°C (550°F). The actual toughness data are extremely good. ***Therefore, 18% delta ferrite is acceptable for centrifugally-cast CF-8 material, even with the higher carbon (only 0.036 for this heat)***.
- Heat 68 of statically-cast CF-8 (15% delta ferrite) has more than adequate toughness, and the comparison between actual and predicted data is excellent. The predicted saturation toughness at both room temperature and 290°C (550°F) is well above the threshold value.

Clearly, 15% delta ferrite is below the level of concern, and the carbon in this case (0.063%) puts any additional concern about excess carbide precipitation to rest.

- The KRB pump cover (CF-8 with 28% delta ferrite) data show a reasonable comparison between predicted and actual toughness, but the aging time is too short to draw a definitive conclusion. If saturation levels are reached, the crack growth resistance at both room temperature and 290°C (550°F) is very close to 350 kJ/m^2 (2,000 in-lb/in^2) at a crack extension of 2.5 mm (0.1 in), marginal but above the threshold value. ***Therefore, even at 28% delta ferrite, low-molybdenum CASS has adequate toughness.***
- Heat P2 of centrifugally-cast CF-3 (12% delta ferrite) has excellent toughness, but the predicted service toughness is extremely conservative. ***Low-molybdenum, centrifugally-cast material should not need evaluation.***
- Heat I of statically-cast CF-3 (20% delta ferrite) has excellent toughness, and the predictions are in reasonable agreement with actual data. Such material should not require any further evaluation, even with the 20% delta ferrite. ***This provides a measure of demonstration that statically-cast, low-molybdenum material with relatively high delta ferrite content (≥ 20%) could be screened out from further evaluation.***
- Heat 69 of statically-cast CF-3 (21% delta ferrite) has excellent toughness, and the predictions are in good agreement with actual data. Such material should not require evaluation, even with the 21% delta ferrite. ***These data provide an additional measure of demonstration that statically-cast, low-molybdenum material with relatively high delta ferrite content (≥ 20%) could be screened out from further evaluation.***
- The EPRI heat of statically-cast CF-3 (36% delta ferrite) has moderately good toughness at both room temperature and 290°C (550°F), although the conservatively predicted saturated crack growth resistance curves indicate marginal toughness, about 420 kJ/m^2 (2,400 in-lb/in^2) at a crack extension of 2.5 mm (0.1 in). This is still well above the screening threshold value. At operating temperatures of 290°C to 300°C for 56 effective full power years, the actual toughness data are much higher and even more acceptable. Further evaluation should not be required, even with the 36% delta ferrite. ***These data provide a strong argument that, even for high delta ferrite content, low-molybdenum, statically-cast material is more than adequate.***
- The predicted saturation toughness of Heat 75 (statically-cast CF-8M with 25% delta ferrite) is marginal at both room temperature and 290°C (550°F), with a value of about 230 kJ/m^2 (1,300 in-lb/in^2) at a crack extension of 2.5 mm (0.1 in). The actual toughness is somewhat higher, even in the excessively-aged condition, and can probably be shown by evaluation to be fit for continued service unless large flaws exist. ***Evaluation should be required, but the results of any evaluation should be favorable.***
- Heat C1488 of centrifugally-cast CF-8M (21% delta ferrite) has marginal predicted toughness at both room temperature and 290°C (550°F), but excellent actual toughness. The predicted value of 200 kJ/m^2 (1,150 in-lb/in^2) at a crack extension of 2.5 mm (0.1 in) is less than one-half of the measured values at 66 effective full power years (EFPY) of aging. The predictions of saturated behavior seem to have major difficulties with centrifugally-cast material, even with high molybdenum and high delta ferrite. This material should require no further evaluation. ***The actual performance of this material provides strong evidence that***

high-molybdenum, centrifugally-cast material with relatively high delta ferrite content (≥ 20%) can be screened out from further evaluation.

In summary, both the saturated and partially-aged predictions of fracture toughness are very conservative for all but the most extreme cases. The best agreement between prediction and measurement can be found for the statically-cast product forms with high molybdenum content. The comparison also shows that, for statically-cast CF-3 and CF-8 material, the predicted elastic-plastic fracture toughness is in moderate agreement and very conservative relative to saturation toughness, except for very high delta ferrite (36%). Statically-cast material with delta ferrite levels of 15%, 20% and 21% (at 290°C) show little aging out to equivalent service times of 44 EFPY, 43 EFPY and 21 EFPY, respectively.

Collectively, these comparisons show that, when compared to flaw tolerance elastic-plastic fracture toughness thresholds of real concern, which are of the order of 255 kJ/m^2 (1,450 $in\text{-}lb/in^2$), the fracture toughness of CASS materials operating under typical service conditions for both the current and the license renewal terms is more than adequate. The only exceptions are those extreme combinations of high-molybdenum and high delta ferrite material, or moderately high delta ferrite, statically-cast material that the screening criteria are intended to identify.

It should be noted that, based upon a review of the literature, including data from Reference 2, the effects of high loading rate are not significant, and therefore do not affect these conclusions. In Reference 2, fracture toughness results were presented for both as-cast and aged CF-3 and CF-8 material with between 30 and 40% delta ferrite content. The data are obtained at three different loading rates, termed “quasi-static”, “intermediate”, and “impact.” No significant difference in fracture toughness as a function of loading rate was observed.

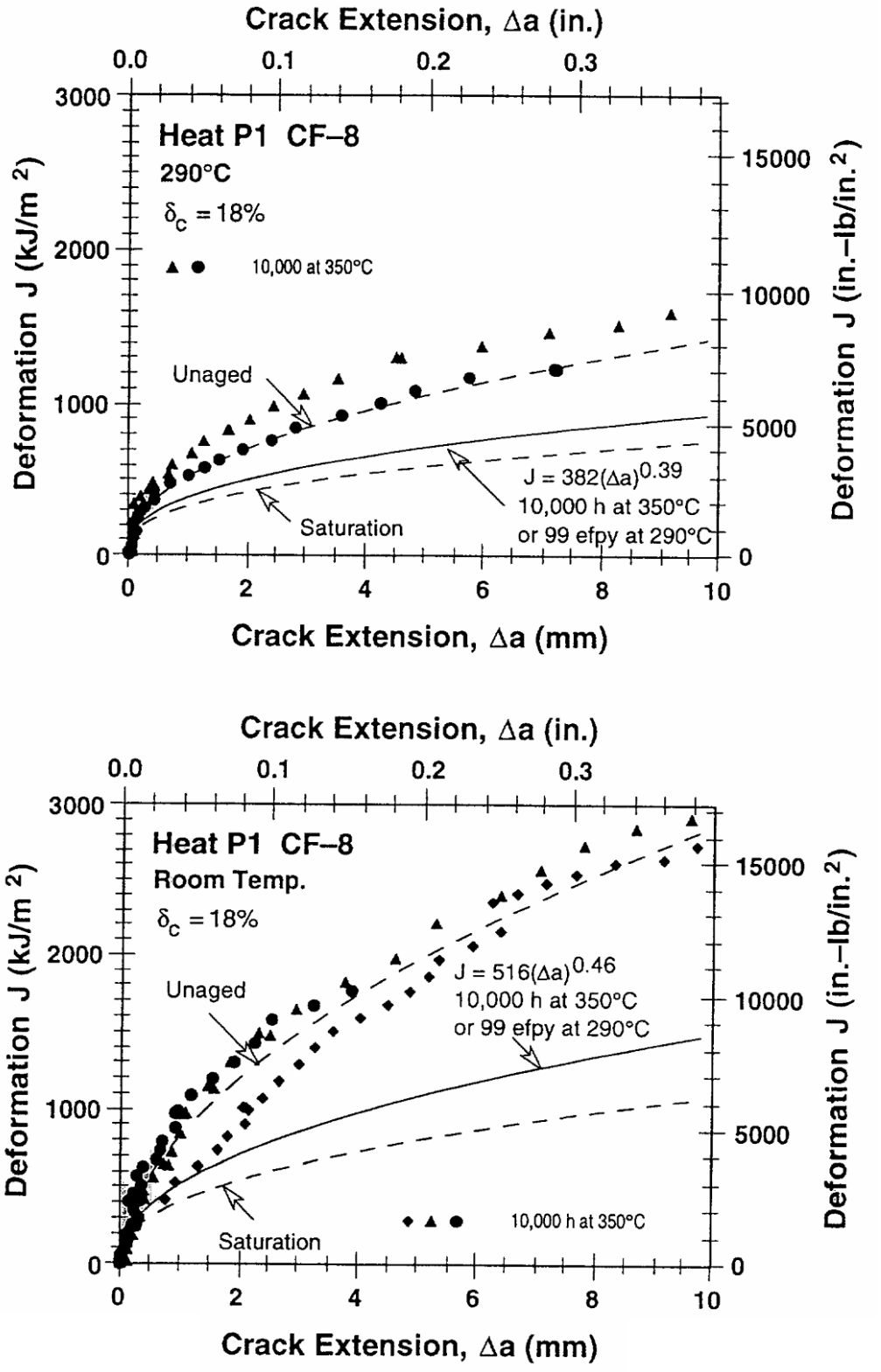

Figure 2-14
Experimental and Estimated J-R Curves for Partially-Aged Centrifugally-Cast Pipe of CF-8 Steel (Figure 22 from Reference 11)

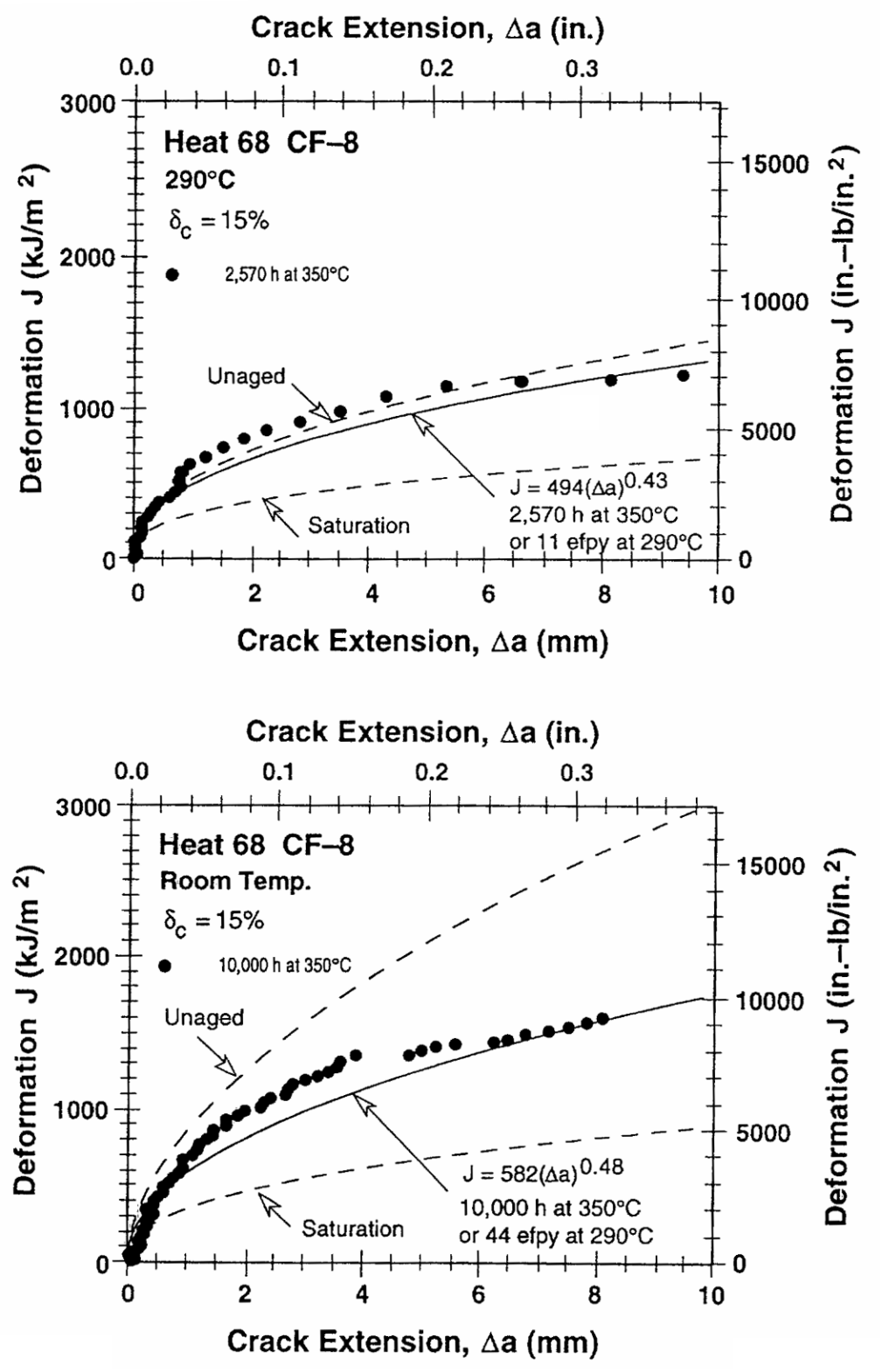

Figure 2-15
Experimental and Estimated J-R Curves for Partially-Aged Statically-Cast Pipe of CF-8 Steel (Figure 23 from Reference 11)

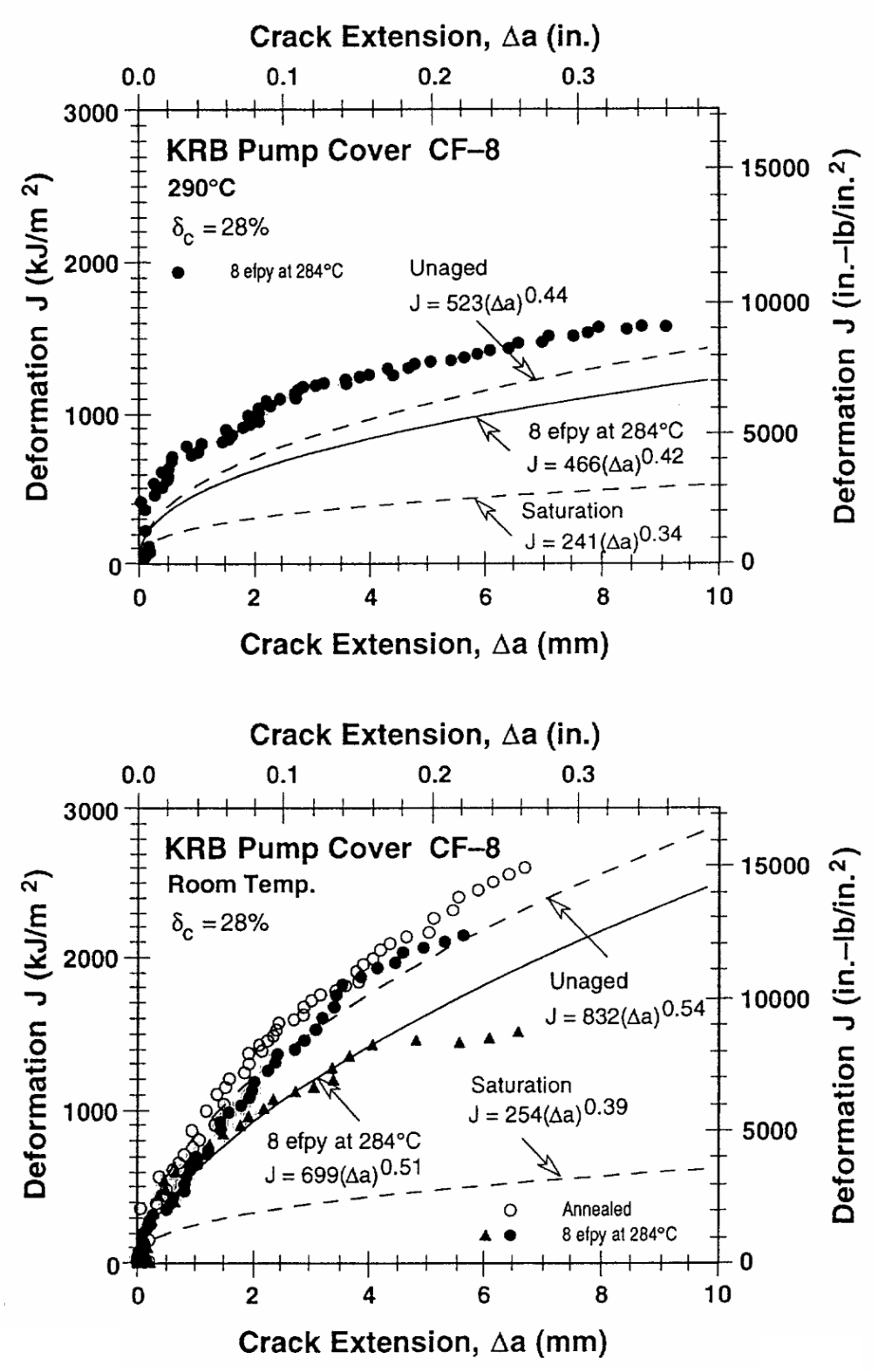

Figure 2-16
Experimental and Estimated J-R Curves for Partially-Aged Pump Cover Plate of CF-8 Steel (Figure 24 from Reference 11)

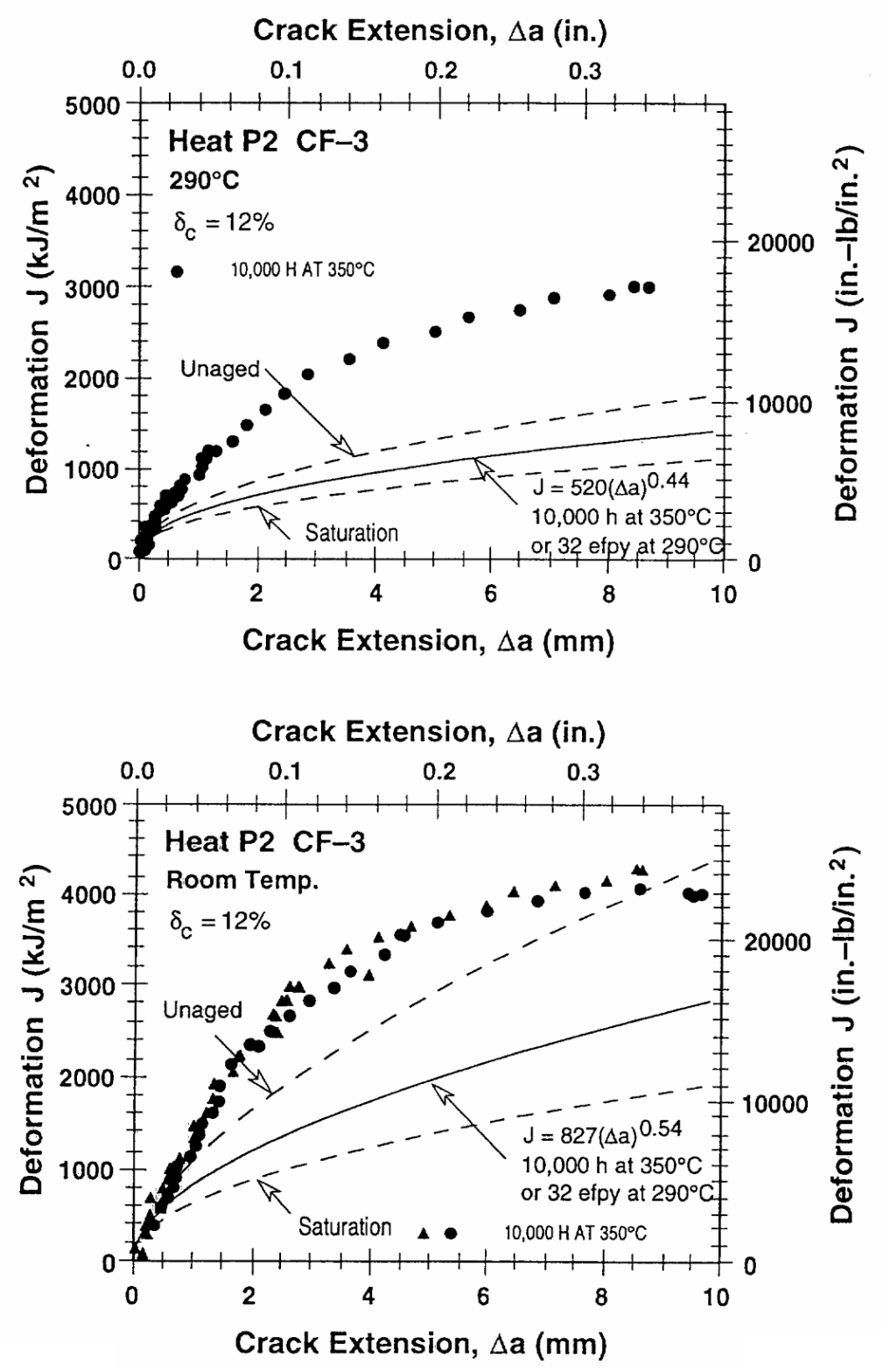

Figure 2-17
Experimental and Estimated J-R Curves for Partially-Aged Centrifugally-Cast Pipe of CF-3 Steel (Figure 25 from Reference 11)

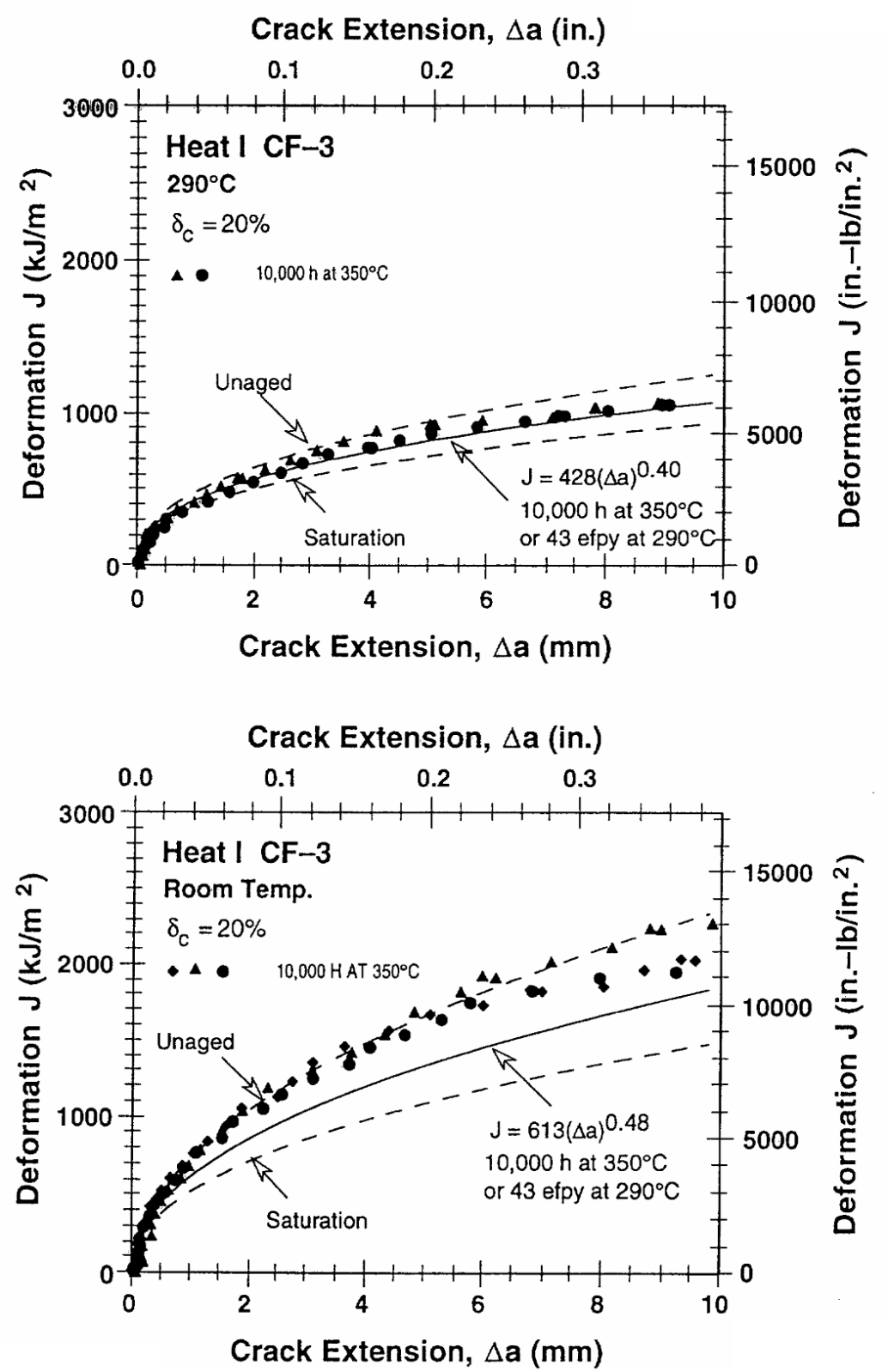

Figure 2-18
Experimental and Estimated J-R Curves for Partially-Aged Statically-Cast Pump Impeller of CF-3 Steel (Figure 26 from Reference 11)

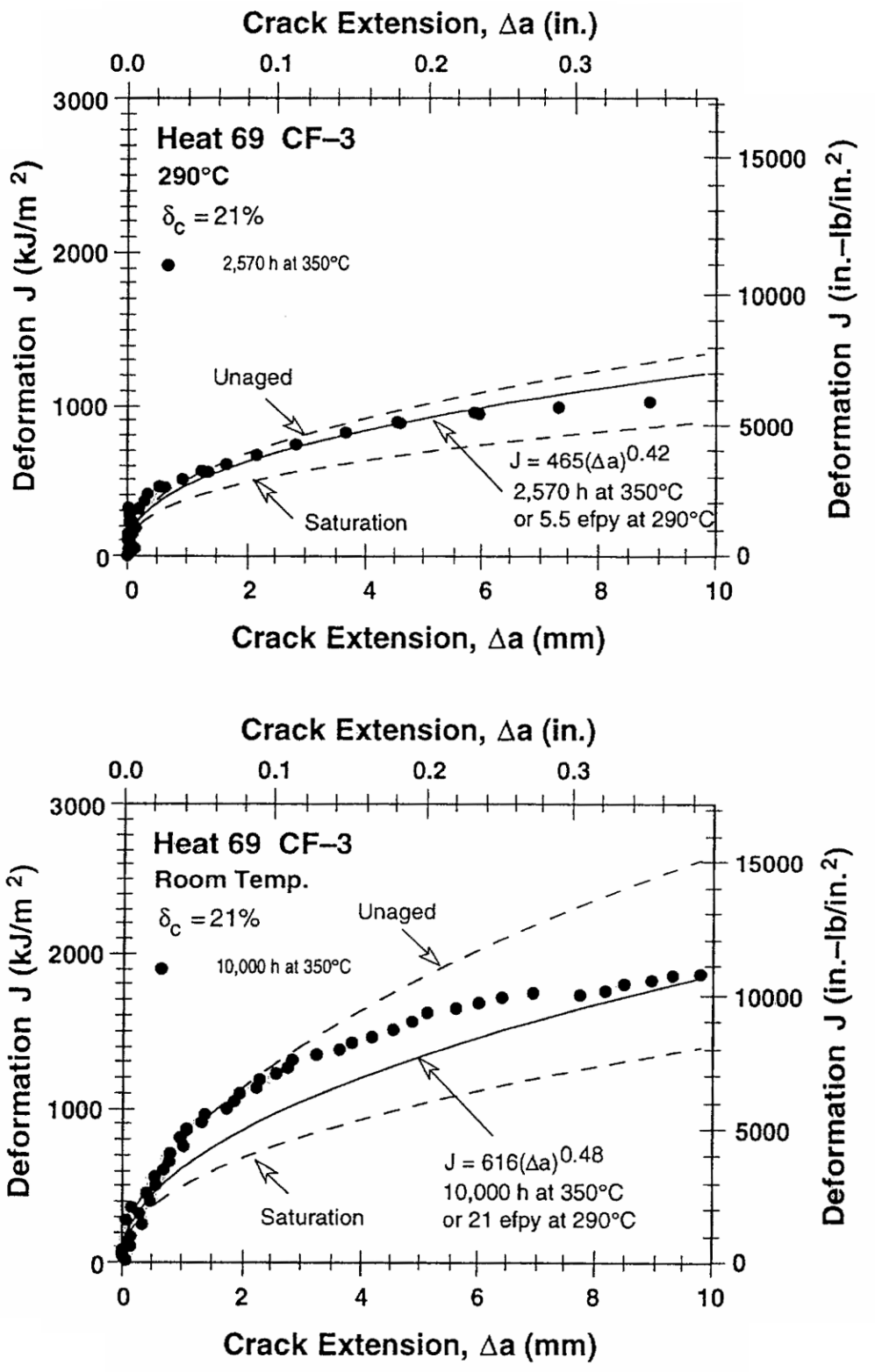

Figure 2-19
Experimental and Estimated J-R Curves for Partially-Aged Statically-Cast Slab of CF-3 Steel (Figure 27 from Reference 11)

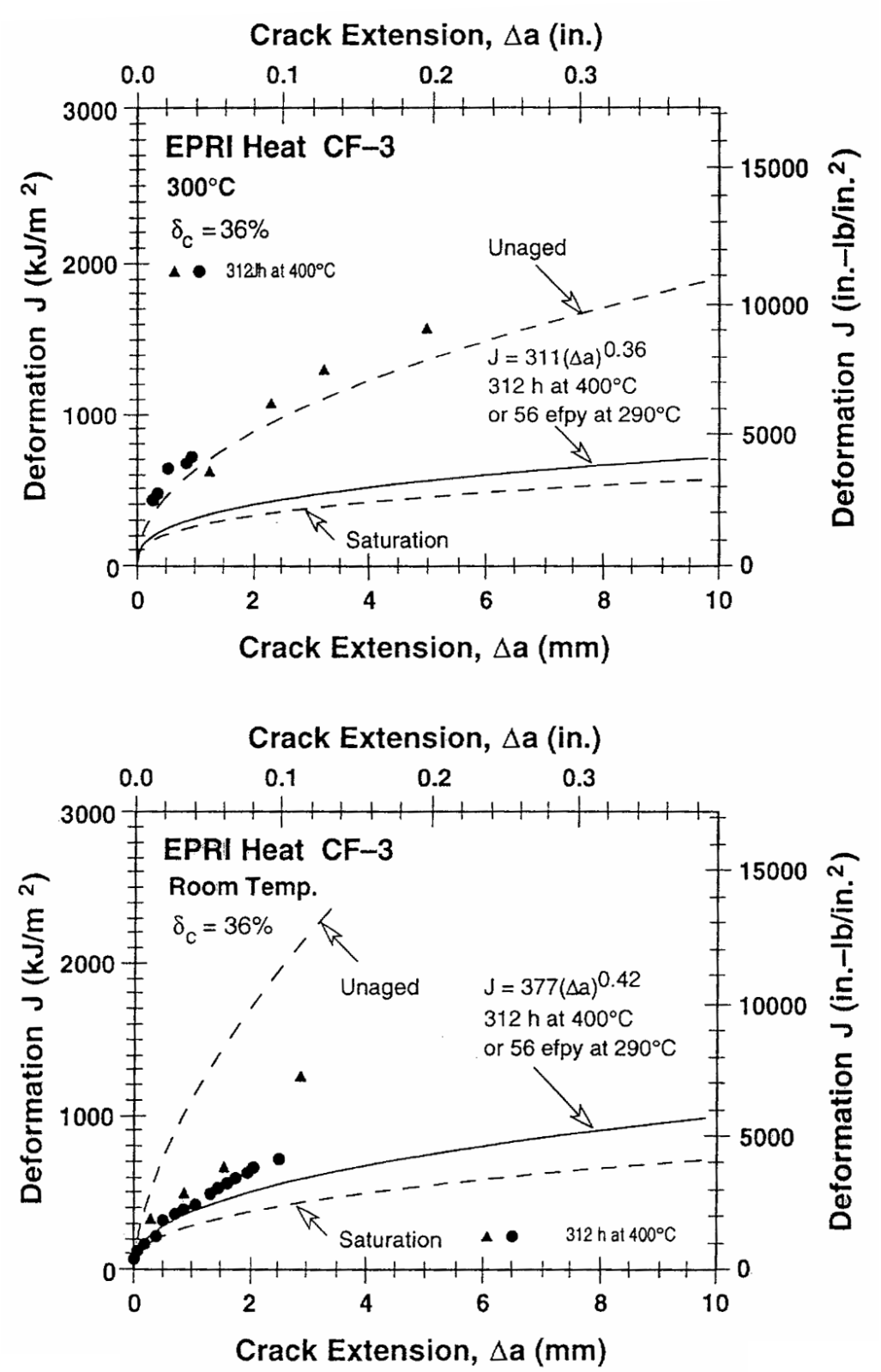

Figure 2-20
Experimental and Estimated J-R Curves for Partially-Aged Statically-Cast Plate of CF-3 Steel (Figure 28 from Reference 11)

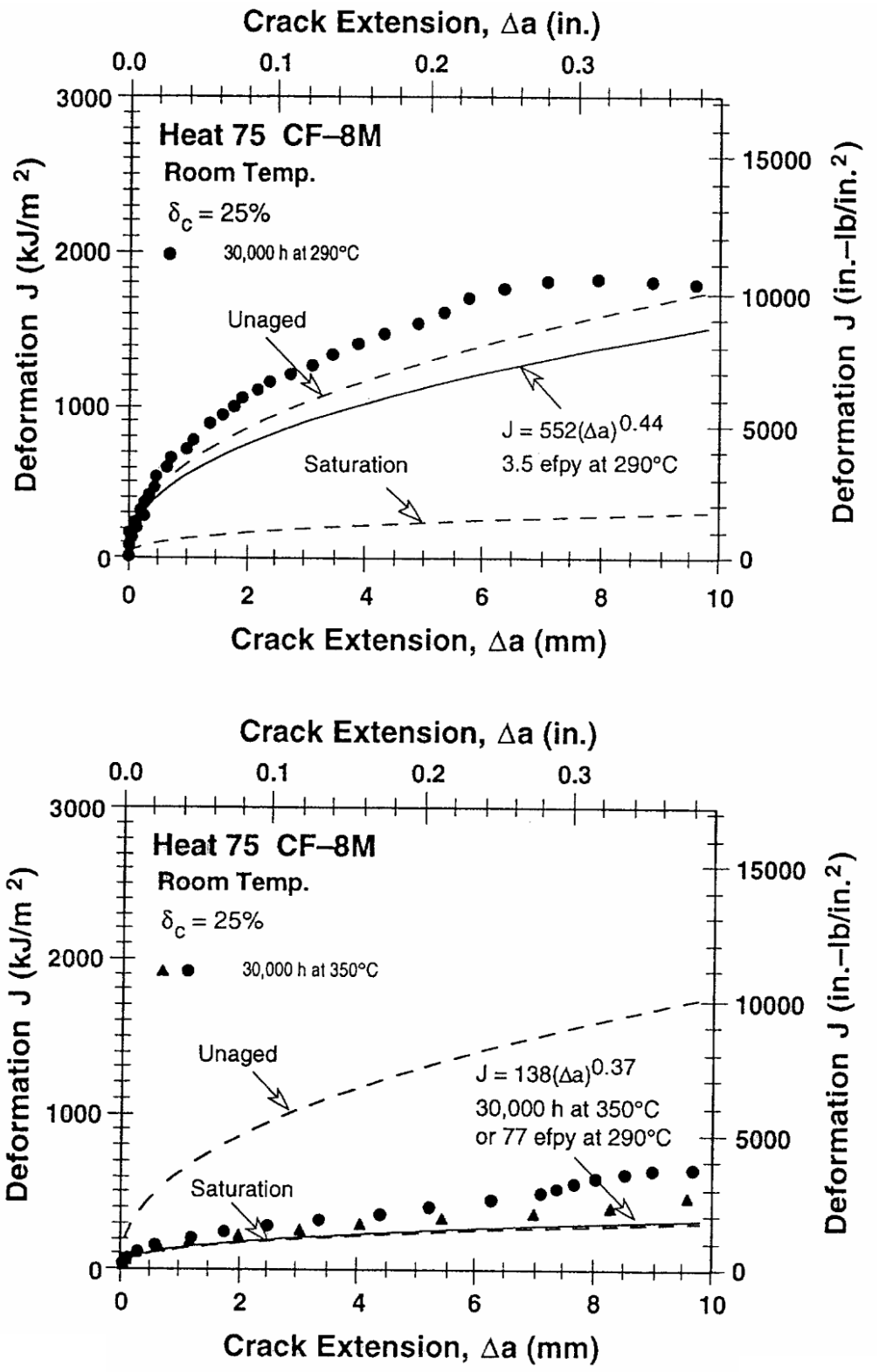

Figure 2-21
Experimental and Estimated J-R Curves for Partially-Aged Statically-Cast Slab of CF-8M Steel (Figure 29 from Reference 11)

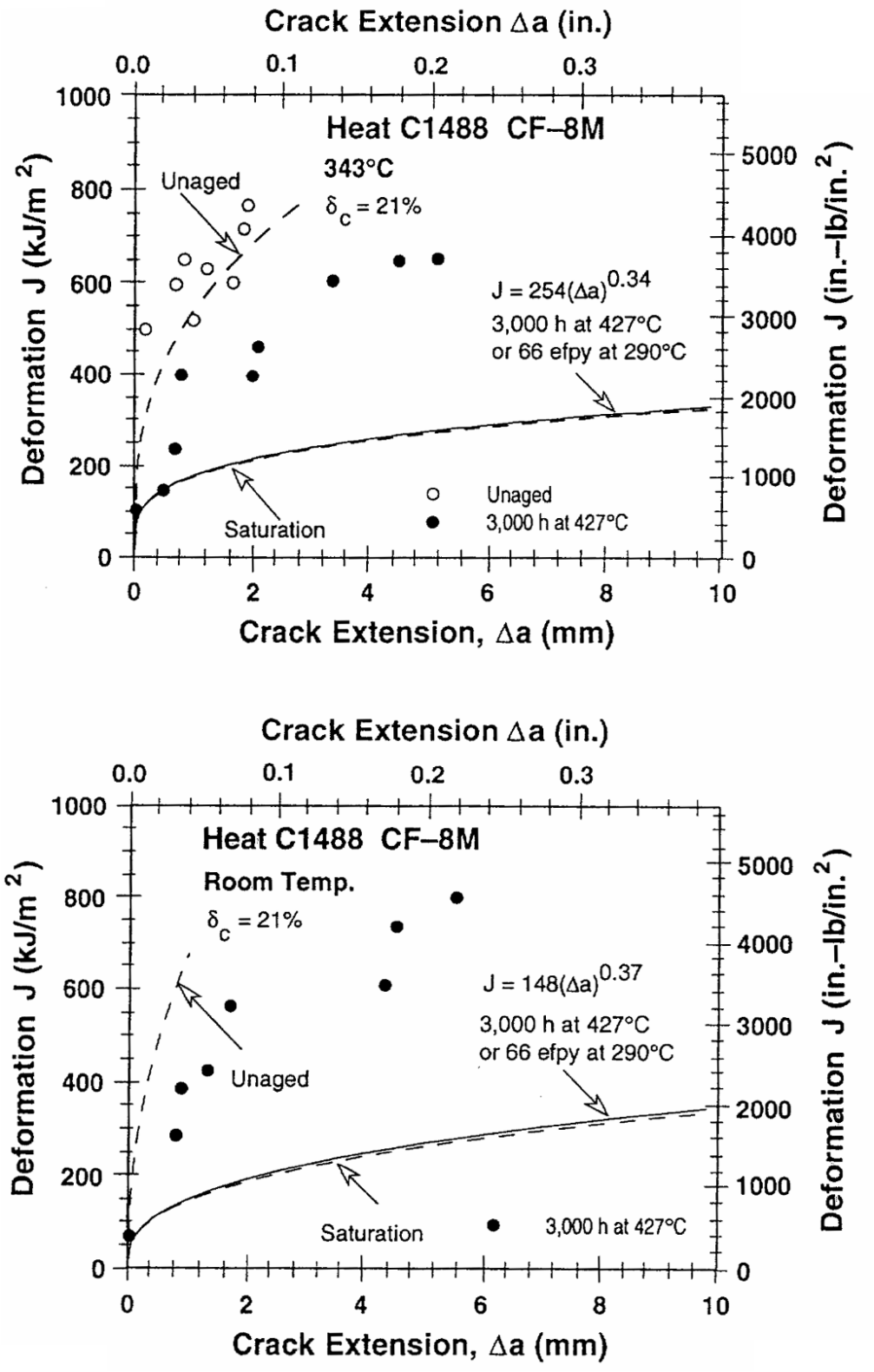

Figure 2-22
Experimental and Estimated J-R Curves for Partially-Aged Centrifugally-Cast Pipe of CF-8M Steel (Figure 30 from Reference 11)

2.4 Comparisons to Fracture Toughness of Weldments

A comparison of fracture toughnesses for aged CASS material and those for austenitic stainless steel weld metal is instructive. Mills [13] has offered a microstructural explanation for the lower toughness of submerged-arc welds (SAW) and shielded-metal-arc welds (SMAW), relative to gas-tungsten-arc welds (GTAW), that explains the microstructural changes in CASS materials during thermal aging embrittlement, as well. He observed that the failure mode for all of the welds was a dimple rupture mechanism, but that the SAW and SMAW failures were initiated by a combination of decohesion of second-phase particles of manganese silicide and local rupture/decohesion of delta ferrite particles. Using a composite plot of fracture toughness data, as shown in Figure 2-23 (Figure 11 from Reference 13), he suggested lower-bound J_c values for SAW, SMAW and GTAW at 427°C (800°F) to 538°C (1000°F) of 40, 70, and 230 kJ/m^2 (228, 400, and 1300 in-lb/in^2), respectively. At 24°C (75°F) the recommended lower-bound values of J_c were 100 kJ/m^2 (571 in-lb/in^2) for SAW and SMAW, and 350 kJ/m^2 (2000 in-lb/in^2) for GTAW.

Jaske and Shah [14], in their review of available fracture toughness data for aged CASS materials, point out that very few of the data fall below the very conservative component end-of-life lower-bound limit recommended by Framatome of 100 kJ/m^2 (571 in-lb/in^2), even for fully-aged conditions. A more direct comparison can be obtained by plotting the lower-bound J-R curve data for statically-cast and centrifugally-cast CF-8M material with delta ferrite ranging from 15% to about 28%, as tabulated by Chopra and Shack [15], against J-R curve data for Type 316 SAW metal, as given in Reference 16. Figure 2-24 shows that statically-cast CF-8M material with delta ferrite less than 10% has considerably greater crack growth resistance at reactor operating temperature than does SAW metal, while statically-cast CF-8M material with delta ferrite levels between 10 and 15% has a resistance to crack growth that is quite similar, but slightly greater, to that of SAW metal at reactor operating temperature.

Only statically-cast CF-8M material with delta ferrite greater than 15% displays a crack growth resistance below that for SAW metal, and then only for very large crack extensions. Figure 2-25 shows that, even for centrifugally-cast CF-8M material with delta ferrite greater than 15%, the crack growth resistance is similar, but slightly greater, than that for SAW metal at reactor operating temperature. Even though the fracture toughness data for CF-8M material are limited to a delta ferrite content of about 28%, these comparisons are likely to be valid for materials with higher delta ferrite content, based upon fracture toughness trend curves as a function of delta ferrite content for low-molybdenum material. The latter data extends out to the 40% delta ferrite range. This extrapolation is also supported by Figure 2-12, which illustrates the saturation effect of an aging parameter that includes delta ferrite content. Such favorable comparisons justify the use of existing weld metal acceptance criteria for flaws detected and sized during the inservice inspection of CASS components, as discussed in Section 3.

It should be pointed out that this issue of high delta ferrite content (> 25%) is one of the few areas of disagreement between the NRC staff and the industry. Reference 17 stipulates that the limit for comparison of crack growth resistance data between CASS material and SAW/SMAW weld metal is a delta ferrite content of 25%. For CASS material with delta ferrite content above 25%, some other form of justification must be provided for inservice examination flaw acceptance criteria. The industry continues to recommend that the available data, while very

sparse, support the favorable comparison of worst-case CASS material (high Mo, high delta ferrite, statically-cast) with SAW/SMAW weld metal.

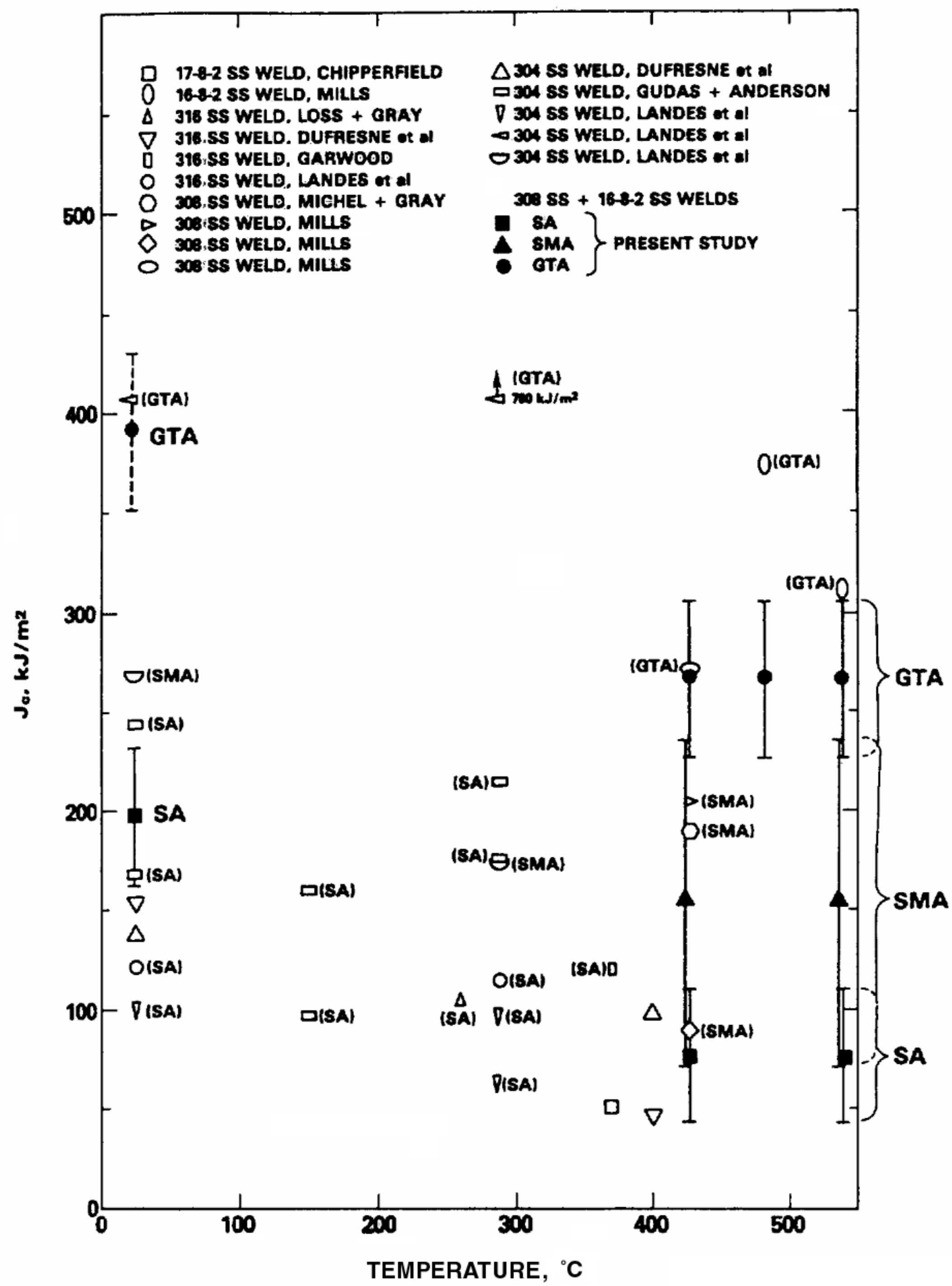

Figure 2-23
Comparison of Measured J_c Results for Weldments with Values Reported in the Literature (Figure 11 from Reference 13)

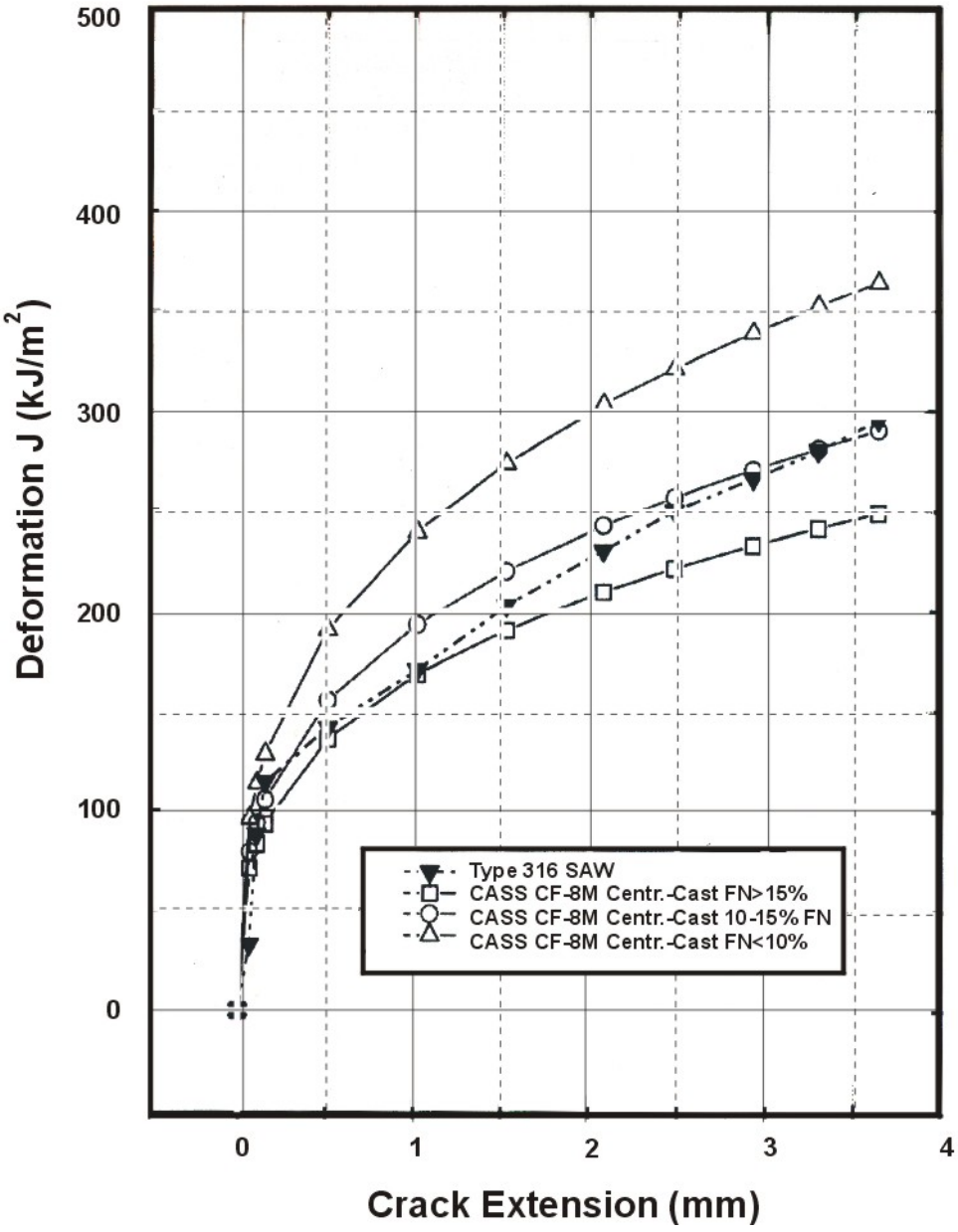

Figure 2-24
Comparison of Crack Growth Resistance (J-R) Curves for Type 316 SAW and Statically-Cast CF-8M Material at 555°F

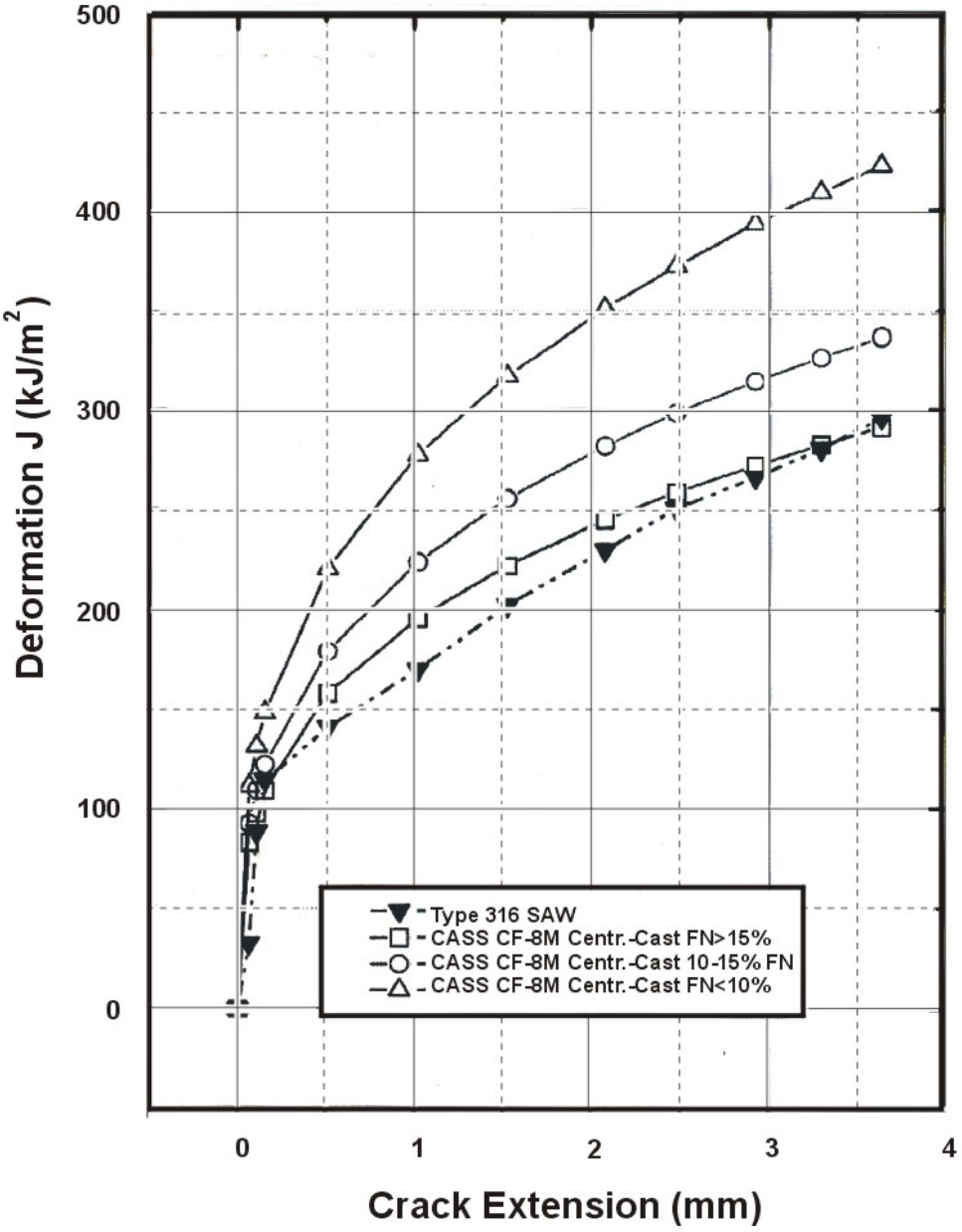

Figure 2-25
Comparison of Crack Growth Resistance (J-R) Curves for Type 316 SAW and Centrifugally-Cast CF-8M Material at 555°F

3
INSERVICE EXAMINATION AND FLAW EVALUATION

3.1 Inservice Inspection Program Elements for Piping, Pumps, and Valves

The effects of thermal aging embrittlement on CASS piping, pump, and valve components of the reactor coolant system and the primary pressure boundary are managed, both during the current license term and in any license renewal period, by elements of the plant inservice inspection program. This program includes the applicable requirements of the ASME Code Section XI, Subsection IWB.

The welds and internal, pressure-retaining surfaces of CASS reactor coolant pump casings are examined periodically, in accordance with Examination Categories B-L-1 and B-L-2. Examination Category B-L-1 calls for either an ultrasonic (UT) or radiographic (RT) volumetric examination of 100% of the length of all welds in at least one pump in each group of pumps that perform a similar function in the reactor coolant system. Examination Category B-L-2 requires the visual (VT-3) examination of the internal, pressure-retaining surfaces of these selected pumps during disassembly for maintenance, repair, or volumetric examination.

Similar requirements apply to CASS valve body welds and internal, pressure-retaining surfaces of these valves under the provisions of Examination Categories B-M-1 and B-M-2, respectively, provided that the valves are at least nominal pipe size (NPS) four inches or greater. For these NPS 4 or larger valves, Examination Category B-M-1 requires the volumetric (UT or RT) inspection of 100% of the weld length in at least one valve within each group of valves that are of the same size, constructional design (e.g., globe, gate, or check valves), and manufacturing method, and that perform similar functions within the system (e.g., containment isolation or system overpressure protection). Examination Category B-M-2 requires the visual (VT-3) inspection of the internal surfaces when the valve is disassembled for maintenance, repair, or volumetric examination. For valves of size less than four inches NPS, Examination Category B-M-1 calls for a periodic surface (e.g., dye penetrant, or PT) examination of the welds for the selected valves, with no visual examination of the internal surfaces. The pumps and valves should be selected for examination based, at least in part, on their susceptibility to thermal embrittlement, with material specifications, type of casting method, and operating temperature as elements of the screening process.

Pressure-retaining welds in CASS piping and fittings are periodically inspected, in accordance with Examination Category B-J. Examination Category B-J requires the surface and volumetric examination of a set of circumferential welds in piping and fittings four inches NPS, or larger. The set must include all terminal ends and all weld joints with relatively high design-basis stresses or fatigue usage factors. The scope of the examination includes 100% of the circumferential weld, plus a strip of CASS base metal 0.5-inch on each side of the weld. At issue

is the extent to which the strip of CASS base metal included in the examination is representative of the CASS material most affected by thermal aging embrittlement.

In addition, Examination Category B-P requires the visual (VT-2) examination of the pressure-retaining boundaries of piping, pumps, and valves during the system leakage tests that are conducted prior to plant startup following each refueling outage.

Acceptance criteria for any indications detected during the volumetric examinations are given in IWB-3514, IWB-3518, IWB-3519, or IWB-3522. Allowable planar flaws for the volumetric examinations are given in Table IWB-3514-2 and Table IWB-3518-2. Allowable planar flaw dimensions are given for both surface and subsurface flaws, and for flaws detected by UT, RT, and by a combination of RT and supplementary surface examination, and are based on acceptance standards for austenitic stainless steel piping [9].

The relevant conditions for the visual examination of the internal, pressure-retaining surfaces of the pump casings and valve bodies include “crack-like surface flaws developed in service or grown in size beyond that recorded during preservice visual examination,” for VT-1 inspections, and “loose, missing, cracked, or fractured parts, bolting, or fasteners,” for VT-3 inspections. The relevant conditions for the visual (VT-2) examinations of the pressure-retaining boundaries during system leakage tests include “through-wall leakage that penetrates the pressure retaining membrane.” When relevant conditions are detected during visual examinations, corrective actions are required, in the form of supplemental volumetric or surface examination, analytical evaluation, repair, or replacement of the component.

An alternative to Examination Category B-L-1 is available in the form of ASME Nuclear Code Case N-481, which permits the volumetric examination of pump casing welds to be replaced by a combination of visual (VT-1) examination of the external surfaces of one (the most susceptible to thermal aging embrittlement) pump casing and a flaw tolerance evaluation of the most critical locations in that pump casing. The VT-2 examination of the exterior of all pumps during hydrostatic pressure testing and the VT-3 examination of the internal surfaces whenever a pump is disassembled for maintenance are still required. The flaw tolerance evaluation includes the explicit consideration of thermal aging embrittlement and any other processes that may degrade the properties of the pump casing during service. The procedure involves assuming a flaw at the most highly-stressed location and in the most damaging orientation in the pump casing. Appendix A of this report provides an example of such a flaw tolerance calculation.

While Nuclear Code Case N-481 strictly applies to reactor coolant pump casings, the industry has maintained that the alternative of flaw tolerance demonstration combined with visual examination should also be adequate for other reactor coolant system and primary pressure boundary components, such as valve bodies. The extension of this code case to valve bodies has been suggested to the appropriate ASME Code Section XI groups, and is under consideration. The flaw tolerance evaluation procedures of N-481 provide a method for demonstrating that the component is capable of maintaining its functional capability in the presence of “mature” flaws; i.e., flaws that are detectable by routine visual examination.

3.2 Inservice Inspection Program Elements for Reactor Pressure Vessel Internals

The effects of thermal aging embrittlement on CASS Class CS reactor pressure vessel internals are also managed, during both the current license term and the period of extended operation, by elements of the plant inservice inspection program. This program includes the requirements of the ASME Code Section XI, Subsection IWB, Examination Categories B-N-2 (for BWR core support structures) and B-N-3 (for PWR core support structures). In both cases, the examination is visual (VT-3) for accessible surfaces of the internals. Remote, as opposed to direct, visual examination is permitted in accordance with IWA-2210 (c).

Acceptance criteria for the CASS internals examinations, including the description of relevant conditions that require corrective action, are provided in IWB-3520. These descriptions include "loose, missing, cracked, or fractured parts, bolting, or fasteners." At issue is the ability to visually detect surface cracking by VT-3 examination. The visual acuity and maximum direct examination distance requirements for VT-1 and VT-3 visual examination are given in Table IWA-2210-1. The maximum examination distance for VT-1 is given as 2 feet, while that for VT-3 is given as 4 feet, with the character recognition heights for the two methods given as 0.044 and 0.105 inches, respectively. In other words, VT-1 examinations require the observer to be closer and require the detection of smaller objects, by about a factor of 2. Remote visual examination techniques, such as cameras or fiber-optic devices, are required to meet the same qualifications.

Recent information from the BWR Vessel and Internals Program [18] provide calibration relative to VT-1 and VT-3 methods. The exercise was directed at the detection of cracks in BWR core shrouds and involved the placement of 0.0005-inch diameter stainless steel wires 20 feet underwater against various backgrounds, using cameras as the remote visual examination device. Detection was assured from a distance of 16 inches, provided that the lighting was adequate and reflection from the various backgrounds minimized. Contrast was not a concern. The wire diameter was considerably smaller than the character recognition height for either VT-1 or VT-3, and the remote camera distance was considerably less than the maximum examination distance for either VT-1 or VT-3. The wire diameter is also somewhere between 1% to 3% of the width of a mature crack under load, defined here to be between 0.015 and 0.050 inches. Such visual examination qualification exercises provide high confidence in the ability to detect mature cracks by either VT-1 or VT-3 methods.

3.3 Flaw Evaluation Procedures

When flaws are detected and sized that are in excess of the allowable limits of Tables IWB-3514-2 or IWB-3518-2, corrective actions are required, either in the form of supplementary examinations, repair, replacement, or engineering evaluation. An example is provided by engineering evaluations, in accordance with Article IWB-3640 (Evaluation Procedures and Acceptance Criteria for Austenitic Piping). These rules are intended for austenitic stainless steel piping components containing a flaw exceeding the allowable flaw standards of IWB-3514.3.

The evaluation procedures specified in IWB-3640 formally apply to austenitic piping and adjoining pipe fittings that are four inches nominal pipe size or greater, per IWB-3641(a); are fabricated from wrought austenitic stainless steel, Ni-Cr-Fe alloy, or CASS with a ferrite number less than 20, per IWB-3641(b)(1); and, for CASS piping materials, adequate fracture toughness to permit the pipe cross section to reach limit load after aging must be demonstrated per IWB-3641(c). However, the flaw evaluation procedures specified in IWB-3640 also may be applied to all CASS components. The most limiting lower-bound fracture toughness reported in Reference 13, using the J-R crack growth resistance curve data for statically-cast SA 351 Grade CF-8M with ferrite number greater than 15, is slightly below but essentially equivalent to the Type 316 SAW fracture toughness (J-R) data used to generate the end-of-evaluation-period acceptance standards for SAW and shielded-metal-arc welds (SMAW), as specified in Tables IWB-3641-5 and IWB-3641-6. Crack growth resistance for Grade CF-8M materials that are cast centrifugally, regardless of ferrite number, or for statically-cast material with delta ferrite less than 15%, is greater than that for Type 316 SAW metal. The comparisons are shown graphically in Figures 2-24 and 2-25.

Therefore, the use of the flaw acceptance criteria for SAW and SMAW contained in IWB-3640 for evaluating detected and sized flaws found during inservice inspection, or for flaws assumed in a flaw tolerance evaluation of high-molybdenum, statically-cast CASS components has been justified. These flaw acceptance criteria are conservative for evaluating inservice inspection or flaw tolerance results for low-molybdenum or centrifugally-cast CASS components.

Flaw evaluations of CASS components documented in Appendix A, Appendix B, and the EPRI Cast Austenitic Stainless Steel Sourcebook [12] support this type of evaluation, and demonstrate the tolerance of CASS components to very large flaws, even under extreme loading conditions. These critical flaw size calculations show that elastic-plastic fracture toughness at saturation levels of thermal aging (for example, 60 years at 320°C, leading to an impact energy of 40 ft-lb and an elastic-plastic fracture toughness of 255 kJ/m^2 (1450 $in\text{-}lb/in^2$)) provides more than adequate structural integrity for components of interest.

3.4 Regulatory Evaluation

Reference 17 provides the regulatory evaluation of the industry technical position on the adequacy of ASME Code Section XI inservice inspection program elements for managing the effects of thermal aging embrittlement for CASS components. The staff of the U. S. Nuclear Regulatory Commission (NRC) appear to have accepted the adequacy of the ASME Code Section XI inservice inspection program elements, with three exceptions. Those exceptions are discussed below.

1. The NRC staff does not think that the Examination Category B-J inspections are adequate, because an insufficient amount of CASS base metal is included in the scope of the examinations. It would appear that they have determined that the 0.5-inch strip on either side of pressure-retaining circumferential welds in Class 1 piping and fittings does not represent the most limiting CASS material. Reference 17 states that “The volumetric examination should be performed on the base material of each heat, with the scope of the inspection covering the portions determined to be limiting from the standpoint of applied stress level, operating time and environmental considerations. Alternatively, a plant/component-specific

flaw tolerance evaluation, using specific geometry and stress information, can be used to demonstrate that the thermally-embrittled material has adequate toughness."

The license renewal applicant should first attempt to demonstrate that the CASS piping and fittings satisfy the screening criteria. If the material can be shown to satisfy the screening criteria, no further action is required. If the material fails to satisfy the screening criteria, three alternatives are available. First, it can be argued that the base metal adjacent to the pressure-retaining circumferential welds is the limiting material, because of stress level and material condition. This volume of base metal is not only generally subject to the highest stresses in the piping system, but has also been exposed to an additional penalizing temperature history during the field welding process. Second, a more limiting location in the base metal can be sought, perhaps in an elbow or a tee junction. Finally, saturated thermal embrittlement J-R curves can be used in a plant/component flaw tolerance evaluation.

2. The NRC staff does not think that the Examination Category B-N-2 (BWR) and B-N-3 (PWR) VT-3 visual examinations are adequate, apparently because of uncertainty about the flaw tolerance of internals components. The staff also has concerns about the embrittlement enhancement caused by the combination of neutron irradiation and thermal aging of CASS. Therefore, a supplemental visual examination is thought to be necessary for susceptible components, with a demonstration of visual acuity well beyond the requirements of either VT-1 or VT-3 examinations. No credit for the ability to tolerate a mature crack is given, unless a mechanical loading assessment or a flaw tolerance evaluation is provided.

   The staff recognizes that a mechanical loading assessment for the internals component might show that the loading is either compressive or is tensile, but low enough in amplitude to preclude fracture. In such a case, no supplemental examination is required.

   Therefore, the license renewal applicant should first attempt to demonstrate that the CASS internals satisfy the screening criteria, including exposure of the internals component to a neutron fluence that is limited to 1×10^{17} n/cm^2 (E > 1 MeV). If the material can be shown to satisfy the screening criteria, then no further action is required. If the material fails to satisfy the screening criteria, three alternatives are available. First, the mechanical loads can be shown to result in compressive stresses, or low tensile stresses. Low is undefined, but the industry has used 8 to 10 ksi as the threshold in earlier discussions with the NRC staff. Second, in accordance with arguments provided above, the internals component can be shown to be tolerant to mature flaws, flaws for which the existing visual acuity standards in the ASME Code for VT-3 visual examination are adequate. Finally, a supplemental visual examination following the BWRVIP visual acuity recommendations can be undertaken.

3. The NRC staff believes that a delta ferrite limit of 25% applies to the adequacy of the ASME Code Section XI inservice inspection and flaw evaluation requirements of IWB-3640. The NRC staff had previously accepted the comparison of lower-bound CASS fracture toughness data to that for SAW and SMAW welds for the entire range of CASS materials. For CASS materials with delta ferrite content that exceeds 25%, Reference 17 states "the flaw evaluation would be on a case-by-case basis using fracture toughness data supplied by the licensee."

4
PROPOSED EVALUATION PROCEDURE

The proposed procedure for evaluating the effects of thermal aging embrittlement effects (e.g., reduction of fracture toughness) in Class 1 reactor coolant system and primary pressure boundary cast austenitic stainless steel components is composed of two parts: (1) screening to determine whether or not the effects of thermal aging embrittlement are potentially significant to the continued function of a particular CASS component during the license renewal term; and (2) when the effects of thermal aging embrittlement are found to be potentially significant for CASS components, an aging management program based upon periodic inservice inspection and flaw evaluation criteria that provides the basis for demonstrating aging management during the license renewal term. This same approach, with minor modifications, also applies to Class CS internals components.

The recommended screening criteria are listed in Section 1 of this report, and are repeated here for completeness. These screening criteria apply to both Class 1 reactor coolant system and primary pressure boundary, and to Class CS internals CASS components.

- *Low-molybdenum (e.g., SA 351 Grade CF-3 and Grade CF-8) material that has been cast centrifugally is not subject to potentially significant reduction of fracture toughness after exposure to service temperatures less than 320°C (610°F) for 525,000 hours (60 years). Low-molybdenum material that has been cast statically is not subject to potentially significant loss of fracture toughness after exposure to service temperatures less than 320°C (610°F) for 525,000 hours (60 years), provided that the delta ferrite content of the material can be shown by calculation or measurement to be 20% or less. Further evaluation of low-molybdenum, statically-cast components is required, in terms of inservice examination and flaw evaluation program elements, if the delta ferrite content of the material cannot be shown to be 20% or less.*
- *High-molybdenum (e.g., SA 351 Grade CF-3M and Grade CF-8M) material that has been cast centrifugally is not subject to potentially significant reduction of fracture toughness after exposure to temperatures less than 320°C (610°F) for 525,000 hours (60 years), provided that the delta ferrite content of the material can be shown by either calculation or measurement to be 20% or less. Further evaluation of high-molybdenum, centrifugally-cast components is required, in terms of inservice examination and flaw evaluation program elements, if the delta ferrite content of the material cannot be shown to be 20% or less.*
- *High-molybdenum (e.g., SA 351 Grade CF-3M and Grade CF-8M) material that has been cast centrifugally is not subject to potentially significant reduction of fracture toughness after exposure to temperatures less than 320°C (610°F) for 525,000 hours (60 years), provided that the delta ferrite content of the material can be shown by either calculation or measurement to be 14%, or less. Further evaluation of high-molybdenum, statically-cast components is required, in terms of inservice examination and flaw evaluation program elements, if the delta ferrite content of the material cannot be shown to be 14%, or less.*

The application of these screening criteria is illustrated by the flow chart shown in Figure 4-1. This flow chart is intended to depict the steps in screening CASS material and method of casting only, using information on molybdenum content, delta ferrite content, and casting method.

When the material and casting process screening steps lead to a requirement for aging effects management, the recommended aging effects management program elements are based upon the favorable comparison of fracture toughness data for SAW/SMAW weld metal and high-molybdenum, statically-cast, high-delta-ferrite CASS material, as described in Section 2.4. This comparison permits any detected and sized flaws from the periodic inservice inspections of Class 1 reactor coolant system and primary pressure boundary CASS components, such as CASS pump casings and valve bodies, to be evaluated in one of three ways:

- When adequate fracture toughness can be demonstrated such that the component can achieve limit load prior to unstable crack extension, in accordance with IWB-3641(c), using J-R data in Reference 9, the end-of-evaluation-period acceptance standards to be applied to detected and sized flaws are those for wrought stainless steel base metal, gas-metal-arc weld (GMAW) metal, and gas-tungsten-arc weld (GTAW) metal; or
- When adequate fracture toughness cannot be demonstrated such that the component cannot be shown to achieve limit load prior to unstable crack extension, in accordance with IWB-3641(c), or for conservatism, the end-of-evaluation-period acceptance standards to be applied are those for SAW and SMAW metal.
- Otherwise, case-by-case evaluation using representative material toughness properties in accordance with References 11a, 11b, and 15 can be justified.

In the first option, acceptable circumferential flaw size limits are prescribed in Tables IWB-3641-1 (Service Level A and B Loadings) and IWB-3641-2 (Service Level C and D Loadings). In the second option, acceptable circumferential flaw size limits are prescribed in Tables IWB-3641-5 (Service Level A and B Loadings) and IWB-3641-6 (Service Level C and D Loadings). The axial flaw size acceptance criteria for the two material categories do not differ, and are given in Tables IWB-3641-3 (Service Level A and B Loadings) and IWB-3641-4 (Service Level C and D Loadings).

The differences in acceptable circumferential flaw sizes are substantial, reflecting the reduced fracture toughness in the SAW and SMAW properties. For example, for comparable flaws and applied loadings, the SAW/SMAW end-of-evaluation-period flaw depth limit may be less than half the depth of the limiting circumferential flaw for wrought base metal or GMAW/GTAW metal.

These evaluation requirements can be used directly for all CASS Class 1 reactor coolant system and primary pressure boundary components. Even when the alternative rules of ASME Nuclear Code Case N-481 are shown to apply, the flaw growth procedures of the non-mandatory Appendix C can be used in conjunction with the end-of-evaluation-period flaw acceptance criteria of IWB-3640 for the flaw tolerance evaluation. These same flaw evaluation requirements can also be used for Class CS internals CASS components, with a slight modification. The basic inservice examination requirements for Class CS internals components calls for visual (VT-3) examination. For any observed relevant condition, such as a surface manifestation of an apparent crack (e.g., a crack-like indication), one of the possible actions to be taken is a supplemental

surface or volumetric examination to further characterize the relevant indication and, if necessary, to size any potential flaw. In such a case, the flaw evaluation procedures outlined above apply for Class CS CASS internals components, as well.

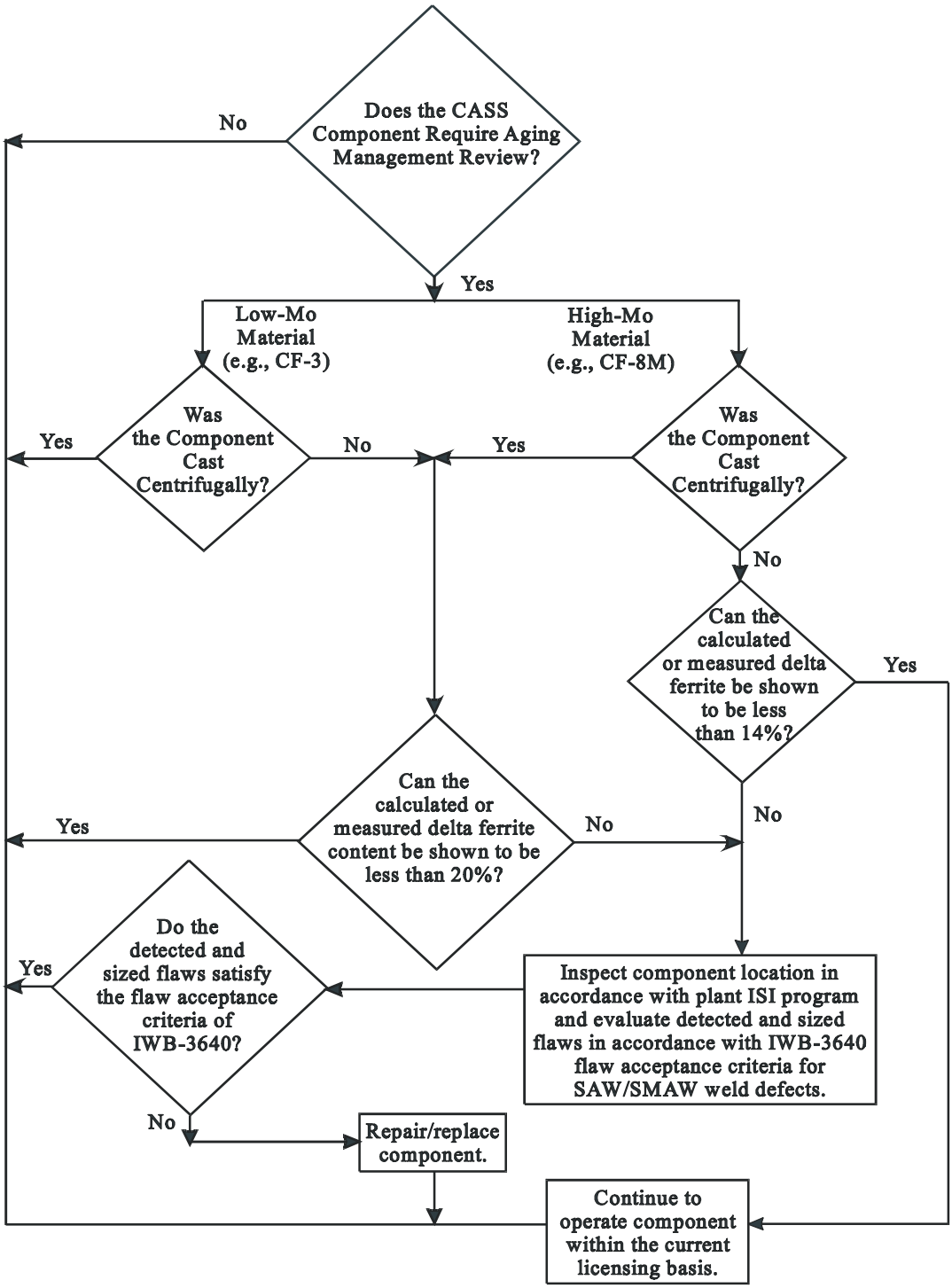

Figure 4-1
Flow Chart Illustrating Screening Criteria for Potential Significance of Thermal Aging Effects for Class 1 Reactor Coolant System and Primary Pressure Boundary Components

For evaluation of either actual or hypothetical flaws, if it can be determined that a particular casting is relatively unaffected by the effects of thermal aging embrittlement, a more favorable crack growth resistance (J-R) curve can be determined on a case-by-case basis. Such a case-by-case justification will ensure that the GMAW/GTAW material properties and procedures of Appendix C can be applied, and will then guarantee the satisfaction of IWB-3641(c), since the Appendix C "methodology is based on a limit load evaluation of the pipe section reduced by the flaw area for flaws in ductile material when the ability to reach limit load is assured, and on elastic-plastic fracture mechanics evaluations for flaws in or near less ductile material where limit load action is not assured."

The screening criteria for potential significance of CASS thermal aging embrittlement effects outlined above apply to all CASS Class 1 reactor coolant system and primary pressure boundary components, and to all Class CS CASS internals components manufactured from Grade CF3, CF3A, CF8, CF8A, CF3M, CF3MA, and CF8M material. However, the inservice examination requirements for Class 2 and Class 3, which emphasize surface and visual examination methods, and the associated evaluation of indications and relevant conditions can use similar techniques. As with Class CS components, the screening criteria apply directly, provided that material property and chemistry information is available. The flaw evaluation procedures also apply, following the observation of relevant conditions and supplemental surface or volumetric examinations. In some cases, flaw tolerance calculations can help to determine the need for supplemental volumetric examination. For example, flaw tolerance evaluations of Class 2 components can be used to determine the necessity for augmented examinations, with the results of Appendix A, Appendix B, and Reference 12 used as guidance.

In summary, the effects of thermal aging embrittlement on Class 1 CASS reactor coolant system and primary pressure boundary components, and for CASS Class CS internals components are found to be either not significant for the license renewal term, based upon material chemistry and casting type screening criteria, or, if the effects are potentially significant, can be managed adequately through the license renewal term by the periodic volumetric, surface, and visual inservice inspection program elements specified in the ASME Code Section XI, Subsection IWB, or the alternative inservice examination and flaw tolerance evaluation procedures of ASME Nuclear Code Case N-481. When conditions are detected during these inservice inspections that exceed the allowable limits given in Table IWB-3518-2, engineering evaluations of either detected or postulated flaws shall be carried out using material properties and acceptance criteria applicable to SAW and SMAW metal per the evaluation procedures presented in IWB-3640. More favorable material properties and acceptance criteria may be justified, on a case-by-case basis, using the fracture toughness data in Reference 15.

5
REFERENCES

1. P. McConnell and W. Sheckherd, "*Fracture Toughness Characterization of Thermally Embrittled Cast Duplex Stainless Steel*," Report No. EPRI NP-5439, Fracture Control Corporation, Goleta, California (September 1987).

2. P. McConnell, W. Sheckherd, and D. Norris, "*Properties of Thermally Embrittled Cast Duplex Stainless Steel,* " Journal of Materials Engineering, Volume 11, No. 3, pp. 227-236 (1989).

3. Chopra and A. Sather, "*Initial Assessment of the Mechanisms and Significance of Low-Temperature Embrittlement of Cast Stainless Steels in LWR Systems*," NUREG/CR-5385 (ANL-89/17), Argonne National Laboratory, Argonne, Illinois (August 1990).

4. "*PWR Reactor Coolant System License Renewal Industry Report, Revision 1,*" Report No. 90-07, Nuclear Management and Resources Council (NUMARC), Washington, D. C. (May 1992); also EPRI Report No. TR-103844s (July 1994).

5. "*BWR Primary Coolant Pressure Boundary License Renewal Industry Report, Rev. 1,*" Report No. 90-09, Nuclear Management and Resources Council (NUMARC), Washington, D. C. (April 1992); also EPRI Report No. TR-103843s (July 1994).

6. "*Requirements for Class 1 Components of Light-Water Cooled Plants*," in: Rules for Inservice Inspection of Nuclear Power Plant Components, ASME Boiler & Pressure Vessel Code, Section XI, Subsection IWB, The American Society of Mechanical Engineers, New York, New York (July 1989).

7. "*Case N-481: Alternative Examination Requirements for Cast Austenitic Pump Casings*," in: Code Cases, Nuclear Components, ASME Boiler & Pressure Vessel Code, The American Society of Mechanical Engineers, New York, New York (March 5, 1990).

8. "*Demonstration of the Management of Aging Effects for the Reactor Coolant System Piping*," Report No. BAW-2243, The B&W Owners Group Generic License Renewal Program (GLRP), B&W Nuclear Technologies, Lynchburg, Virginia (March 1995).

9. "*Evaluation of Flaws in Austenitic Steel Piping*," ASME Code Section XI Task Group for Piping Flaw Evaluation, Report No. EPRI NP-4690-SR, Electric Power Research Institute, Palo Alto, California (July 1986).

10. P. Hedgecock, "*The Evaluation of Significant Deterioration Mechanisms in Cast Austenitic Stainless Steel Primary Coolant Pressure Boundary Components*," Draft Report, EPRI Contract RP 2643-26, NUTECH Engineers, San Jose, California (May 1989).

11a. O. K. Chopra, "*Estimation of Fracture Toughness of Cast Stainless Steels During Thermal Aging in LWR Systems*," NUREG/CR-4513 (ANL-90/42), Revision 5, Argonne National Laboratory, Argonne, Illinois (May 1991).

11b. O. K. Chopra, "*Estimation of Fracture Toughness of Cast Stainless Steels During Thermal Aging in LWR Systems*," NUREG/CR-4513 (ANL-93/22), Revision 1, Argonne National Laboratory, Argonne, Illinois (August 1994).

12. P. Riccardella, et al., "*Evaluation of Cast Austenitic Stainless Steel Components*," in: Cast Austenitic Stainless Steel Sourcebook, Report No. EPRI TR-100034, Attachments E & F, Structural Integrity Associates, San Jose, California (October 1991).

13. W. J. Mills, "*Fracture Toughness of Stainless Steel Welds*," in: Fracture Mechanics: Nineteenth Symposium, ASTM STP 969, pp. 330-355, T. A. Cruse, Editor, American Society for Testing and Materials, Philadelphia, Pennsylvania (1986).

14. C. E. Jaske and V. N. Shah, "*Life Assessment Procedures for Major LWR Components: Cast Stainless Steel Components*," NUREG/CR-5314 (EGG-2562), Volume 3, Idaho National Engineering Laboratory, Idaho Falls, Idaho (October 1990).

15. O. K. Chopra and W. J. Shack, "*Assessment of Thermal Embrittlement of Cast Stainless Steels*," NUREG/CR-6177 (ANL-94/2), Argonne National Laboratory, Argonne, Illinois (May 1994).

16. J. D. Landes and D. E. McCabe, "*Toughness of Austenitic Stainless Steel Pipe Welds*," Report No. EPRI NP-4768, Westinghouse Electric Corporation, Pittsburgh, Pennsylvania (October 1986).

17. C. I. Grimes, Chief, License Renewal and Standardization Branch, USNRC, Letter to D. J. Walters, Nuclear Energy Institute, plus Attachment, "Staff Evaluation of License Renewal Issue No. 98-0030: Thermal Aging Embrittlement of Cast Austenetic Stainless Steel Components," May 19, 2000.

18. EPRI TR-105696, "BWR Vessels and Internals Project: Reactor Pressure Vessel and Internals Examination Guidelines (BWRVIP-03)," EPRI, Palo Alto CA, October 1995.

A
APPENDIX A – ELASTIC-PLASTIC FRACTURE TOUGHNESS EVALUATION

Introduction

Previous evaluations of cast austenitic stainless steel (CASS) nuclear components, such as that described in Reference A1 (see Appendix B), have shown that severe thermal aging embrittlement does not compromise structural integrity. These evaluations have used both naturally-aged and artificially-aged material property data from the open literature, including crack growth rates and saturated elastic-plastic fracture toughness values, to demonstrate that extremely large flaws, well above the size that would be detected readily during inservice examination, are needed in order to threaten structural integrity. Reference A1 provides calculations to support the continued operation of a cast CF-8 elbow with an end-of-life elastic-plastic fracture toughness that has been reduced to 255 kJ/m^2 (1450 $in\text{-}lb/in^2$) through exposure to service temperatures for periods of 40 years or longer. The stresses used for the evaluation were obtained from plant component stress reports.

In this appendix, a similar but more elementary set of calculations is used to also justify an elastic-plastic fracture toughness of 255 kJ/m^2 (1450 $in\text{-}lb/in^2$) as a screening criterion for license renewal thermal aging embrittlement evaluation of CASS components, in essential agreement with the findings in Reference A1. In this case, the elastic-plastic crack driving force for a postulated reference flaw is calculated for a simple, but typical component geometry, a thick-walled cylinder with a hypothetical internal, circumferential crack.

Application of Elastic-Plastic J-Estimation

Elastic-plastic J-estimation methods [A2] show that the applied crack driving force, J_{appl}, is given by the sum of an elastic term, J_E, and a plastic term, J_P, so that

$$J_{appl} = J_E + J_P.$$

The elastic term for the geometry under consideration is given by

$$J_E = \pi\, a\, (\sigma)^2\, F^2\, (a, R_i, R_o) / E_1,$$

where a is the effective crack depth, including any correction for plasticity at the crack tip; σ is the remote axial tensile stress acting across the cylinder wall; F is a shape function that depends on a and the cylinder inner and outer radii, R_i and R_o, respectively; and E_1 is the reduced elastic modulus, given by

$$E_1 = E / (1 - \upsilon^2),$$

where E is the elastic modulus of the material and υ is Poisson's ratio. For simplicity, the equivalent crack depth will be chosen to be one-quarter of the wall thickness. The shape function F can be found from tables in Reference A2, as a function of a/b and R_i/R_o, where $b = R_o - R_i$.

The plastic term is given by

$$J_P = \alpha \sigma_o \varepsilon_o c (a / b) h_1 (a / b, n ; R_i / R_o) (P / P_o)^{n+1}.$$

Here the plastic material parameters α, n, σ_o, and ε_o are derived from a Ramberg-Osgood deformation theory plasticity model for the material (see Reference A2),

$$\varepsilon / \varepsilon_o = \sigma / \sigma_o + \alpha (\sigma / \sigma_o)^n.$$

The function c (a/b) is the remaining ligament, so that c = b - a; the shape function h_1 can be found from charts in Reference A2; and the limit load P_o is given by

$$P_o = 2 \sigma_o \pi (R_o^2 - R_c^2) / \sqrt{3},$$

where $R_c = R_i + a$.

These expressions can be used to derive a crack driving force for a thick-walled cylinder with inner radius, R_i = 25 inches; an outer radius, R_o = 30 inches; thickness b = 5 inches; crack depth a = 1.25 inches; R_c = 26.25 inches; R_i/R_o = 0.833; b/R_i = 0.2; a/b = 0.25; and c = 3.75 inches. For austenitic stainless steel, $E = 28 \times 10^6$ psi, υ = 0.3, $\sigma_o = 30 \times 10^3$ psi, α = 1.63, and n = 5.42.

Then

$$P_o = 2 \pi (30{,}000) (900 - 689.1) / \sqrt{3} = 22.96 \times 10^6 \text{ lb}$$

and

$$P = 275 \pi \sigma = 863.9 \sigma,$$

where the effective axial stress σ will be estimated from existing component stress reports. F is found from Reference A2 to be F (0.25,0.833) = 1.26, so that

$$J_E = 2.03 \times 10^{-7} (\sigma)^2.$$

Also, h_1 is found from Reference A2 to be h_1 (0.25, n; 0.833) = 6.58. Therefore, J_P is found to be

$$J_P = 1291 (P / P_o)^{6.42}.$$

Determining the crack driving force has then been reduced to an assumption on effective axial stress. For example, if the remote axial membrane stress is assumed to be 20,000 psi (about 2/3 of the yield strength and approximately equal to S_m), then

$J_E = 81.2$ in-lb/in^2,

and

$J_P = 208.1$ in-lb/in^2,

for a total crack driving force of 289 in-lb/in^2. This force is considerably less than the value of 100 kJ/m^2 (570 in-lb/in^2) that is recommended by Framatome (see Reference A3) as a lower bound J_{IC} for component assessment, illustrating the conservatism of the Framatome criterion.

Applied J-Integral Methods (Appendix K)

This simple estimate of the crack driving force can be confirmed by using the procedures of the non-mandatory Appendix K to Section XI of the ASME Code. Although Appendix K is provided for the assessment of reactor pressure vessels with low upper shelf Charpy impact energies, the acceptance criteria are useful for other applications. For example, one of the methodologies available in the Appendix K calls for the calculation of the applied J-integral from the combination of Mode 1 pressure and thermal stress intensity factors, with appropriate safety factors and plastic zone size corrections. This applied J-integral must be less than the J-integral fracture resistance for the material at a ductile flaw extension of 2.5 mm (0.1 inch).

This applied J-integral approach was examined relative to a set of PWR reactor coolant pumps, with potential crack-driving stresses for the pump casings obtained from certified stress reports. The critical locations for primary membrane stress, or primary membrane plus bending stress, were found to be the diffuser vanes, a section of the volute wall, the junction of the suction nozzle and the lower flange, and the junction of the discharge nozzle with the volute/flange (crotch region). The critical locations for the combination of primary and secondary stress are the upper flange and the junction of the volute with the upper/lower flanges.

For Design Conditions, a combination of internal (Design) pressure (2485 psi) and mechanical load resultants causes a stress intensity for the suction nozzle to vary from about 17,800 to 20,300 psi in the worst locations. The stress intensities for the junction of the volute and lower flange, due to discontinuity stresses and internal pressure, range from about 11,500 to 19,200 psi in the worst locations. The junction of the upper flange with the pump casing causes (discontinuity) stresses that vary from about 3,000 to 19,000 psi. Primary plus secondary stress intensities, which include substantial thermal bending stresses, met the 3 S_m limit of 58,050 psi at almost all locations, except for the upper flange and crotch areas where elastic-plastic analysis was required to satisfy stress limits. The worst-case location had a stress intensity of 63,420 psi.

The 1.25-inch deep flaw was analyzed with two sets of worst-case stresses. In one case, the inner surface stress intensity of about 63,000 psi was converted into an axial stress distribution, including thermal bending stresses, through the 5-inch thick wall and fitted to a quadratic distribution. The procedures of Reference A5 were used to compute a linear elastic fracture

mechanics stress intensity factor of about 89 ksi√in, which was converted to an applied J-integral of 257 in-lb/in^2. This value is in reasonable agreement with the 289 in-lb/in^2 calculated by simple elastic-plastic J-estimation methods.

The other worst-case calculation was extremely and unrealistically conservative, using the stress intensity of 63,420 psi as the axial stress for the linear elastic fracture mechanics calculation. In this case, K_{IC} was calculated to be 125 ksi√in and the applied J-integral became 509 in-lb/in^2. Even in this very conservative case, the applied J-integral turned out to be less than the lower bound value of 570 in-lb/in^2 recommended for component evaluation by Framatome. Again, this result confirms the conservatism of the Framatome criterion.

Fully-Plastic Conditions

When the remote axial stress is assumed to approach the limit load itself, the elastic-plastic crack driving force from the J-estimation method becomes 183 + 1291 = 1474 in-lb/in^2. This value is well above the lower-bound limit of 570 in-lb/in^2 given by Framatome, and this calculated crack driving force is not realistic, since the axial stress would be at yield strength levels over the complete cross section. However, this calculation provides an extremely conservative basis for an elastic-plastic fracture toughness screening threshold, above which the resistance to crack growth is such that loss of structural integrity from thermal aging embrittlement should not be a concern. For purposes of screening existing crack growth resistance curves for naturally-aged or artificially-aged CASS materials, a threshold value of 1450 in-lb/in^2 at a crack extension of 2.5 mm (0.1 inch), essentially in agreement with the results in Appendix, has been selected.

This screening threshold can be used to evaluate the data assembled in Reference A4, which contains lower-bound crack growth resistance (J-R) curves at room temperature and at 290°C (550°F) for both statically-cast and centrifugally-cast stainless steels with ferrite content in three ranges–less than 10%, between 10 and 15%, and greater than 15%. The J-R curves also explicitly include a separate set of curves for ASTM SA-351 Grade CF-8M, one of the possible high-molybdenum grades (the other is Grade CF-3M). From these J-R curves (see Figures 2-2 and 2-3 from Reference A4) and the 1450 in-lb/in^2 screening threshold at a crack extension of 2.5 mm (0.1 inch), the material of greatest concern is statically-cast CF-8M. Of the other statically-cast materials, only CF-3 and CF-8 material at 290°C with delta ferrite greater than 15% is marginal. Considering the conservatism of the screening threshold, CF-3 and CF-8 materials should also be of no concern. For centrifugally-cast material, only CF-8M with delta ferrite greater than 10% is a concern. No other materials are affected significantly. Therefore, this screening threshold permits an evaluation methodology that distinguishes between those situations involving a significant reduction of fracture toughness and those with an insignificant reduction.

References

A1. P. Riccardella, et al., "*Evaluation of Cast Austenitic Stainless Steel Components*," in: Cast Austenitic Stainless Steel Sourcebook, Report No. EPRI TR-100034, Attachments E and F, Structural Integrity Associates, San Jose, California (October1991).

A2. V. Kumar, et al., "*An Engineering Approach for Elastic-Plastic Fracture*," Report No. EPRI NP-1931, General Electric Company, Schenectady, New York (July 1981).

A3. C. E. Jaske and V. N. Shah, "*Life Assessment Procedures for Major LWR Components: Cast Stainless Steel Components*," NUREG/CR-5314 (EGG-2562), Volume 3, Idaho National Engineering Laboratory, Idaho Falls, Idaho (October 1990).

A4. O. K. Chopra and W. J. Shack, "*Assessment of Thermal Embrittlement of Cast Stainless Steels*," NUREG/CR-6177 (ANL-94/2), Argonne National Laboratory, Argonne, Illinois (May 1994).

A5. I. S. Raju and J. C. Newman, Jr., "*Stress-Intensity Factors for Internal and External Surface Cracks in Cylindrical Vessels*," Transactions of the ASME, Journal of Pressure Vessel Technology, Vol. 104, No. 4, pp. 293-298 (November 1982).

B
APPENDIX B – FLAW TOLERANCE EVALUATION OF CAST AUSTENITIC STAINLESS STEEL COMPONENTS

Introduction

This appendix briefly describes a generic worst case flaw tolerance evaluation for statically-cast austenitic stainless steel elbows for both PWR reactor coolant system piping and BWR reactor recirculation system piping. This case study is intended to represent the upper bound case using typical elbow geometries, design and operation conditions, piping stresses, material fatigue crack growth and fracture toughness data. Conservative assumptions are used throughout as appropriate and described in the corresponding sections. For example, all defects are considered to be 360-degree crack-like flaws located in regions of maximum stress intensity. Each defect is considered to open to the inside surface and exposed to the process fluid environment. The loss of fracture toughness due to thermal aging embrittlement is predicted using conservative estimates based on current research results. The assumed flaw is grown analytically using environmentally-assisted fatigue crack growth data from the literature.

Analysis Input

Typical geometries for PWR and BWR elbows are used in this "worst case" generic evaluation. The dimensions of the analyzed elbows are as shown in Table B-1.

Table B-1
Elbow Geometries

	PWR	BWR
OD	36.2 in (919.48 mm)	28.363 in (720.42 mm)
ID	31.0 in (787.40 mm)	25.867 in (657.02 mm)
Thickness	2.6 in (66.04 mm)	1.248 in (31.70 mm)

The operating conditions used in the analyses for the PWR and BWR elbows are described in Table B-2.

Table B-2
Operating Conditions

	PWR	BWR
Design Pressure	2485 PSIG	1148 psig
Oper. Pressure	2235 psig	1050 psig
Design Temp.	650°	562°F
Peak Pressure	—	1361 psig

Representative loadings at the elbow location are used in the fatigue crack growth evaluation. The loadings were obtained from References B1 and B2 and are shown in Table B-3.

Table B-3
Elbow Loadings

BWR					
Loadings	F_a (kips)	M_b (in-kips)	M_c (in-kips)	Stress (psi) $\sigma_{tensile}$	Stress (psi) $\sigma_{bending}$
DW	3.1	-344.8	-257.7	29.0	620.0
Thermal	-0.5	-310.8	-305.9	-4.7	630.0
OBE_1	10.0	511.0	245.0	15.0	820.0
OBE_2	14.8	481.6	413.3	21.4	920.0
PWR					
	Loadings		Stress (psi)		
	DW		127.0		
	Thermal		3569.0		
	½ SSE		6600.0		

For the BWR case, the force and moments were obtained at the mid-point of the elbow element in the piping model. Only the axial force and the two bending moments were used because these were the pertinent driving forces for the analytical crack model used in the crack growth analyses. For the BWR elbow, the appropriate stress intensification factors were included in the stress calculation from the forces and moments to account for the elbow geometry effects.

For the PWR elbow, bounding stresses for the entire reactor coolant piping system were taken from Reference B3, which were assumed to apply to the elbow location. These stress values were also assumed to include the appropriate stress intensification factors. Therefore, no adjustment to these stress value was made in the fatigue crack growth calculation.

The pressure stresses were computed for both PWR and BWR elbows using the equation for thin wall cylinder under internal pressure. These pressure stresses were also multiplied by stress intensification factors for use in the crack growth evaluation.

Two residual stress cases were considered in the fatigue crack growth evaluation. The first residual stress case is a linear through-wall bending stress distribution, denoted as the "worst case" residual stress. The second case is a stress distribution fitted to a third order

polynomial and is called the "best estimate" residual stress. These stress distributions are shown in Figure B-1.

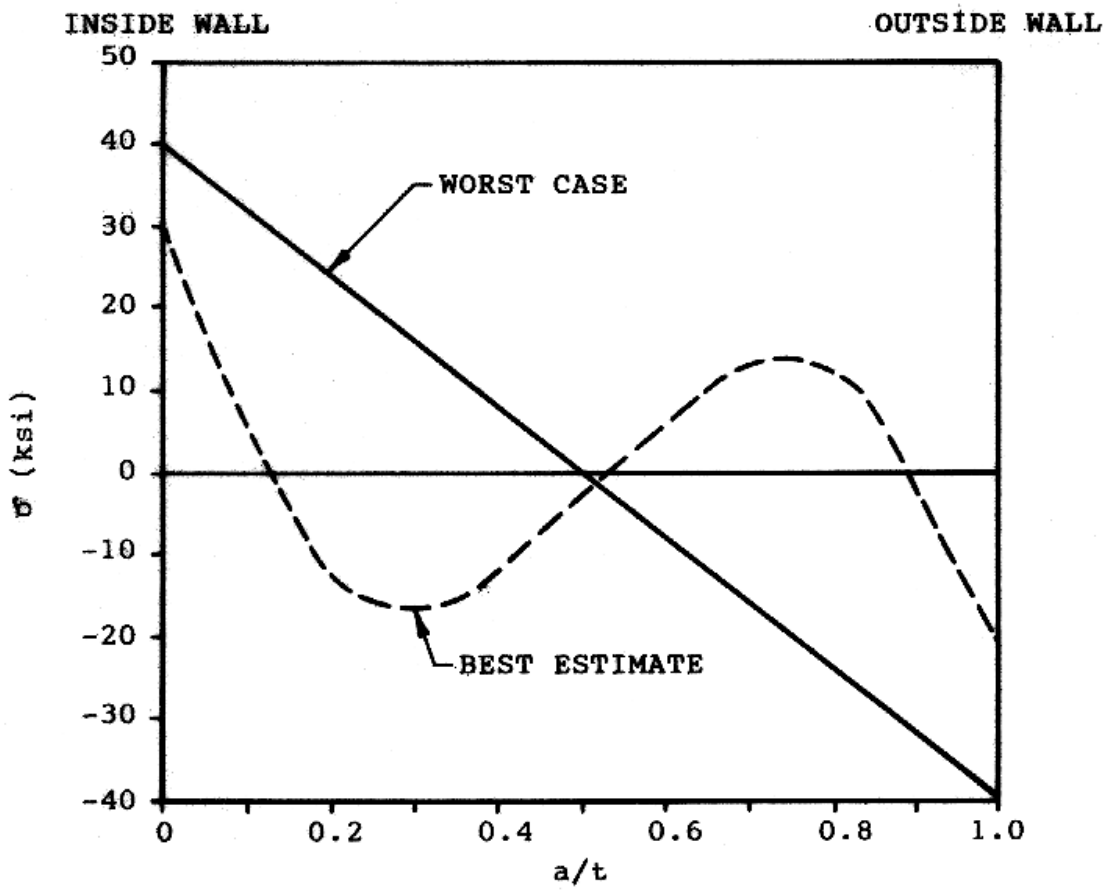

Figure B-1
Distribution of Axial Residual Stress

Fatigue Crack Growth Evaluation

Fatigue crack growth data, Figure B-2, for the CF8M cast austenitic stainless steel, are taken from Reference B4. The data presented are for the PWR primary water environment air tests at 320°C (608°F). The upper bound curve for all the crack growth data is represented by the following equation:

$$da/dN = 5.1465 \times 10^{-11} \left(K_{max} (1-R)^{0.5}\right)^4$$

where:

a = Crack depth (in)
N = Number of cycles
R = K_{min}/K_{max}
K_{max}, K_{min} = Maximum and minimum stress intensity factor in units of $ksi\sqrt{in}$

The above fatigue crack growth equation includes the R ratio effect in the crack growth calculation, and has been converted to English units.

Typical design transients for both PWR and BWR piping systems are shown in Tables B-4 and B-5, taken from a number of references identified in the tables.

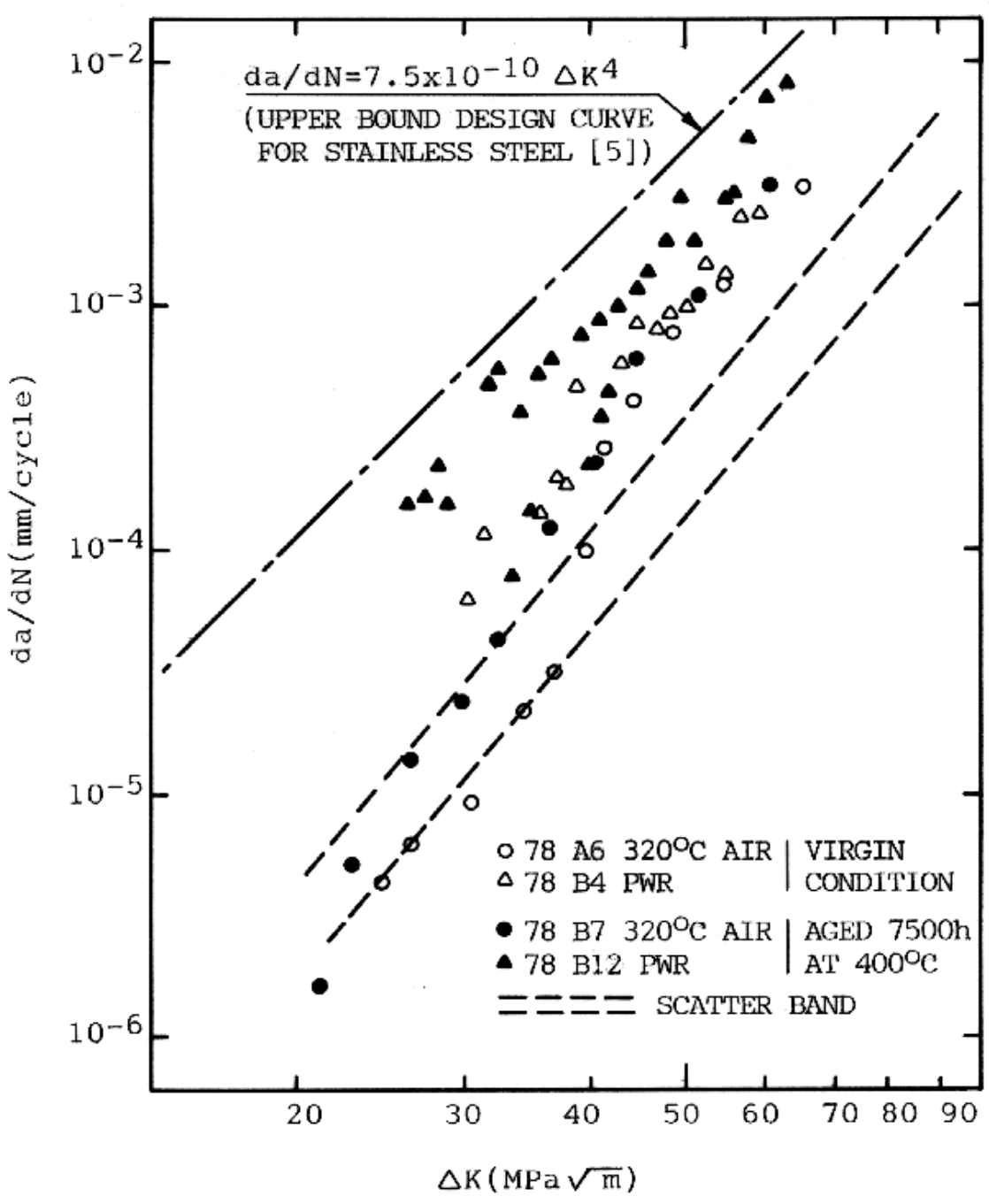

Figure B-2
Fatigue Crack Growth Rate at 320°C (608°F) in Air and in PWR Environment at 1 cpm for CF-8M, Heat L (Reference B4)

Table B-4
PWR Transients

Number of Cycles/40 Years			
Transients	**Ref. B5**	**Ref. B2**	**Ref. B6**
Heat Up/Cool Down	200	500	200
Unit Loading/Unloading at 5% of Full Power/Min	18400	–	18300
Step Load Increase/Decrease of 10% Full Power	2000	–	2000
Large Step Load Decrease with Steam Dump	200	–	200
Reactor Trip	400	480	400
Loss of Load (without Turbine/Reactor Trip)	80	–	80
Loss of Flow	80	–	80
Turbine Roll Test	10	–	10
Cold Hydro Test	5	–	
Hot Hydro Test	40	–	
Upset	–	210	–
OBE	–	200	–
Loss of Power	–	–	40
Accident (Pipe Break)	–	–	21

Table B-5
BWR Transients

Number of Cycles/40 Years	
Transients	**Ref. B7**
Start Up/Shut Down	130
Scram to Low Pressure Hot Standby	349
Scram to High Pressure Hot Standby	62
Hydro Test	130

A semi-elliptical defect in the crotch area of an elbow presents a three-dimensional crack problem whose solution is not readily available and which would be too expensive to analyze. Thus, a full circumferential crack in a cylinder with t/R ratio of 0.1 was selected to conservatively model the semi-elliptical defect and should conservatively represent the defect, in the piping elbow. Stress intensity factors were calculated for all the loading cases for both PWR and BWR elbows. The results are shown in Figures B-3 and B-4. In general, the worst case residual stress produces the highest stress intensity factor among all the loading cases.

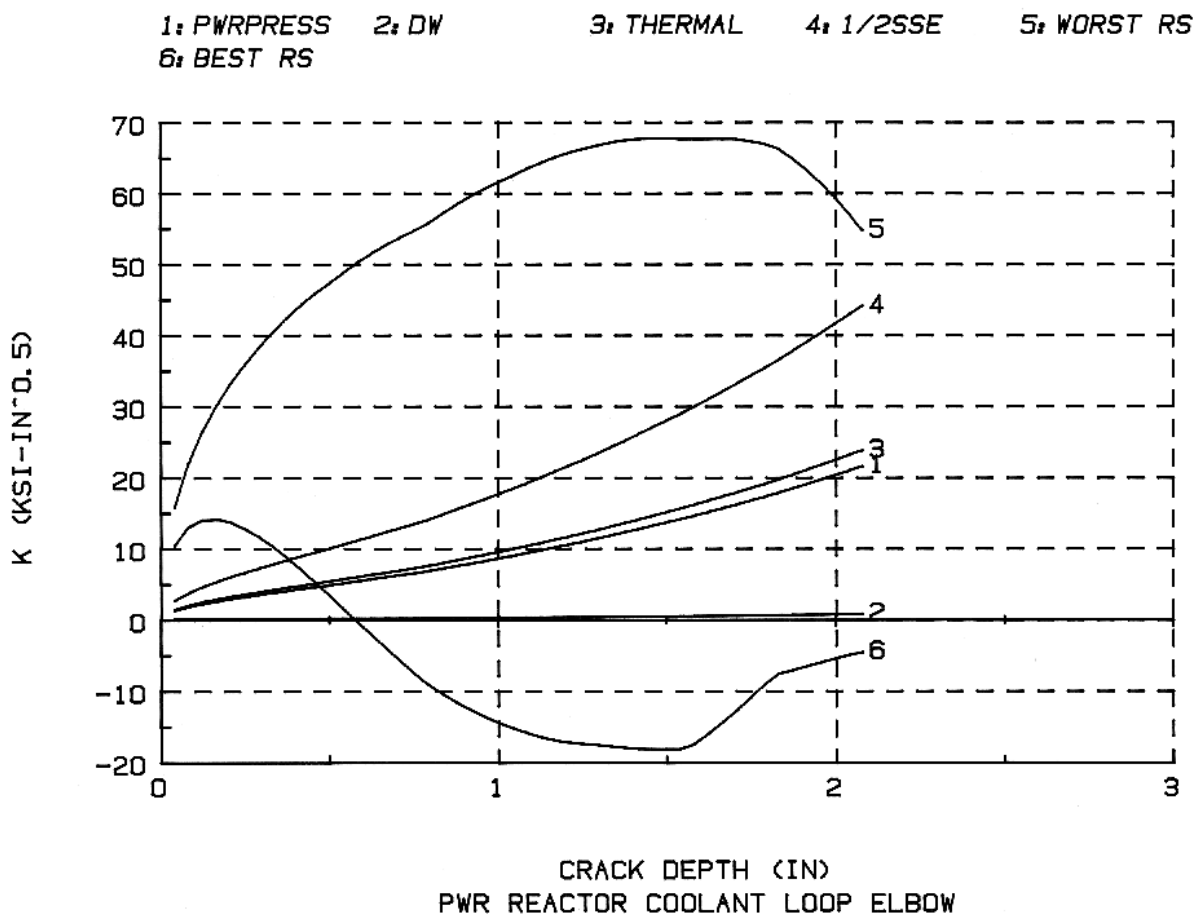

Figure B-3
PWR Reactor Coolant Loop Elbow

The design transients for both the PWR and BWR cases were assumed to be evenly distributed over the 40 years design period. Due to the large number of transient types for the PWR case, the transients were further reduced to four major types of transients as shown in Table B-6. Also if the number of transients was not be evenly divisible by 40 (design life) as in the BWR case, the number of cycles for each type of transient was rounded up to the nearest integer per year. Also for each type of transient, the corresponding change in pressure and temperature were determined so that the appropriate scale factor could be applied, to the base stress intensity factor cases of Figures B-3 and B-4. The number of cycles for each design transient, and the corresponding pressure and temperature changes (Δp and ΔT) are also shown in Table B-6.

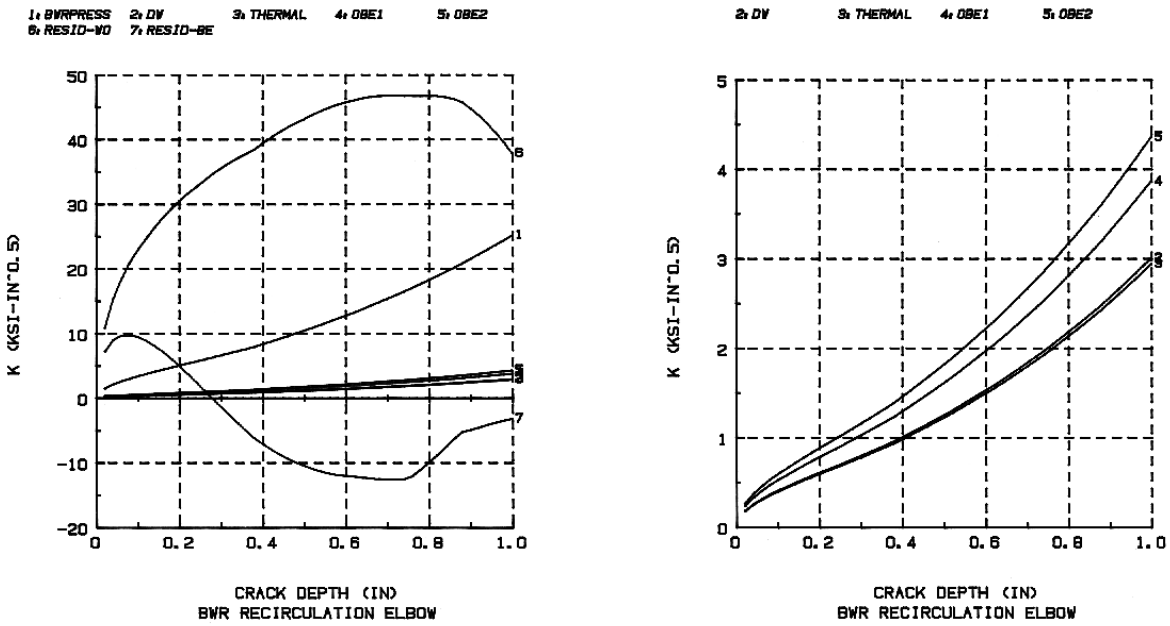

Figure B-4
BWR Recirculation Elbow

Table B-6
PWR Case

Transients	Number of Cycles per Year	Δp(psig)	ΔT(°F)
Hydro Test	4	3107	300
Heat Up/Cool Down and Other Significant Transients	24	2235	580
Unit Loading (5% power)	460	150	70
Step Loading (10% power)	50	150	16

BWR Case

Transients	Number of Cycles per Year	Δp(psig)	ΔT(°F)
Hydro Test	4	1361	0
Start Up/Shut Down	4	1045	480
Scram to LP Hot Standby	9	1080	480
Scram to HP Hot Standby	2	270	480

This input data was used to perform fatigue crack growth evaluations for both the PWR and the BWR elbows. Three hypothetical initial crack sizes of 0.2362 in. (6 mm), 0.4724 in. (12 mm) and 1.1811 in. (30 mm) were used. The 1.1811 in. (30 mm) crack size was not used for the BWR elbows since it would be essentially through-wall at the start. For each of these initial crack sizes, three evaluation cases were performed: no residual stress, best estimate residual stress, and worst case residual stress, in addition to the other loadings as specified in Tables B-4 and B-5.

The fatigue crack growth results are presented in Figures B-5 to B-9. In all but one of the cases (30 mm initial flaw depth), the fatigue crack growth is minimal over the 40 years design life, even using the worst case residual stress distribution.

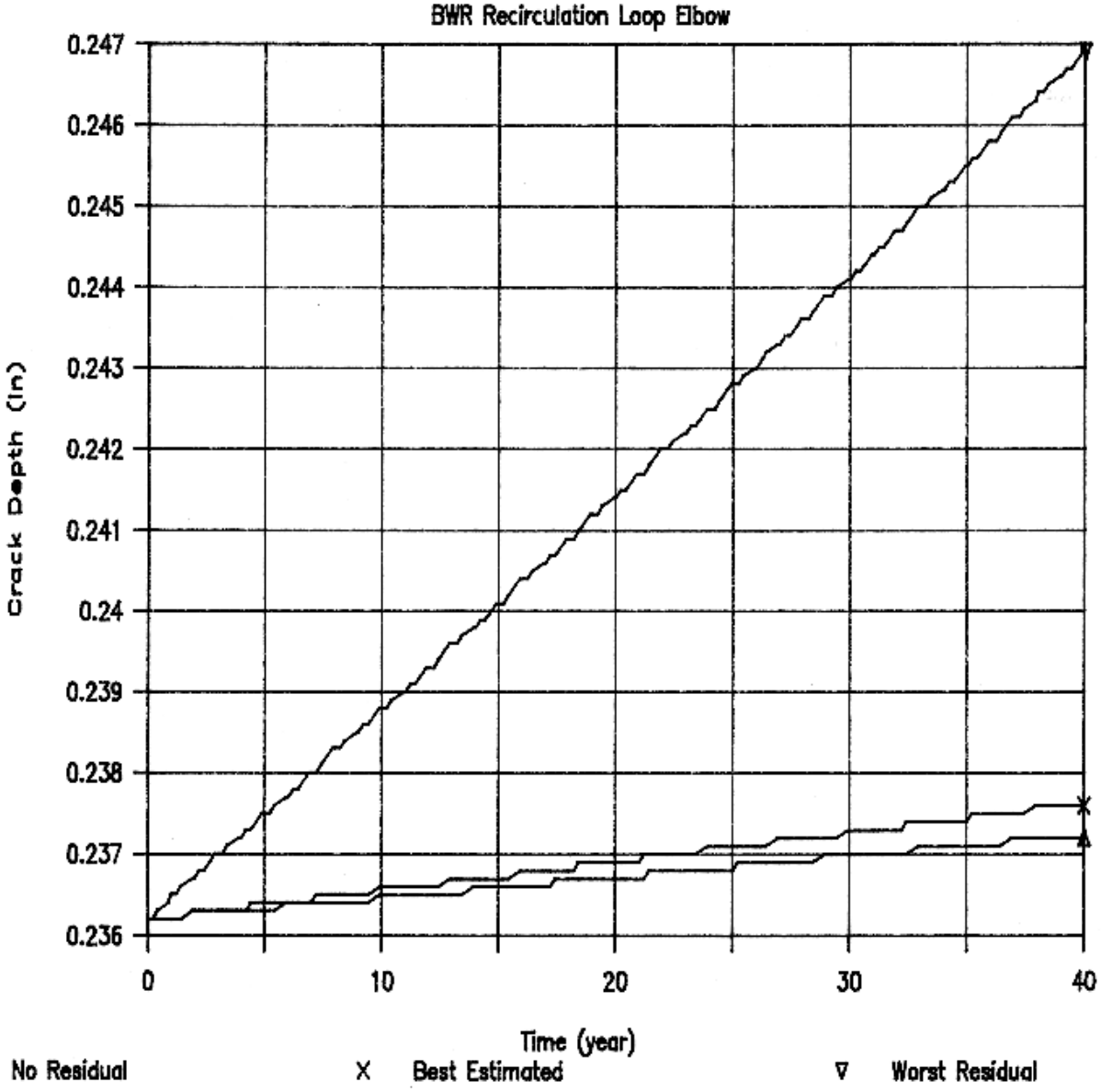

Figure B-5
Fatigue Crack Growth (6 mm Initial Defect)

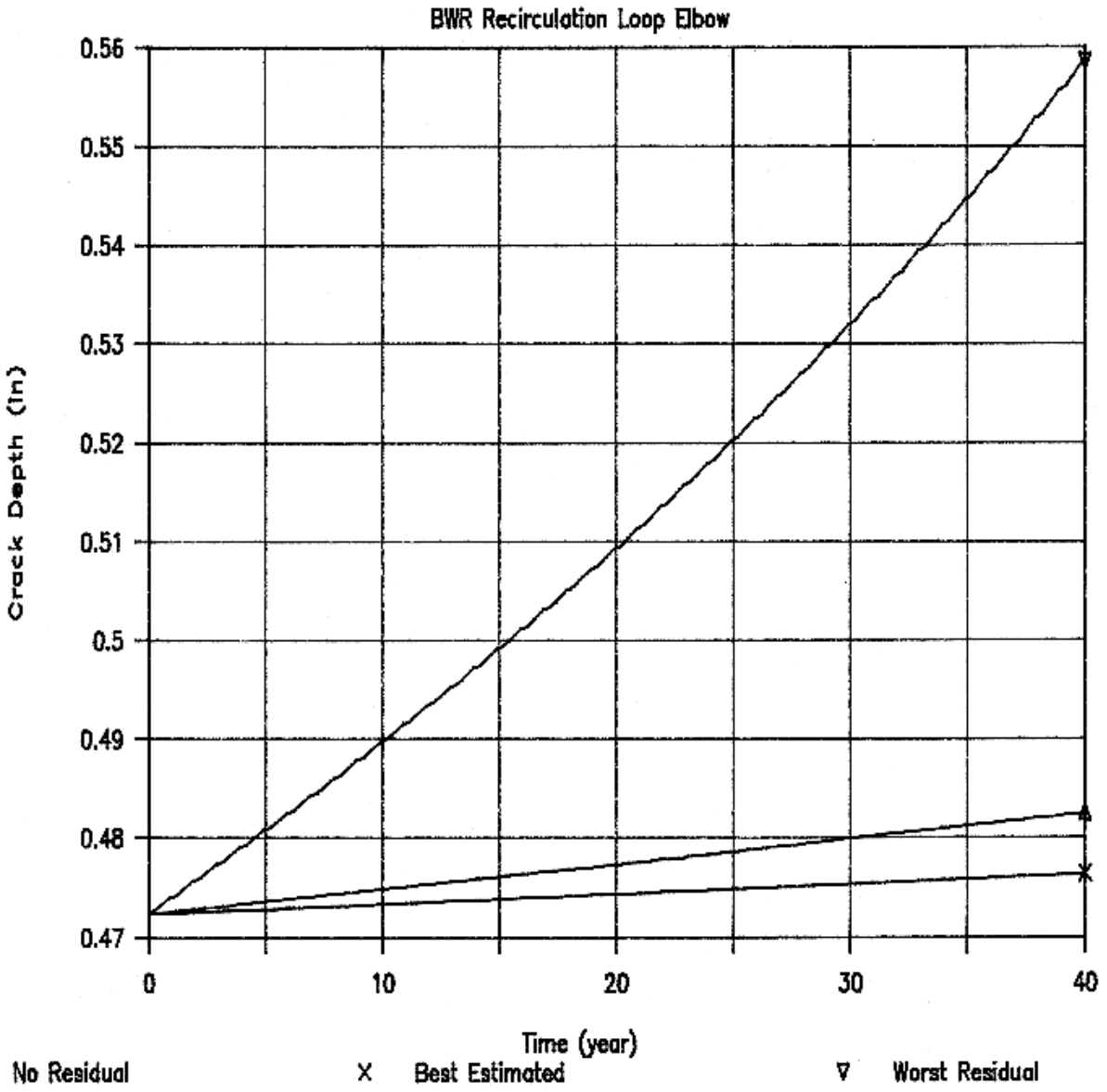

Figure B-6
Fatigue Crack Growth (12 mm Initial Defect)

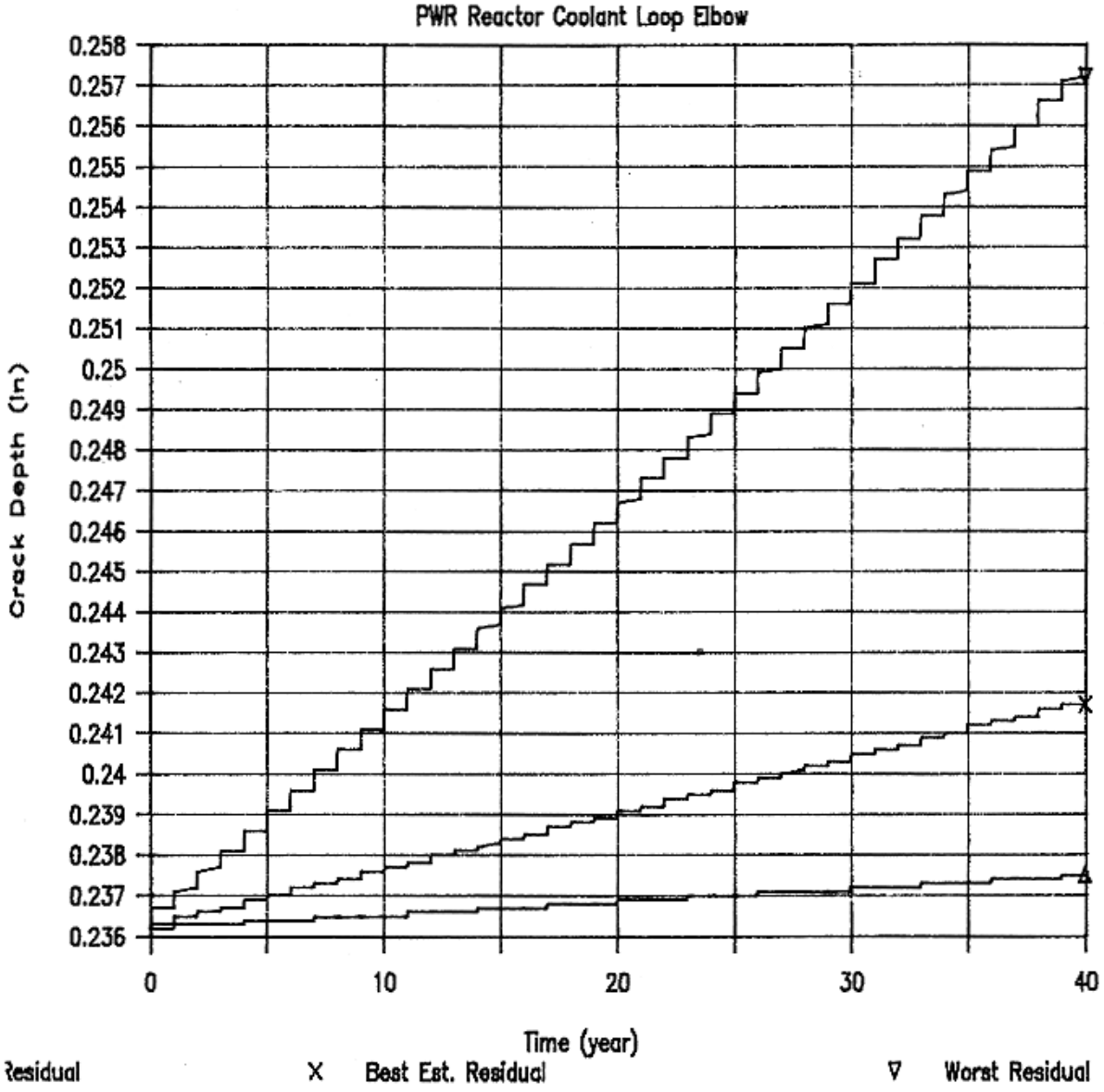

Figure B-7
Fatigue Crack Growth (6 mm Initial Defect)

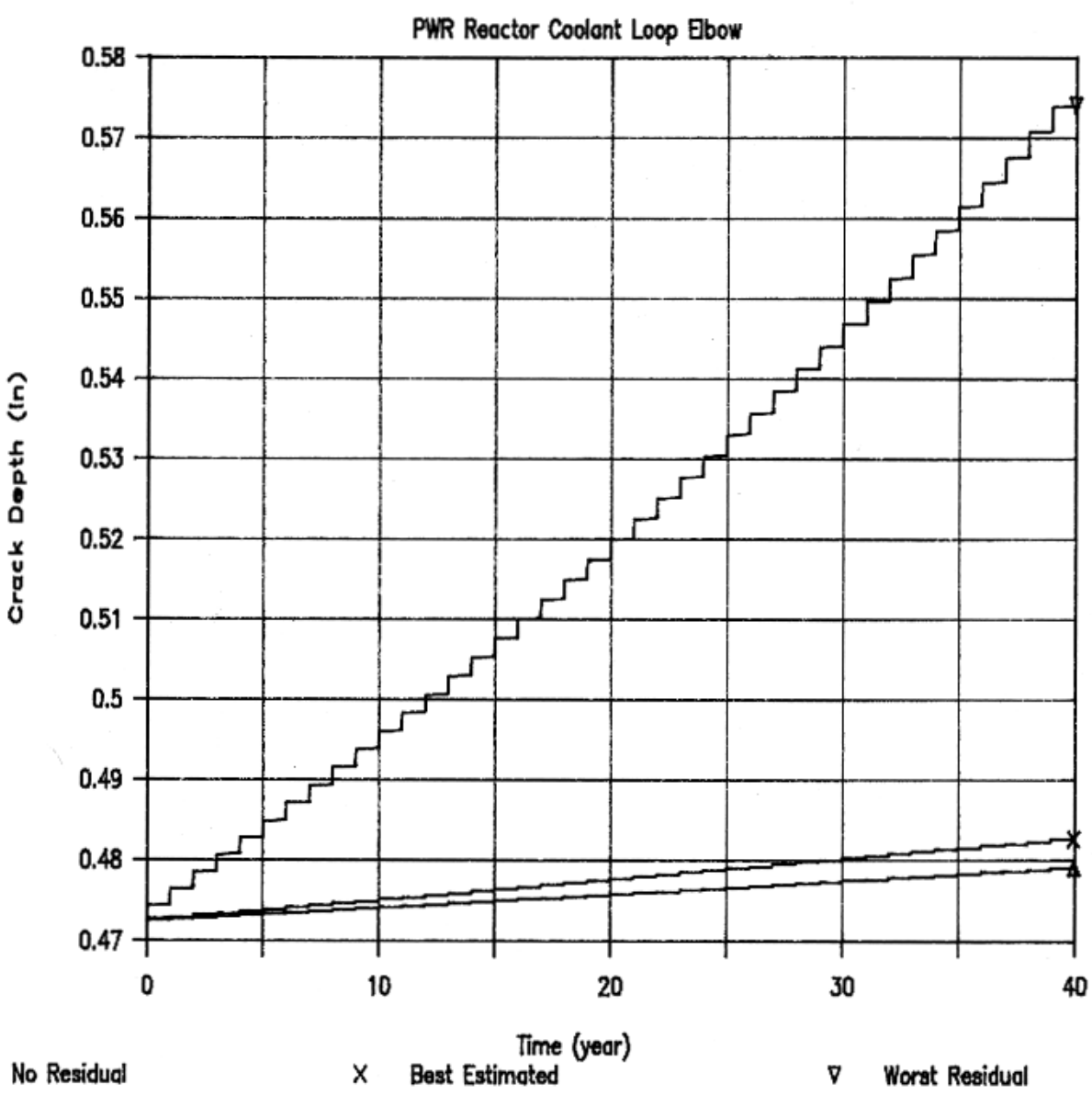

Figure B-8
Fatigue Crack Growth (12 mm Initial Defect)

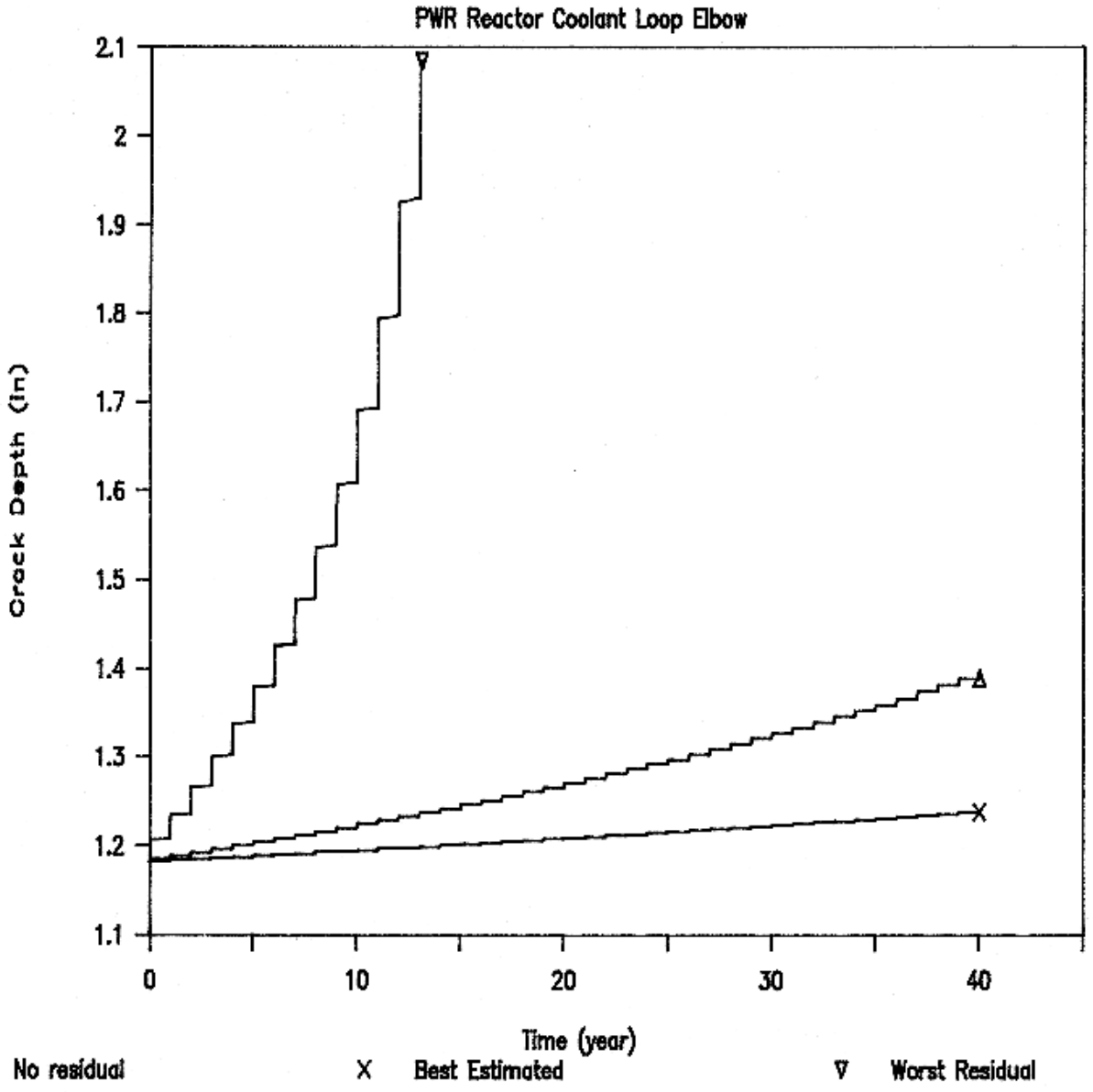

Figure B-9
Fatigue Crack Growth (30 mm Initial Defect)

These generic evaluation cases incorporated a number of conservative assumptions, including the upper bound crack growth data for the CF8M cast austenitic steel in the PWR environment, highest stress value for the PWR elbow, and full circumferential crack model. The analysis indicate that if a fabrication defect of substantial depth were located in a high stress location, e.g. combination of worst residual stress and high applied load, with aged material; it may warrant an inservice inspection during the latter part of the plant life.

Critical Flaw Size Evaluation

Thermal aging of cast austenitic stainless steel has been identified as resulting in a decrease in the ductility of the material. This decrease in ductility has a direct effect on the fracture toughness of the material and thus the critical flaw size. The critical flaw size decreases as the fracture toughness of the material decreases.

Figure B-10 presents the effect of thermal aging at 280°C and 320°C on cast CF-8 stainless steel [B8]. These aging temperatures approximately correspond to the operating temperature of a BWR and a PWR, respectively. Upper shelf Charpy impact energies (C_v) are shown in this figure for aging at 70,000 hours (8 years) and at 300,000 hours (34 years). Figure B-11 presents a correlation between the material fracture toughness, J_{IC}, and upper shelf Charpy impact energy for cast duplex stainless steel. This correlation is presented as impact energy per unit area, while the results in Figure B-10 are in total energy (Joules or ft-lb). No description was given in [B9] as to whether the impact energy was presented per unit area or as total impact energy. One reference was made that the test results were obtained from Charpy V-notch test specimens. Using the ASTM E24 testing standard, the fracture area of a Charpy V-notch test specimen is 8 mm x 10 mm (0.8 cm^2).

In calculating the fracture toughness, the impact energy presented in Figure B-11 was assumed to be per unit area (cm^2). This gives a conservative fracture toughness estimation (25% lower) compared to if the results were meant to be per 0.8 cm^2. Table B-7 presents the corresponding J_{IC} values and conversions to K_{IC} in English units.

Table B-7
Fracture Thoughness Property Correlations

Time (hrs)	Aged At		Impact Energy		J_{IC}	K_{IC}
70000	320°C	(608°F)	95 J	(70 ft-lb)	500 kJ/m^2	270 ksi$\sqrt{in}$
	280°C	(536°F)	140 J	(103 ft-lb)	900 kJ/m^2	362 ksi$\sqrt{in}$
300000	320°C	(608°F)	65 J	(48 ft-lb)	350 kJ/m^2	226 ksi$\sqrt{in}$
	280°C	(536°F)	90 J	(66 ft-lb)	500 kJ/m^2	270 ksi$\sqrt{in}$
Extrapolated to						
60 Yrs	320°C	(608°F)	54 J	(40 ft-lb)	250 kJ/m^2	191 ksi$\sqrt{in}$
	280°C	(536°F)	54 J	(40 ft-lb)	250 kJ/m^2	191 ksi$\sqrt{in}$

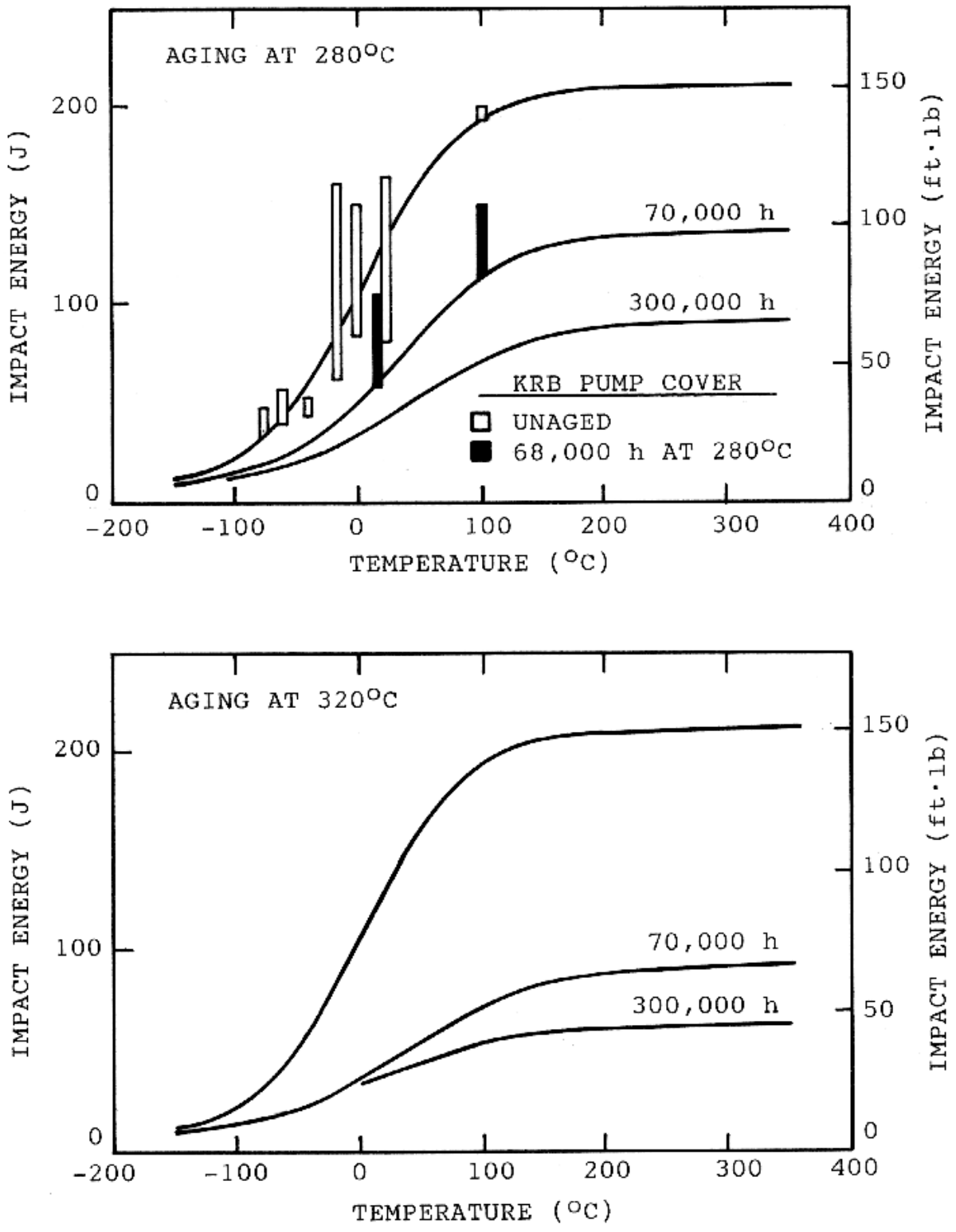

Figure B-10
Effect of Thermal Aging at 280° and 320°C on the Transition Curves for Impact Energy of Cast CF-8 Stainless Steel (Reference B8)

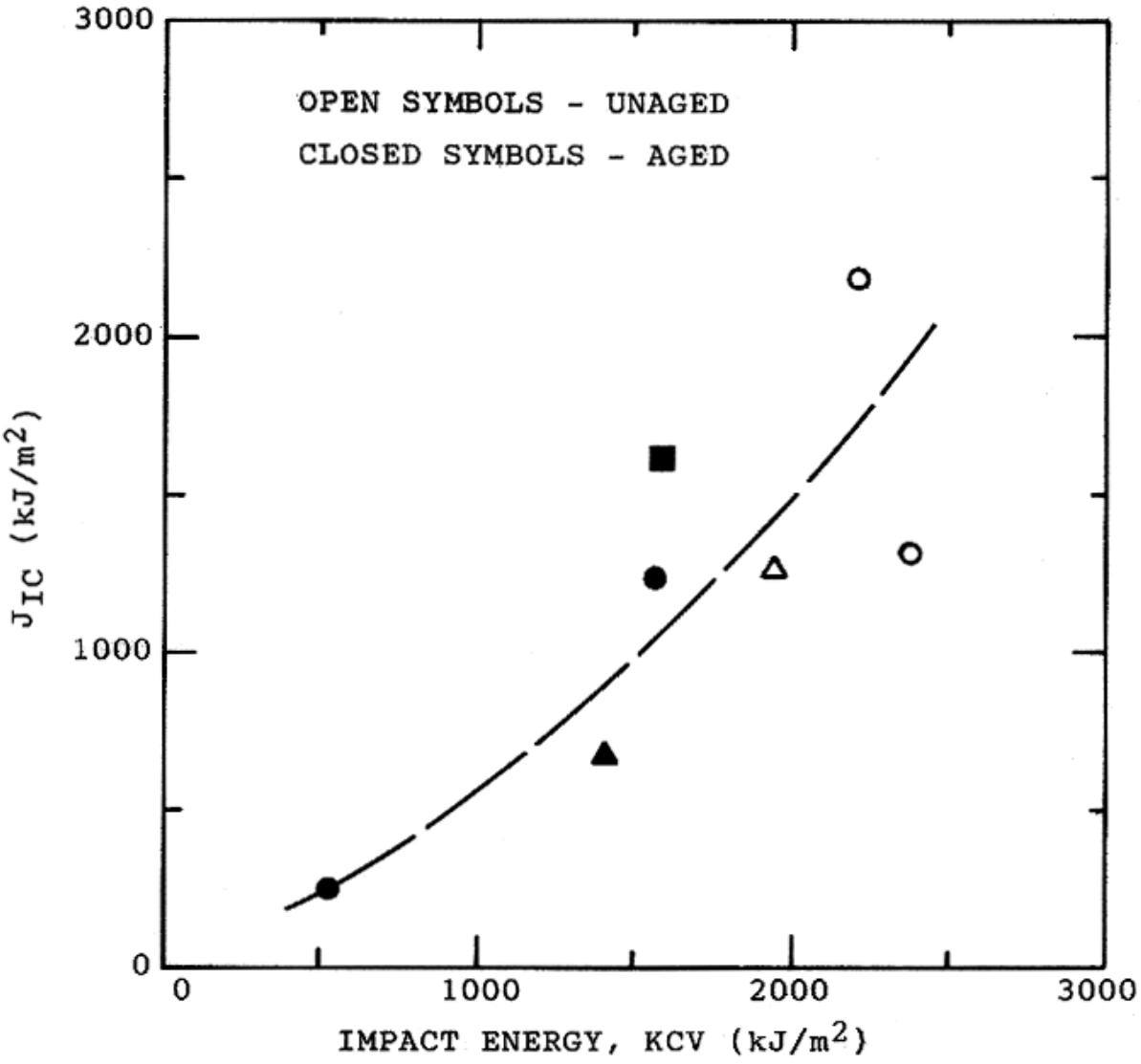

Figure B-11
Correlation Between J_{ic} and Impact Energy for Cast Duplex Stainless Steel (Reference B9)

Figures B-12 and B-13 present the resulting critical flaw size evaluation of the PWR and BWR elbows based on these toughness data. The total stress intensity factor curve is the worst combination among all the fatigue crack growth loading cases, with the addition of the seismic loading which was not included in the fatigue crack growth evaluation. In both the PWR and BWR cases, the total stress intensity factor curve is well below the K_{IC} curve at the end of 300,000 hours. Using the extrapolated K_{IC} value at 60 years, the BWR elbow still shows a comfortable margin below K_{IC} while the critical crack depth in the PWR elbow would be about 2 inches. Thus, for a typical plant life of 40 years, the analyses indicate that the component would exhibit leak-before-break behavior in the event that the semi-elliptical defect grows through the pipe wall by fatigue.

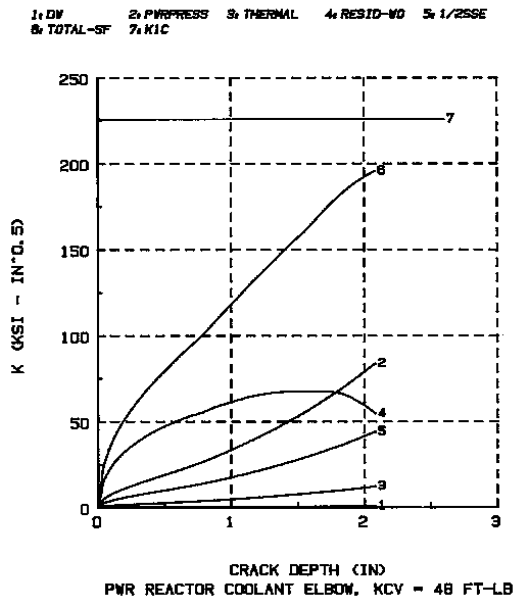

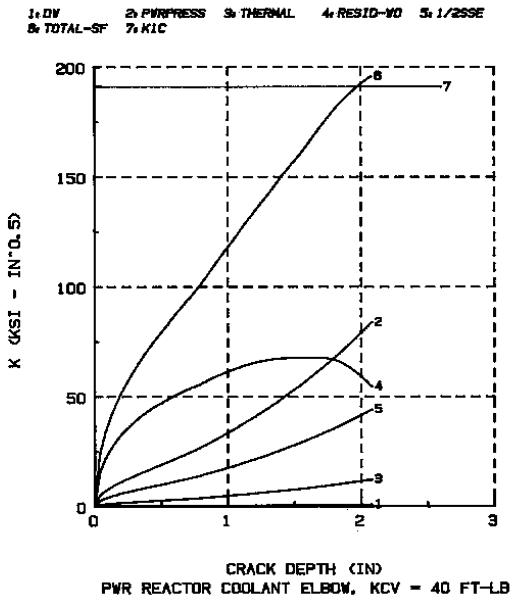

Figure B-12
PWR Reactor Coolant Elbow

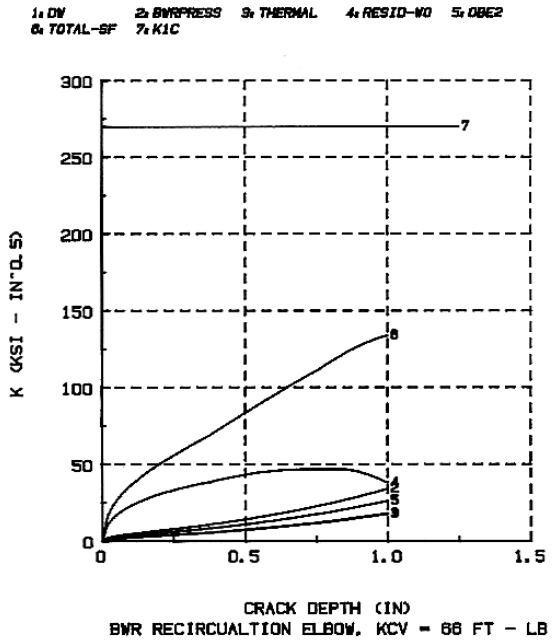

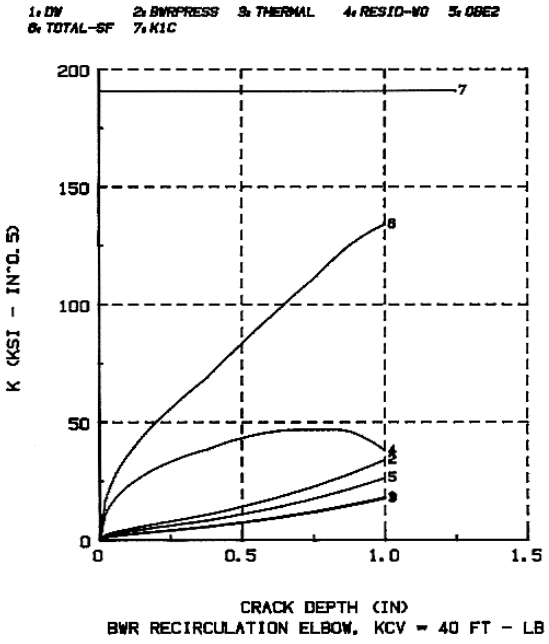

Figure B-13
BWR Recirculation Elbow

Discussion

A generic "worst case" analysis was performed to study the fatigue crack growth of a defect in a cast austenitic stainless steel pipe component. The components chosen were a reactor coolant loop piping elbow for a PWR and a recirculation loop elbow for a BWR. The stresses used in this generic evaluation were the maximum stress value reported for a typical PWR reactor coolant loop piping system, and a value calculated from the reported forces and moments from a plant specific BWR recirculation system stress report. An upper bound fatigue crack growth law was used. A full circumferential crack model was chosen although the defect would most likely be semi-elliptical.

Conservative fracture toughness estimates were obtained considering recent test data on thermal aging of these materials at PWR and BWR temperatures [B8, B9 and B10]. No safety factors were applied to these toughness estimates.

In summary, the analyses show that the predicted fatigue crack growth is small for both initial crack depths of 6 mm (0.24 in) and 12 mm (0.47 in) for all the anticipated residual stress patterns. For an initial crack depth of 30 mm (1.18 in) in the PWR case, the crack growth is also small for the no residual stress and the best estimate residual stress. For the worst residual stress case, the crack would grow through-wall in less than 14 years. The case with initial crack depth of 30 mm was not performed for the BWR elbow since the nominal pipe wall is only 1.24 inch.

In both cases, the predicted critical flaw size for a typical plant life of 40 years indicate that the component would exhibit leak-before-break behavior in the event that the semi-elliptical defect grew through the pipe wall by fatigue. Even extrapolating the thermal aging to 60 years, the BWR elbow shows considerable margin to leak-before-break, while the PWR would require a flaw almost 80% through the pipe wall before fracture would be predicted.

References

B1. GE Report 11A2622, "Design Report, Recirculation System for James A. Fitzpatrick Nuclear Power Station, ANSI B31.1 Calculation", October, 1971.

B2. VA Sequoyah FSAR Update, Vol. 5.

B3. EPRI Special Report NP-4690-SR, "Evaluation of Flaws in Austenitic Steel Piping," July, 1986.

B4. Slama, G., Petrquin, P., Mager, T., "Effect of Aging on Mechanical Properties of Austenitic Stainless Steel Castings and Welds", SMiRT Post Conference Seminar No. 6, Monterey, CA., August, 1983.

B5. Riccardella, P.C., and Mager, T.R., "Fatigue Crack Growth Analysis of Pressurized Water Reactor Vessels," Stress Analysis and Growth of Cracks, ASTM, STP 513, 1972.

B6. SI Report 85-034, "Fracture Mechanics Leak-Before-Break Evaluation of R. E. Ginna Nuclear Power Station High Energy Piping Welds Outside Containment", Rev. 0, February, 1986.

B7. NEDE-21821, Boiling Water Reactor Feedwater Nozzle/Sparger Final Report, March, 1978.

B8. Chopra, O.K., and Chung, H.M., NUREG/CR-42104, "Long Term Embrittlement of Cast Duplex Stainless Steels in LWR Systems - Annual Report, October 1983 – September 1984".

B9. Chopra, O.K., and Chung, H.M., NUREG/CR-42104 Vol. 1, No. 1, "Long Term Embrittlement of Cast Duplex Stainless Steels in LWR Systems – Semi-annual Report, October 1985 - March 1986".

B10. Chopra, O.K., and Chung, H.M., NUREG/CR-4744 Vol. 1, No. 2, "Long Term Embrittlement of Cast Duplex Stainless Steels in LWR Systems: Semi-annual Report, April 1986 - September 1986".

Target:
Nuclear Power

About EPRI

EPRI creates science and technology solutions for the global energy and energy services industry. U.S. electric utilities established the Electric Power Research Institute in 1973 as a nonprofit research consortium for the benefit of utility members, their customers, and society. Now known simply as EPRI, the company provides a wide range of innovative products and services to more than 1000 energy-related organizations in 40 countries. EPRI's multidisciplinary team of scientists and engineers draws on a worldwide network of technical and business expertise to help solve today's toughest energy and environmental problems.

EPRI. Electrify the World

Printed on recycled paper in the United States of America

1000976

EPRI • 3412 Hillview Avenue, Palo Alto, California 94304 • PO Box 10412, Palo Alto, California 94303 • USA
800.313.3774 • 650.855.2121 • askepri@epri.com • www.epri.com